CONTEMPORARY DENTAL IMAGING:

FROM DIAGNOSIS TO QUANTITATIVE ASSESSMENT

Editor:
Dr. Öğr. Üyesi Esra Fidan KARAMADEN

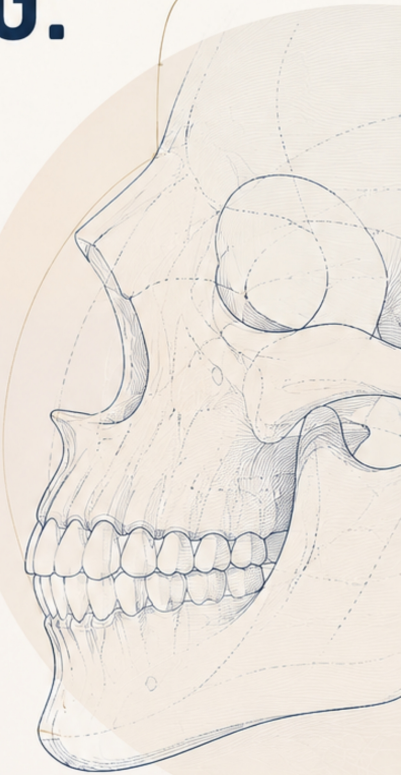

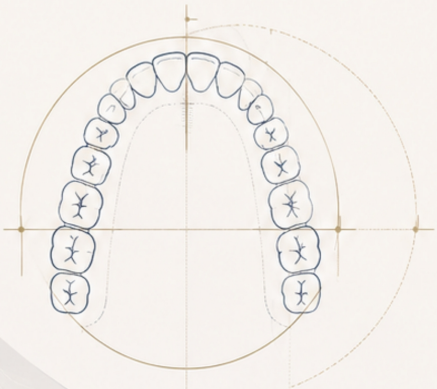

BİDGE Yayınları

BİDGE Yayınları

Contemporary Dental Imaging: From Diagnosis to Quantitative Assessment

Editor: DR. ÖĞR. ÜYESİ ESRA FİDAN KARAMADEN

ISBN: 978-625-8821-80-2

1st Edition
Page Layout By: Gözde YÜCEL
Publication Date: 2026-08-12
BİDGE Yayınları

Certificate No: 71374

www.bidgeyayinlari.com.tr - bidgeyayinlari@gmail.com
Krc Bilişim Ticaret ve Organizasyon Ltd. Şti.
Güzeltepe Mahallesi Abidin Daver Sokak Sefer Apartmanı No: 7/9 Çankaya / Ankara

CONTENTS

CHAPTER 1

Imaging the Living Pulp: Dental MRI and Quantitative Imaging Biomarkers in Vital Pulp Therapy and Regenerative Endodontics

Damla İLKGELEN[1]
Suay Yağmur ÜNAL[2]

Introduction

For most of the history of endodontic diagnosis, the clinician's access to the dental pulp has been almost entirely indirect. Cold, heat, and electric pulp testing infer the physiological state of the pulp from a patient's subjective sensory report, while periapical radiography and, more recently, cone-beam computed tomography (CBCT) visualize the periradicular bone and root canal space but are largely blind to the pulp itself, since these hard-tissue-optimized modalities depend on differential attenuation of ionizing radiation by mineralized structures rather than by the soft, richly vascularized and innervated connective tissue that constitutes the pulp proper.

[1] Dr. Öğr. Üyesi, Nişantaşı Üniversitesi Diş Hekimliği Fakültesi Endodonti Anabilim Dalı İstanbul/Türkiye, Orcid: 0000-0003-1619-173X
[2] Dr. Öğr. Üyesi, Nişantaşı Üniversitesi Diş Hekimliği Fakültesi Ağız Diş ve Çene Radyolojisi İstanbul/Türkiye, Orcid: 0000-0002-8559-7461

Magnetic resonance imaging (MRI) inverts this relationship. Because MR contrast arises from the density and relaxation behavior of tissue water and macromolecular protons rather than from radiographic density, MRI is able to render the dental pulp directly, without ionizing radiation, and with a level of soft-tissue contrast unattainable by CBCT. What began as a series of ex vivo and small feasibility studies has, over roughly two decades, matured into a body of work that increasingly reports not merely qualitative images of the pulp but quantitative, numerically defined imaging biomarkers: relaxation times, apparent diffusion coefficients, and dynamic contrast-enhancement parameters that can, in principle, be measured, thresholded, and compared across time points or between patients.

This chapter examines that literature at the point where it intersects with two clinically distinct but conceptually related domains of contemporary endodontics. Vital pulp therapy (VPT) seeks to preserve an already vital, and often already reactive or inflamed, pulp in the face of caries or trauma; regenerative endodontic procedures (REPs) seek, by contrast, to induce the formation of new vascularized tissue within a canal whose native pulp has already been lost. Both fields share a common diagnostic weakness: the principal available outcome measures — symptom resolution, radiographic healing, and pulp sensibility testing — are indirect, delayed, or of limited reliability, a limitation that has itself motivated a wider search for nontraditional, more objective vitality-assessment methods (Afkhami et al., 2024). The chapter first situates dental MRI within the broader shift from hard-tissue to soft-tissue-capable imaging, then surveys the technical means by which pulp-scale quantitative imaging has become feasible, defines what is meant by a quantitative imaging biomarker in the radiological sense, and reviews the specific quantitative approaches reported for pulp vitality, before turning to their still-emerging application in vital pulp

therapy and regenerative endodontics, their shared limitations, and the direction in which artificial intelligence and radiomics appear likely to take the field.

From Radiography to Magnetic Resonance: A Changing Paradigm in Pulp Imaging

The introduction of CBCT gave endodontics a three-dimensional view of the root canal system and periradicular bone that two-dimensional periapical radiography could not provide, and comparative studies against histopathological reference standards have generally found CBCT more sensitive than periapical radiography for detecting apical periodontitis, even though CBCT still underestimates lesion prevalence relative to histology and periapical radiography retains reasonable accuracy for larger lesions.

What CBCT cannot do, by the nature of x-ray attenuation contrast, is characterize the pulp itself. As a recent comprehensive review of dental MRI observes, conventional radiographic techniques and CBCT are built around the visualization of hard, mineralized tissue, so that the pulp — a soft connective tissue — remains essentially invisible on these modalities regardless of resolution (Han et al., 2025). This is not a minor gap: whether a pulp is vital, reversibly inflamed, irreversibly inflamed, or necrotic is precisely the information a clinician needs in order to choose between vital pulp therapy, regenerative treatment, or conventional root canal treatment, and none of it is directly legible on a CBCT volume.

A systematic review comparing MRI directly against CBCT for periapical pathosis represents an early attempt to test whether MR's soft-tissue sensitivity could be brought to bear on this diagnostic gap in a way that is comparable, rather than merely complementary, to the existing hard-tissue gold standard. Dental

MRI's usefulness beyond pulp vitality alone is illustrated by work differentiating periapical granulomas from radicular cysts using dental-dedicated MRI sequences, a distinction that CBCT's bone-density contrast cannot make since both lesion types present as similar periapical radiolucencies (Juerchott et al., 2018). More recently, a feasibility study of a dental-dedicated MRI (ddMRI) system operating at low field strength (0.55 T) with a purpose-built seven-channel dental coil evaluated pulp vitality and apical periodontitis directly against CBCT and clinical consensus in a small consecutive patient sample, reporting that dedicated dental MRI could visualize pulp vitality status and periapical fluid accumulation with useful agreement to the existing reference standards, while acknowledging that the sample size and single-center design limit how far the findings generalize (Johannsen et al., 2026). Taken together, this recent trajectory illustrates a field moving from asking whether MRI can see the pulp at all toward asking how reliably, and how quickly, it can be made to do so in an ordinary clinical setting.

Technical Foundations of Dental MRI: Coils, Sequences, and Spatial Resolution

The central technical obstacle to dental MRI is not image contrast, which is intrinsically favorable for soft tissue, but signal-to-noise ratio (SNR) within the very small tissue volumes that a dental pulp occupies. Standard head-and-neck receive coils, designed for whole-jaw or whole-face coverage, sit too far from any individual tooth to provide the local sensitivity that high-resolution pulp imaging requires, and this SNR penalty is the main reason early dental MRI work was often confined to ex vivo teeth scanned at high field strength or with long acquisition times (Han et al., 2025; Vaddi et al., 2025).

Two broad hardware strategies have been used to close this gap. The first keeps the receive coil outside the mouth but tailors it

closely to dental anatomy — for example, purpose-built mandibular or maxillary surface coils used together with “Black Bone” gradient-echo sequences (such as short-tau inversion recovery, STIR, and double-echo steady-state, DESS, variants) that render bone as a dark structure against bright soft tissue, improving bone–soft-tissue contrast for surgical and oncological applications in the oral cavity. The second strategy places the receive coil inside the mouth itself. Wireless, inductively coupled intraoral volume coils have achieved voxel sizes on the order of $(350\ \mu m)^3$ in roughly four minutes of scan time, a resolution the original developers reported as comparable, in their sensitive volume, to CBCT (Ludwig et al., 2016). More recent intraoral coil arrays, combining a buccal and a lingual element, have pushed this further to around 250 μm isotropic resolution while also enabling parallel imaging, and disposable, braces-inspired wireless bite coils have been reported to achieve submillimeter resolution (approximately $0.30 \times 0.30 \times 1.5\ mm^3$) with soft-tissue delineation of pulp and periodontal membrane not visible on CBCT, while simplifying placement to something resembling inserting a mouthguard (Özen et al., 2026).

On the pulse-sequence side, three families are relevant to quantitative pulp imaging specifically. Contrast-enhanced T1-weighted sequences, acquired before and after intravenous gadolinium administration, are used to derive signal-intensity ratios or full dynamic contrast-enhanced (DCE) time-intensity curves that are sensitive to pulpal perfusion. Multi-echo spin-echo T2-mapping sequences generate voxel-wise parametric maps of T2 relaxation time, a parameter that reflects tissue water content and has been applied along the length of the root canal from crown to apex. Diffusion-weighted sequences, historically limited in the oral cavity by susceptibility artifact from adjacent air and dental restorations, have more recently been adapted using hybrid turbo-gradient-spin-echo (TGSE) BLADE readouts specifically optimized for the dental

pulp, enabling in vivo apparent diffusion coefficient (ADC) mapping of healthy teeth for the first time under clinically feasible conditions (Sittinger et al., 2025).

These hardware and sequence choices interact with a basic tradeoff between field strength, resolution, scan time, and practicality. Low-field, dental-dedicated systems purpose-built for chairside or office-based use sacrifice some SNR and resolution for shorter, more tolerable examinations and lower cost, whereas high-field (3 T or above) research protocols with dedicated intraoral hardware can resolve sub-millimeter pulp anatomy and support more demanding quantitative sequences, at the cost of specialized equipment, longer scan times, and, so far, confinement to research centers. Any discussion of quantitative dental MRI biomarkers has to be read against this backdrop: the numbers reported in one study were very often generated on hardware and sequences that differ, sometimes substantially, from those used in another.

The Concept of a Quantitative Imaging Biomarker

The Radiological Society of North America's Quantitative Imaging Biomarkers Alliance (QIBA) defines quantitative imaging as the extraction of quantifiable features from medical images for assessing the normal state or the severity, degree of change, or status of a disease, injury, or chronic condition relative to normal (Radiological Society of North America, 2021). QIBA's central concern, since its founding in 2007, has been reducing variability of such measurements across devices, imaging sites, patients, and time, through published “profiles” that specify the acquisition and processing parameters needed for a given biomarker to meet a stated, quantifiable performance claim for accuracy and precision.

This framework is a useful yardstick against which to read the dental-pulp imaging literature, precisely because it names the property that the field is still working to establish. A signal-intensity

ratio, a T2 value, or an ADC measurement is only useful as a clinical biomarker to the extent that a given numerical value means approximately the same thing regardless of which scanner, coil, or center produced it — the same requirement that motivated QIBA's own profile for diffusion-weighted imaging and ADC in other organ systems, where accuracy and precision have had to be established and published explicitly before ADC values could be trusted as comparable across a multicenter trial. Dental pulp imaging has, to date, generated multiple independently plausible quantitative candidates — described in the following section — without yet reaching this stage of cross-site, cross-vendor standardization, a point to which the chapter returns in the discussion of limitations below.

The appeal of pursuing such standardization specifically for pulp vitality is sharpened by the well-documented unreliability of the alternative. A recent scoping review of nontraditional pulp vitality assessment methods was motivated in large part by the recognized limitations of the traditional cold, heat, and electric pulp tests, which depend on a patient's subjective report and can be confounded by apprehension, prior trauma, multi-rooted teeth with partially necrotic pulp, and recently erupted or heavily restored teeth (Afkhami et al., 2024). A quantitative imaging biomarker, by definition, does not depend on the patient's subjective report at all — which is precisely why the imaging literature reviewed below has attracted sustained interest despite its still-early stage of development.

Quantitative MRI Assessment of Pulp Vitality

The earliest attempts at a genuinely quantitative pulp-vitality biomarker used signal intensity itself. Kress et al. (2004) measured T1 and T2 signal intensity in the region of interest of 211 teeth from 35 patients and found that neither the plain T2 sequence nor the non-contrast-enhanced T1 sequence distinguished clinically vital from

avital teeth; a significant difference emerged only when comparing the non-contrast T1 signal against the same tooth's post-contrast T1 signal, which the authors interpreted as reflecting pulpal perfusion — present in vital pulp and absent, or markedly reduced, in necrotic pulp. A companion study by the same group subsequently showed that pulp cavity signal intensity itself varies systematically with patient age and tooth type even in healthy teeth (Kress et al., 2007), a finding with direct implications for any attempt to set a single universal vitality threshold. A later prospective in vivo study of the healthy pulp's contrast-enhancement pattern, using precisely timed post-contrast acquisitions, further characterized the normal range and time course of pulpal enhancement in intact teeth, providing a normative baseline against which pathological enhancement patterns can be compared (Juerchott et al., 2022).

More recent work has extended this contrast-enhanced approach from a single before/after ratio to a full dynamic time-intensity curve (TIC). Using 3 T dynamic contrast-enhanced MRI with time-resolved angiographic imaging, Yomtako et al. (2026) classified the shape of the post-contrast time-intensity curve in teeth with known electric-pulp-test status and found that TIC classification distinguished vital from non-vital teeth with an accuracy comparable to electric pulp testing itself, whereas plain T1-weighted, T2-weighted, or single-time-point gadolinium-enhanced T1 signal intensity again failed to reach statistical significance between the two groups — reinforcing, more than two decades after Kress et al. (2004), that it is specifically the temporal dynamics of perfusion, not a static signal value, that appears to carry most of the diagnostic information.

A second quantitative channel is T2 relaxometry. Cankar et al. (2020) generated voxel-wise T2 maps along the coronal-to-apical length of the root canal in 74 teeth scanned at 3 T and classified according to the International Caries Detection and Assessment

System (ICDAS), finding that mean pulp T2 fell in a graded, caries-severity-dependent manner — averaging around 166 ms in sound coronal pulp (ICDAS 0) and around 115 ms in the most severely carious group (ICDAS 4–6) — with a distinct crown-to-apex T2 profile that additionally differed between single-rooted and multi-rooted teeth. Because this relationship is graded rather than binary, T2 mapping offers, at least in principle, a continuous severity readout rather than a simple vital/non-vital classification. A subsequent histological validation study by a related group correlated pulp T2 parameters directly with graded, morphometrically quantified pulp degeneration in extracted premolars, finding that teeth with histologically confirmed degeneration showed both lower mean T2 and lower T2 variability than non-degenerated teeth, and that degeneration grade correlated positively with ICDAS score and negatively with both T2 parameters (Tenyi et al., 2024) — an important step because it ties the MRI signal to microscopic ground truth rather than only to a clinical or radiographic surrogate.

A third channel exploits water diffusion. In an early ex vivo study, Vidmar et al. (2012) calculated ADC maps of extracted teeth across a range of ICDAS scores and found that affected pulp regions (ADC below approximately 1.0×10^{-9} m²/s) could be reliably separated from intact pulp (ADC above that threshold), with average pulp ADC correlating linearly with both ICDAS score and directly measured dentin demineralization depth. Translating diffusion imaging into the more diagnostically relevant in vivo setting proved considerably harder, owing largely to susceptibility artifact in the oral cavity, until a hybrid turbo-gradient-spin-echo BLADE diffusion sequence, optimized specifically for the dental pulp and validated across 329 healthy teeth in 18 volunteers, established feasible b-value ranges and normative in vivo ADC values, notably finding that ADC did not differ significantly across tooth type or jaw,

which the authors interpreted as evidence that pulp ADC behaves as a stable, comparable marker suitable for future disease-state and necrosis studies (Sittinger et al., 2025).

Read together, this literature converges on three largely independent quantitative channels, each tied to a different biophysical property of the pulp:

1. contrast-enhanced signal intensity and dynamic time-intensity curves, sensitive to pulpal blood perfusion;
2. T2 relaxation time, sensitive to tissue water content and microstructural organization;
3. apparent diffusion coefficient, sensitive to the restriction of water molecular motion by cellular and matrix structure.

Each channel has, at least in a single-center setting, been validated against an accepted external reference — electric pulp testing, ICDAS caries grading, or direct histology — which is a stronger evidentiary position than exists for most other proposed nontraditional vitality-assessment methods (Afkhami et al., 2024). A comprehensive review of the wider dental MRI literature situates this pulp-specific quantitative work within the broader growth of MRI applications across dentistry, from caries detection to implant planning (Han et al., 2025), underscoring that pulp vitality quantification is one strand, albeit a clinically central one, within a fast-growing field.

Table 1 Representative Quantitative MRI Biomarkers Investigated in Dental Pulp Imaging

Biomarker / Technique	**Reported Metric**	**Key Finding**	**Representative Study**
Contrast-enhanced signal intensity	Pre-/post-contrast T1 signal difference	Distinguishes vital vs. avital teeth; plain T1/T2 alone not significant	Kress et al. (2004)

Dynamic contrast-enhanced time-intensity curve (TIC)	TIC pattern classification	Differentiates vital/non-vital teeth with accuracy comparable to electric pulp testing	Yomtako et al. (2026)
T2 relaxometry	Mean pulp T2 (ms)	Decreases with increasing ICDAS score (≈166 ms sound → ≈115 ms severe)	Cankar et al. (2020)
T2 relaxometry + histology	Mean T2 and T2 variability	Lower T2 / variability associated with histologically confirmed pulp degeneration	Tenyi et al. (2024)
Apparent diffusion coefficient (ADC) mapping	ADC ($\times 10^{-9}$ m^2/s)	Affected pulp ADC < ≈1.0; correlates with demineralization depth and ICDAS	Vidmar et al. (2012)
High-resolution diffusion-weighted imaging (in vivo)	Normative pulp ADC	Feasible in vivo at 3 T; ADC stable across tooth and jaw type	Sittinger et al. (2025)
Signal intensity (cell-based regeneration)	SI relative to contralateral pulp over time	SI changes after stem-cell transplantation paralleled histological maturation	Iohara et al. (2016)
Signal intensity (regenerative endodontic outcome)	SI vs. contralateral control tooth	Vital pulp-like tissue regenerated regardless of apical preparation size	El-Kateb et al. (2020)

Imaging-Based Monitoring in Vital Pulp Therapy

Vital pulp therapy comprises a graded set of procedures intended to preserve some or all of an already-vital pulp when it has been exposed, or nearly exposed, by caries or trauma:

- indirect pulp treatment, leaving a thin layer of soft, demineralized dentin over an intact pulp;

- direct pulp capping, placing a biocompatible material directly over a small mechanical or carious exposure;
- partial pulpotomy, removing only the superficially inflamed coronal pulp tissue beneath an exposure;
- full pulpotomy, removing the entire coronal pulp while preserving the radicular pulp.

The American Academy of Pediatric Dentistry's first clinical practice guideline devoted specifically to permanent-tooth VPT, based on a systematic review of literature through mid-2024 and graded using the GRADE framework, recommends any of these four procedures — using a calcium silicate-based cement — for teeth with deep caries diagnosed with a normal pulp or reversible pulpitis, provided hemostasis can be achieved (American Academy of Pediatric Dentistry, 2025). The companion systematic review and meta-analysis underlying that guideline found 24-month success rates of 91–97% across indirect pulp treatment, direct pulp capping, partial pulpotomy, and full pulpotomy in such teeth, with no statistically significant difference between techniques, and no significant difference between indirect pulp treatment and direct pulp capping even at 36 months when calcium silicate cement was used for the latter (Coll et al., 2025).

What is notably absent from this evidence base is any routine quantitative imaging endpoint. Outcome in VPT trials is still defined, essentially, by the absence of pain or infection signs together with radiographic absence of periapical pathology — an endpoint that is reliable but slow, since a failing pulp may remain radiographically silent for months, and that says nothing directly about the physiological state of the pulp tissue that has been left in place. This is exactly the gap that the quantitative MRI literature reviewed above was not designed to fill, but plausibly could: if dynamic contrast-enhanced time-intensity curves can already separate vital from non-

vital teeth with accuracy comparable to electric pulp testing (Yomtako et al., 2026), and if T2 relaxometry can grade pulp response to caries on a continuous scale that correlates with histological degeneration (Cankar et al., 2020; Tenyi et al., 2024), then in principle the same measurements could be repeated on a treated tooth over time and compared against its own baseline or against the contralateral control tooth, offering an earlier and more graded signal of an at-risk pulp than waiting for symptoms or radiolucency to appear. It is important to be explicit, however, that this specific application — quantitative MRI as a longitudinal monitoring tool after vital pulp therapy — remains an extrapolation from the vitality-classification and caries-response literature reviewed above rather than an established body of VPT outcome studies in its own right; no study identified here has yet reported quantitative MRI follow-up of a VPT-treated cohort against the reference standards used in the trials synthesized by Coll et al. (2025). It represents, at present, a translational opportunity rather than a validated clinical tool.

Imaging in Regenerative Endodontics: Revascularization and the Question of Tissue Identity

Regenerative endodontic procedures (REPs) trace their conceptual origin to mid-twentieth-century observations that a blood clot induced in the apical portion of a cleaned and disinfected canal could support the ingrowth of new, vascularized tissue; this was refined into a named “revascularization” procedure applied to a necrotic immature premolar in the early 2000s, and subsequently formalized as a disinfection-then-blood-clot protocol using sodium hypochlorite and chlorhexidine irrigation followed by a multi-antibiotic intracanal medicament. The primary original indication was the immature, necrotic permanent tooth, where continued root maturation — thickening canal walls and apical closure — served as the principal radiographic marker of success; more recently,

comparable cell-homing-based protocols have been applied experimentally to mature teeth with fully formed roots and periapical lesions, where root maturation is not a relevant endpoint and some other measure of pulp-like tissue formation is required instead (El-Kateb et al., 2020).

MRI has been used in exactly this role — as a direct, noninvasive readout of intracanal tissue formation — in both cell-transplantation and cell-homing regenerative paradigms. In a stem-cell-transplantation context, Iohara et al. (2016) tracked the MR signal intensity of pulp-like tissue regenerated after mobilized dental pulp stem cell (MDPSC) therapy and reported that its evolution toward, and eventual convergence with, the signal intensity of normal contralateral pulp was consistent with the histological findings in the same cases, an early demonstration that a purely imaging-based signal could track a biologically meaningful regenerative process over time. The subsequent pilot clinical study of autologous MDPSC transplantation in five patients with irreversible pulpitis, monitored for up to 24 weeks, reported no adverse events and a robust positive electric-pulp-test response as early as four weeks post-transplantation, with imaging used alongside clinical and laboratory measures to corroborate regeneration (Nakashima et al., 2017).

In the more common cell-homing paradigm — blood-clot-based REPs performed without exogenous cell transplantation — El-Kateb et al. (2020) used MRI signal intensity, measured at the middle and apical thirds of the canal at 3, 6, and 12 months and compared against the contralateral normal tooth, to quantitatively assess intracanal tissue regeneration in mature necrotic anterior teeth randomized to two different apical-preparation sizes; the regenerated tissue's signal intensity converged toward that of the normal contralateral pulp in both groups, independent of apical preparation size, and the authors concluded that MRI could assess this

regeneration in a quantitative, noninvasive manner. A related retrospective cohort from the same research group subsequently correlated post-REP MRI signal intensity directly with cold and electric pulp-test responses in the same class of mature necrotic teeth, adding a second, independent line of convergent evidence for the same imaging signal (El-Kateb et al., 2024).

This body of work, however, sits alongside a persistent and important caveat about what, exactly, quantitative imaging in this context is measuring. Histological studies of tissue actually retrieved from canals after cell-homing-based revascularization have repeatedly found that the new intracanal tissue frequently resembles cementum, periodontal-ligament, or bone rather than a genuine, odontoblast-lined dentin-pulp complex, a pattern attributed to the likely recruitment of periodontal-ligament and perivascular stem cells into the canal rather than of true dental-pulp progenitors (Yang et al., 2016). A directly imaging-and-histology-paired case illustrates the point with unusual clarity: in an autotransplanted mature molar, contrast-enhanced MRI demonstrated clear pulp revascularization only four weeks after surgery — a genuine, quantifiable positive imaging signal — yet histological examination of the same tooth after its later extraction, necessitated by unrelated external cervical root resorption, found uninflamed fibrovascular connective tissue with neither odontoblasts nor cementoblast-like cells, most consistent with a bone-marrow- or periodontal-ligament-derived regenerate rather than true pulp (Rugani et al., 2023).

The implication for this chapter's central theme is a genuinely important limitation rather than a minor technical caveat: a positive, reproducible, and even quantitatively graded MRI signal after a regenerative endodontic procedure is currently good evidence that some vascularized, perfused, and probably viable tissue has formed in the canal — but it is not, by itself, evidence that this tissue is a functionally and histologically faithful dental pulp. Closing that

specific gap will require more of the kind of paired imaging–histology correlation exemplified by Rugani et al. (2023) and by the earlier stem-cell work of Iohara et al. (2016), applied across a wider range of regenerative protocols and patient populations than currently exists.

Limitations, Artifacts, and the Need for Standardization

Several limitations recur across the studies reviewed above, and are worth stating plainly rather than leaving implicit. First, there is a basic field-strength and hardware tradeoff: low-field, dental-dedicated systems purpose-built for office-based feasibility, such as the 0.55 T system evaluated by Johannsen et al. (2026), sacrifice signal and resolution for shorter scan times and lower cost, and to date have only been evaluated in small, single-center feasibility cohorts; high-field, intraoral-coil-based research protocols achieve much finer resolution and support more demanding quantitative sequences (Ludwig et al., 2016; Özen et al., 2026; Sittinger et al., 2025), but remain confined to specialized research centers and have not been replicated across multiple independent sites using shared acquisition protocols.

Second, dental MRI as a whole remains susceptible to the ordinary practical constraints of imaging a small, mobile, and metal-rich anatomical region: motion of the jaw or tongue during longer acquisitions, susceptibility artifact near metallic restorations, and partial-volume averaging within regions of interest that may be only a few voxels across, all of which threaten the precision of any quantitative map derived from a clinical, rather than a carefully positioned volunteer or ex vivo, examination (Han et al., 2025).

Third, and perhaps most consequentially for the field's near-term development, dental pulp imaging has not yet reached the stage of cross-vendor, cross-site standardization that other, more mature quantitative MRI biomarkers have achieved. The Quantitative

Imaging Biomarkers Alliance's own published profiles exist precisely because a given quantitative value is not automatically comparable across different scanners, sequences, and sites without explicit, tested acquisition and processing constraints (Radiological Society of North America, 2021). No equivalent profile yet exists for pulp T2 mapping, contrast-enhanced time-intensity curve classification, or pulp ADC; the normative values reported in this chapter — a coronal pulp T2 around 166 ms in sound teeth (Cankar et al., 2020), or a pulp ADC threshold near 1.0×10^{-9} m²/s separating affected from intact tissue (Vidmar et al., 2012) — were generated on specific scanners, field strengths, and sequences and should not yet be assumed to transfer directly to another center's equipment without local validation. Multicenter studies using harmonized acquisition protocols, ideally developed with the same profile-based methodology QIBA has applied elsewhere, represent a precondition for any of these biomarkers to move from a promising research finding to an accepted clinical or trial endpoint.

Artificial Intelligence, Radiomics, and Future Directions

Artificial intelligence applications in endodontic imaging have so far concentrated almost entirely on CBCT rather than MRI. Convolutional neural networks have been developed for automated segmentation of the pulp cavity and root canal system, detection of periapical radiolucent lesions, and classification of specific canal anatomies, and radiomic analysis — the extraction of texture, shape, and intensity features from three-dimensional CBCT data — has been proposed as a means of detecting sub-visual pathological change within the pulp cavity and surrounding tissue and of linking such image-derived features to treatment outcomes (Fontenele & Jacobs, 2025).

The natural extension of this trajectory is to apply comparable segmentation and radiomic pipelines to the quantitative

MRI maps discussed in this chapter — T2 maps, ADC maps, and DCE parameter maps of the pulp — potentially in combination with CBCT's superior spatial and hard-tissue detail, an approach that has not, to this chapter's knowledge, yet been reported in the pulp-imaging literature but that follows directly from developments already under way in both subfields separately.

Any such extension will have to reckon with limitations already flagged for CBCT-based AI and that would likely apply with at least equal force to MRI radiomics: current models are frequently trained and validated on comparatively small, single-center, and sometimes in vitro or ex vivo datasets that do not fully replicate the variability of a real clinical population, raising open questions about generalizability, and broader concerns about data governance and privacy remain unresolved as imaging datasets of this kind move toward multicenter sharing (Fontenele & Jacobs, 2025). Given that the dental-pulp quantitative MRI literature reviewed in this chapter is, if anything, smaller and more heterogeneous in acquisition protocol than the CBCT literature these AI limitations were identified in, any future radiomic application to pulp MRI should be expected to face these constraints from an even earlier starting point.

Conclusion

Magnetic resonance imaging offers something that periapical radiography and CBCT cannot: a direct, radiation-free view of the dental pulp as living, vascularized connective tissue, rather than an inference drawn from the surrounding mineralized structures. Over roughly two decades, that direct view has progressively been converted from a qualitative image into a set of quantitative, numerically defined biomarkers — perfusion-sensitive contrast-enhanced signal and time-intensity curves, T2 relaxometry, and apparent diffusion coefficient mapping — each independently linked, at least within single-center studies, to an accepted external

reference standard such as electric pulp testing, caries severity grading, or direct histology.

The evidentiary gap that remains is less about proof of concept, which now exists in some form across both vital-pulp-therapy-adjacent vitality assessment and regenerative-endodontic tissue-formation monitoring, and more about translation: standardized, multicenter acquisition and processing protocols of the kind the Quantitative Imaging Biomarkers Alliance has already modeled for other organ systems; direct imaging–histology validation of what a given quantitative signal actually represents, which matters especially acutely in regenerative endodontics given the documented tendency of "regenerated" intracanal tissue to be cementum-, periodontal-ligament-, or bone-like rather than true pulp; and integration with the artificial intelligence and radiomic pipelines already emerging around CBCT elsewhere in endodontic imaging. Addressing these three translational gaps, rather than generating further isolated proof-of-concept studies, is likely to determine how much of the promise surveyed in this chapter is ultimately realized in everyday clinical practice.

References

Afkhami, F., Wright, P. P., Chien, P. Y., Xu, C., Walsh, L. J., & Peters, O. A. (2024). Exploring approaches to pulp vitality assessment: A scoping review of nontraditional methods. *International Endodontic Journal*, 57(9), 1065–1098. https://doi.org/10.1111/iej.14073

American Academy of Pediatric Dentistry. (2025). Guideline for use of vital pulp therapy in permanent teeth. *Pediatric Dentistry*, 47(5), 299–311.

Cankar, K., Vidmar, J., Nemeth, L., & Serša, I. (2020). T2 mapping as a tool for assessment of dental pulp response to caries progression: An in vivo MRI study. *Caries Research*, 54(1), 24–35. https://doi.org/10.1159/000501901

Coll, J. A., Dhar, V., Guelmann, M., Crystal, Y. O., Chen, C.-Y., Marghalani, A. A., AlShamali, S., Xu, Z., Glickman, G., Ather, A., Sabeti, M., & Wedeward, R. (2025). Vital pulp therapy in permanent teeth: A systematic review and meta-analyses. *Pediatric Dentistry*, 47(3), 137–150.

El-Kateb, N. M., El-Backly, R. N., Amin, W. M., & Abdalla, A. M. (2020). Quantitative assessment of intracanal regenerated tissues after regenerative endodontic procedures in mature teeth using magnetic resonance imaging: A randomized controlled clinical trial. *Journal of Endodontics*, 46(5), 563–574.

El-Kateb, N. M., Abdallah, A. M., & ElBackly, R. N. (2024). Correlation between pulp sensibility and magnetic resonance signal intensity following regenerative endodontic procedures in mature necrotic teeth: A

retrospective cohort study. *BMC Oral Health, 24*, Article 330. https://doi.org/10.1186/s12903-024-04095-y

Fontenele, R. C., & Jacobs, R. (2025). Unveiling the power of artificial intelligence for image-based diagnosis and treatment in endodontics: An ally or adversary? *International Endodontic Journal*, 58(2), 155–170. https://doi.org/10.1111/iej.14163

Han, B., Chen, N., Luo, J., Afkhami, F., Peters, O. A., & Wang, X. (2025). Magnetic resonance imaging for dental pulp assessment: A comprehensive review. *Journal of Magnetic Resonance Imaging*, 62(2), 362–388. https://doi.org/10.1002/jmri.29742

Iohara, K., Fujita, M., Ariji, Y., Yoshikawa, M., Watanabe, H., Takashima, A., & Nakashima, M. (2016). Assessment of pulp regeneration induced by stem cell therapy by magnetic resonance imaging. *Journal of Endodontics*, 42(3), 397–401. https://doi.org/10.1016/j.joen.2015.11.021

Johannsen, K., Christensen, J., & Kirkevang, L. (2026). Dedicated MRI in the assessment of pulp vitality and apical periodontitis: A feasibility study. *International Endodontic Journal*, 59, 776–787. https://doi.org/10.1111/iej.70101

Juerchott, A., Pfefferle, T., Flechtenmacher, C., Mente, J., Bendszus, M., Heiland, S., et al. (2018). Differentiation of periapical granulomas and cysts by using dental MRI: A pilot study. *International Journal of Oral Science, 10*, Article 17. https://doi.org/10.1038/s41368-018-0017-y

Juerchott, A., Jelinek, C., Kronsteiner, D., Jende, J. M. E., Kurz, F. T., Bendszus, M., et al. (2022). Quantitative assessment of contrast-enhancement patterns of the healthy dental pulp by magnetic resonance imaging: A prospective in vivo study.

International Endodontic Journal, 55(3), 252–262. https://doi.org/10.1111/iej.13662

Kress, B., Buhl, Y., Anders, L., Stippich, C., Palm, F., Bähren, W., et al. (2004). Quantitative analysis of MRI signal intensity as a tool for evaluating tooth pulp vitality. *Dentomaxillofacial Radiology*, 33(4), 241–244. https://doi.org/10.1259/dmfr/33063878

Kress, B., Buhl, Y., Hähnel, S., Eggers, G., Sartor, K., & Schmitter, M. (2007). Age- and tooth-related pulp cavity signal intensity changes in healthy teeth: A comparative magnetic resonance imaging analysis. *Oral Surgery, Oral Medicine, Oral Pathology, Oral Radiology, and Endodontology*, 103(1), 134–137.

Ludwig, U., Eisenbeiss, A.-K., Scheifele, C., Nelson, K., Bock, M., Hennig, J., von Elverfeldt, D., Herdt, O., Flügge, T., & Hövener, J.-B. (2016). Dental MRI using wireless intraoral coils. *Scientific Reports, 6*, Article 23301. https://doi.org/10.1038/srep23301

Nakashima, M., Iohara, K., Murakami, M., Nakamura, H., Sato, Y., Ariji, Y., & Matsushita, K. (2017). Pulp regeneration by transplantation of dental pulp stem cells in pulpitis: A pilot clinical study. *Stem Cell Research & Therapy, 8*, Article 61. https://doi.org/10.1186/s13287-017-0506-5

Özen, A. C., et al. (2026). Intraoral coil arrays for single-tooth dental MRI. *Magnetic Resonance in Medicine*. Advance online publication. https://doi.org/10.1002/mrm.70153

Radiological Society of North America. (2021). RSNA's Quantitative Imaging Biomarkers Alliance (QIBA) is transforming patient care through quantitative science.

RSNA News. https://www.rsna.org/news/2021/april/qiba-a-quantitative-success

Rugani, P., Brcic, I., Magyar, M., Schwarze, U. Y., Jakse, N., & Ebeleseder, K. (2023). Pulp revascularization in an autotransplanted mature tooth: Visualization with magnetic resonance imaging and histopathologic correlation. *Journal of Clinical Medicine, 12*(18), Article 6008. https://doi.org/10.3390/jcm12186008

Sittinger, M. A., Sandner, C., Zhou, K., Mente, J., Lauer, A., Özen, A. C., Vollherbst, D. F., Breckwoldt, M. O., Bendszus, M., Heiland, S., & Hilgenfeld, T. (2025). Feasibility of high-resolution diffusion-weighted imaging of the healthy dental pulp in humans using a hybrid TGSE BLADE sequence. *Scientific Reports, 15*. https://doi.org/10.1038/s41598-025-16272-2

Tenyi, A., Milutinović, A., Vidmar, J., Serša, I., & Cankar, K. (2024). Assessment of dental pulp response to caries via MR T2 mapping and histological analysis. *BMC Oral Health, 24*. https://doi.org/10.1186/s12903-024-04165-1

Vaddi, A., Parasher, P., & Khurana, S. (2025). Beyond X-rays: Unveiling the future of dental diagnosis with dental magnetic resonance imaging. *Diagnostics, 15*(9), Article 1153. https://doi.org/10.3390/diagnostics15091153

Vidmar, J., Cankar, K., Nemeth, L., & Serša, I. (2012). Assessment of the dentin-pulp complex response to caries by ADC mapping. *NMR in Biomedicine*, 25(9), 1056–1062. https://doi.org/10.1002/nbm.2770

Yang, J., Yuan, G., & Chen, Z. (2016). Pulp regeneration: Current approaches and future challenges. *Frontiers in Physiology, 7*, Article 58. https://doi.org/10.3389/fphys.2016.00058

Yomtako, S., Kume, S., Watanabe, H., Kuribayashi, A., Nakamura, S., Imaizumi, A., Tomisato, H., Nomura, Y., Taguchi, M., Oki, A., & Miura, M. (2026). Dynamic contrast-enhanced magnetic resonance imaging for distinguishing vital and non-vital teeth in jaw lesions: A pilot study. *Oral Surgery, Oral Medicine, Oral Pathology and Oral Radiology*, 141(2), 239–244. https://doi.org/10.1016/j.oooo.2025.09.019

CHAPTER 2

FROM PIXELS TO PHENOTYPES AND PROGNOSIS: RADIOMICS AND IMAGING BIOMARKERS OF APICAL PERIODONTITIS

Suay Yağmur ÜNAL[1]
Damla İLKGELEN[2]

Introduction

Apical periodontitis has traditionally been reduced, radiographically, to a binary question: whether a periapical radiolucency is present. This reduction is no longer regarded as sufficient. Contemporary literature supports a shift from simple lesion detection toward quantitative lesion phenotyping, in which lesion volume, shape, cortical interaction, internal heterogeneity, and peri-lesional bone response are treated as measurable imaging biomarkers. This shift has been enabled by cone-beam computed tomography (CBCT), volumetric segmentation and, more recently, CBCT-based texture analysis and radiomics.

The chapter title reflects an intended translational trajectory rather than an accomplished one. As is discussed throughout this chapter, most of the evidence currently available concerns lesion detection, volumetric phenotyping, and diagnostic characterization;

[1] Dr. Öğr. Üyesi, Nişantaşı Üniversitesi Diş Hekimliği Fakültesi Ağız Diş Ve Çene Radyolojisi İstanbul/Türkiye, Orcid: 0000-0002-8559-7461
[2] Dr. Öğr. Üyesi, Nişantaşı Üniversitesi Diş Hekimliği Fakültesi Endodonti Anabilim Dalı İstanbul/Türkiye, Orcid: 0000-0003-1619-173X

genuinely prognostic, externally validated models remain aspirational. Where texture-based prognostic signals have been reported, they are best regarded as early proof-of-concept findings rather than clinically deployable predictors.

The field remains methodologically immature. Studies published through early 2026 are predominantly single-center, retrospective, and modest in scale, and true external validation has not been demonstrated for any of the apical-periodontitis-specific radiomics studies reviewed here. Periapical radiographs remain the first-line imaging modality because of accessibility and lower radiation dose, and the European Society of Endodontology, together with the American Association of Endodontists and the American Academy of Oral and Maxillofacial Radiology, have consistently maintained that CBCT use should be justified by an anticipated diagnostic benefit rather than applied routinely. (Patel et al., 2019; Sousa Melo et al., 2026) Even so, CBCT has repeatedly demonstrated higher sensitivity for lesion detection than periapical radiography, particularly for small lesions, lesions masked by anatomic superimposition, or lesions confined to cancellous bone, as shown in a histopathology-correlated study and corroborated by pooled meta-analytic estimates. (Abesi & Golikani, 2023; de Paula-Silva et al., 2009)

The transition from indices to phenotypes has already begun. Only a moderate relationship has been reported between two-dimensional periapical index scores and true three-dimensional lesion volume, with roughly one-third of index variance explained by volume, indicating that conventional scoring captures lesion burden incompletely. (Maia Filho et al., 2018) Subsequent development of a CBCT-based volumetric periapical index, followed by studies of lesion sphericity and peri-lesional radiodensity gradients, has shown that lesion morphology and the surrounding osseous response are not adequately summarized by maximum diameter alone. A 2024 study extended this framework by

demonstrating significant differences in first-order, texture, and shape features across lesions stratified by volumetric size, cortical erosion, and overall shape. (Lozano González et al., 2024)

The strongest proof-of-concept evidence for lesion characterization has come from cyst-granuloma discrimination studies. In 2020, biopsy-confirmed lesions were shown to be distinguishable, at least in part, by CBCT texture features. (de Rosa et al., 2020) In 2026, this direction was extended using volumetric segmentation, 48 radiomic features, and a hybrid deep-learning model, with accuracy, sensitivity, and precision figures around 90% reported for differentiating radicular cysts from apical granulomas in histologically verified cases. (Çetin et al., 2026) These findings suggest that radiomics can move beyond "is a lesion present" toward "what kind of lesion is this," although the evidence remains confined to small, single-center datasets, and periapical scar tissue is essentially unstudied within this framework.

The prognostic literature is conceptually the most important strand, yet it is also the least mature. Conventional volumetric studies indicate that larger lesions, older age, cortical defects, and greater preoperative bone loss are associated with slower or less complete healing after nonsurgical treatment. More novel work suggests that early texture change may precede visually obvious radiographic healing: in a 2025 study, CBCT texture parameters differed significantly between two intracanal medication groups at only three months, suggesting that microstructural reorganization can be quantified before gross radiographic resolution becomes evident. (Lopes et al., 2025) This finding is clinically interesting, but it has not been validated against long-term healing endpoints or multicenter cohorts, and it should not be read as evidence of a working prognostic model.

The principal barriers to clinical translation are technical rather than conceptual. Radiomic features are highly sensitive to segmentation choices, voxel geometry, gray-level discretization,

preprocessing, scanner variability, and reconstruction settings. CBCT gray values are not standardized as Hounsfield units, and recent methodological work indicates that CBCT-derived attenuation values should, at most, be treated as relative indicators under tightly standardized acquisition conditions rather than as portable quantitative biomarkers. (Eguren et al., 2022) Failure to nest feature selection within cross-validation can additionally produce materially inflated performance estimates. For apical-periodontitis radiomics to become clinically credible, multicenter prospective studies, histologic co-measurement, harmonized acquisition and preprocessing, external validation, and explicit adherence to reporting standards such as the Image Biomarker Standardisation Initiative and the CheckList for EvaluAtion of Radiomics research will be required. (Koçak et al., 2023; Zwanenburg et al., 2020)

Conventional quantitative imaging biomarkers

These are directly interpretable geometric or densitometric measurements — lesion volume, maximum diameter, sphericity, elongation, flatness, and peri-lesional radiodensity — obtained from segmented CBCT volumes without the large-scale feature extraction characteristic of radiomics. The CBCT-based volumetric periapical index and the sphericity and radiodensity studies discussed in "Classical Radiographic Evaluation and the Shift to Three-Dimensional Phenotypes" belong to this category. (Boubaris et al., 2021; Boubaris et al., 2022; Boubaris et al., 2024) These measures are comparatively easy to interpret clinically, but their reliability still depends entirely on segmentation quality.

Handcrafted radiomics

This category comprises the systematic, often high-dimensional extraction of first-order, shape, and texture features (for example, gray-level co-occurrence matrix or gray-level run-length

matrix features) from a defined region or volume of interest, typically followed by statistical comparison or classical machine-learning classification. The cyst-granuloma discrimination studies and the healing-texture study discussed in "Radiomics for Lesion Characterization and Biological Interpretation" and "Treatment Response, Bone Healing Prediction, and Multimodal Integration" fall into this category. (Çetin et al., 2026; de Rosa et al., 2020; Lopes et al., 2025; Lozano González et al., 2024)

AI- and deep-learning-based image analysis

This category includes convolutional neural network-based lesion detection and segmentation models, which learn image representations directly rather than relying on predefined feature families. The nnU-Net-based segmentation work and CNN-based detection study discussed in "Segmentation variability and data leakage" below belong here. (Hadzic et al., 2024; Öksüzoğlu et al., 2026) These models can incorporate handcrafted radiomic features as auxiliary inputs (hybrid models), which is the case for at least one of the diagnostic studies discussed below. (Çetin et al., 2026)

These three categories share a common methodological vulnerability — dependence on consistent, well-documented segmentation and acquisition — but they differ in interpretability, sample-size requirements, and validation practice. Throughout this chapter, the specific category is named wherever it affects how a finding should be interpreted, and the term "radiomics" is used only for categories (ii) and (iii); category (i) is referred to as a conventional or volumetric imaging biomarker.

Classical Radiographic Evaluation and the Shift to Three-Dimensional Phenotypes

Periapical radiography remains the standard entry point for diagnosing and monitoring apical periodontitis, favored for its

accessibility and low radiation dose. Its principal limitation is structural: a three-dimensional inflammatory process is collapsed into a two-dimensional projection, which is subject to magnification, superimposition, cortical masking, and angulation error. This limitation has long been recognized by professional societies. Both the European Society of Endodontology position statement and the joint statement of the American Association of Endodontists and the American Academy of Oral and Maxillofacial Radiology maintain that CBCT should not be used indiscriminately, while acknowledging that three-dimensional imaging may be justified when conventional imaging cannot answer a clinically relevant question. (Patel et al., 2019; Sousa Melo et al., 2026) An updated joint position statement was published in January 2026, reaffirming this selective-use principle and placing continued emphasis on clinician training in CBCT interpretation. (Sousa Melo et al., 2026)

CBCT generally demonstrates higher lesion-detection sensitivity than conventional radiography under appropriate clinical conditions, although the magnitude of the difference depends on study design and reference standard. In a histopathology-correlated study, periapical radiography detected apical periodontitis in 71% of roots, compared with 84% for CBCT, corresponding to sensitivities of 0.77 and 0.91, respectively; specificity was 1.00 for both methods, but the negative predictive value of radiography was poor. (de Paula-Silva et al., 2009) A subsequent meta-analysis reported pooled sensitivity and specificity of approximately 95% and 90% for CBCT, again substantially exceeding digital periapical radiography. (Abesi & Golikani, 2023) Because diagnostic accuracy alone does not establish clinical utility, professional guidance has consistently favored selective rather than routine CBCT use.

This inadequacy of two-dimensional scoring is precisely what motivated the shift toward volumetric phenotypes. The classical two-dimensional periapical index remains clinically useful but relates only moderately to true lesion burden. In a study of 35

single-rooted teeth, a positive but moderate correlation was reported between the periapical index and CBCT-derived lesion volume, with a Spearman correlation coefficient of approximately 0.60 ($r^2 \approx 0.36$), meaning that only around one-third of the variance in the index reflected volumetric variation. (Maia Filho et al., 2018) In practical terms, lesions that appear similar by a two-dimensional score can differ materially in three-dimensional extent.

Volumetric refinements followed directly from this inadequacy. The CBCT periapical index, (Estrela et al., 2008) which is essentially diameter-based, was shown to contain substantial within-category volumetric heterogeneity, particularly for intermediate and larger lesions, indicating that it performs poorly as a surrogate for true lesion size; a volume-based index (CBCTPAVI) was proposed to address this limitation. (Boubaris et al., 2021) Subsequent work reported that periapical lesions with larger volume-index scores were, on average, less spherical, suggesting that lesion growth reflects directional remodeling shaped by local anatomy and cortical constraints rather than isotropic expansion alone. (Boubaris et al., 2022) A further study of peri-lesional radiodensity reported that bone radiodensity increased significantly up to 1.0 mm around lesion borders, and that larger lesions displayed greater radiodensity gradients between lesion core, border, and adjacent bone — an observation consistent with inflammatory biology, although direct histologic-radiomic pairing remains sparse. (Boubaris et al., 2024)

A 2024 study made this conceptual transition explicit. (Lozano González et al., 2024) One hundred small-field-of-view scans were analyzed following lesion classification by volume, cortical expansion, cortical erosion, and regular versus irregular shape. Significant differences were found in energy, total energy, neighboring gray-tone difference matrix contrast, gray-level co-occurrence matrix contrast, sphericity, elongation, and flatness according to lesion size, erosion, and overall shape, whereas cortical expansion showed no significant radiomic differences. This study is

notable for treating apical periodontitis not as a binary present/absent finding but as a family of measurable three-dimensional phenotypes.

The major diagnostic and phenotyping studies underpinning this shift are summarized in **Table 1**. The external-validation column reflects a synthesis of the primary reports by the present authors and should be read as a reviewer's judgment rather than as a verbatim statement by the original investigators.

Segmentation, Standardization, ROI Definition, and Feature Families

A radiomics pipeline in apical periodontitis is only as reliable as its least stable preprocessing step. In small dental datasets, differences in region-of-interest definition, volume cropping, gray-level discretization, voxel spacing, and preprocessing choices can alter extracted features as much as, or more than, the underlying biology does. For this reason, standardization has become a central theme in the general radiomics literature, and the apical-periodontitis-specific literature should be judged against the same criteria. The CheckList for EvaluAtion of Radiomics research (CLEAR) specifies 58 reporting items for radiomics research, and European Society of Radiology practice recommendations emphasize explicit reporting of discretization strategy, voxel resampling, and validation procedure. (Koçak et al., 2023; Santinha et al., 2025) The European Society of Radiology/European Organisation for Research and Treatment of Cancer consensus on lesion segmentation similarly treats lesion definition and segmentation policy as core determinants of biomarker validity rather than as minor technical details. (deSouza et al., 2022)

The Image Biomarker Standardisation Initiative (IBSI) remains central to this discussion because it formalized feature definitions, benchmark values, and standardization principles for quantitative image biomarkers. (Zwanenburg et al., 2020) Its relevance to dental radiomics is indirect but fundamental: a texture

feature that is not stably defined or reproducibly computed cannot function as a biomarker, regardless of how promising it appears in a single dataset.

Segmentation in apical-periodontitis studies has generally followed one of two strategies. The first is **slice-based ROI analysis**, in which a representative two-dimensional section is selected and texture is measured within a manually or semi-automatically defined region; this approach was used both in the earliest cyst-granuloma texture study, which selected the most representative sagittal view of each lesion, and in the short-term healing study, which used a circular two-dimensional region of interest centered within the lesion. (de Rosa et al., 2020; Lopes et al., 2025) Slice-based approaches are comparatively simple and less labor-intensive, but they discard through-plane heterogeneity and remain sensitive to observer choice of the "representative" slice.

The second strategy is **volume-based segmentation**, which better reflects the biological reality of a three-dimensional lesion. Semi-automatic segmentation in dedicated three-dimensional modeling software was used for CBCTPAVI development, and a 2024 radiomics study used a semi-automatic "grow from seeds" tool after voxel resampling to segment both the lesion and surrounding bone. (Boubaris et al., 2021; Lozano González et al., 2024) A comparable semi-automatic three-dimensional workflow was used for a 2026 cyst-granuloma differentiation study prior to feature extraction and model development. (Çetin et al., 2026) Although volumetric segmentation is methodologically preferable for phenotype analysis, it is more sensitive to boundary ambiguity and interobserver variability than slice-based methods.

The standardization problem is especially acute for CBCT because image intensity is not equivalent to standard CT attenuation. A systematic review concluded that CBCT gray values cannot simply be converted into Hounsfield units, largely because the available primary literature on this question remains too limited and

heterogeneous to support a validated conversion. (Eguren et al., 2022) A subsequent 2026 methodological study reinforced this position, indicating that CBCT gray values may function as **relative local indicators of attenuation** under a standardized acquisition and reconstruction protocol, but should not be treated as robust absolute quantitative biomarkers across different devices and protocols. (Wieczorek et al., 2026) Intensity-based radiomic features may therefore provide useful discriminatory information within a single apical-periodontitis study, while their generalizability across imaging systems cannot presently be assumed.

Radiomic features investigated in apical-periodontitis studies can broadly be grouped as **first-order**, **shape**, and **texture** features. First-order features describe the distribution of gray-level values without incorporating spatial relationships; among these, energy, entropy, total energy, and uniformity have been evaluated most frequently. In the 2024 study noted above, energy-related features were associated with lesion volume and erosion, indicating that both the magnitude and distribution of gray-level values may vary with lesion extent and its interaction with surrounding bone. (Lozano González et al., 2024)

Shape features describe the geometric characteristics of a segmented lesion — sphericity, elongation, flatness, and mesh volume have received particular attention. An inverse association between lesion size and sphericity was reported in the sphericity study, while the 2024 study identified significant differences in elongation and flatness between lesions of regular and irregular morphology. (Boubaris et al., 2022; Lozano González et al., 2024) Compared with many texture parameters, shape features are typically more readily interpreted in anatomical and clinical terms, although their reliability remains directly dependent on segmentation accuracy and reproducibility.

Texture features characterize the spatial distribution and relationships of gray-level values within a lesion. Most apical-

periodontitis studies have focused on gray-level co-occurrence matrix features, although gray-level run-length matrix, gray-level size-zone matrix, gray-level dependence matrix, and neighboring gray-tone difference matrix features have also been evaluated. In the earliest cyst-granuloma texture study, angular second moment, sum of squares, sum average, contrast, and correlation were among the parameters associated with lesion differentiation. (de Rosa et al., 2020) In the 2025 healing study, gray-level co-occurrence matrix-derived features including inverse difference moment, difference entropy, and difference variance were examined. (Lopes et al., 2025) In the 2026 cyst-granuloma study, the feature set was expanded to include first-order, shape, and several texture-matrix families, providing a more comprehensive radiomic characterization. (Çetin et al., 2026)

Biological interpretation of these features should nevertheless remain cautious. A low texture-entropy value, for example, cannot be considered a specific imaging marker of a cyst; rather, such measurements indicate differences in the spatial organization of gray-level variation under defined acquisition, reconstruction, and preprocessing conditions. Differences in fluid content, inflammatory or fibrous tissue composition, epithelial organization, reactive sclerosis, and immature reparative bone could plausibly contribute to the observed texture patterns, but in the absence of systematic correlation with histopathologic findings, these associations remain hypotheses rather than established biological correlates.

Radiomics for Lesion Characterization and Biological Interpretation

Among diagnostic applications of apical-periodontitis radiomics, differentiation between radicular cysts and apical granulomas has received the greatest attention. Throughout this chapter, the terms **radicular cyst** (synonymous with periapical cyst)

and **apical granuloma** (synonymous with periapical granuloma) are used consistently to refer to the two principal histopathologic categories; the term **periapical scar** is reserved for the separate, non-inflammatory fibrous-healing entity discussed below. This distinction may be clinically relevant because differences in lesion pathology can influence healing after treatment: pocket cysts may resolve following nonsurgical root canal treatment, whereas true radicular cysts may be less likely to heal without surgical intervention. (Nair, 1998) Histopathologic heterogeneity among periapical lesions has long been recognized; in a review of 1,108 specimens, granulomas were identified more frequently than cysts, while periapical scars accounted for a smaller but clinically relevant proportion of lesions. (Stockdale & Chandler, 1988)

One of the earliest CBCT texture-analysis studies addressing this distinction evaluated 19 patients with 25 biopsy-confirmed lesions, comprising 14 radicular cysts and 11 apical granulomas. (de Rosa et al., 2020) Eleven texture parameters were calculated from intralesional regions of interest, of which five demonstrated predictive value for lesion differentiation across the eight lesion positions analyzed. Detailed acquisition parameters and complete diagnostic-performance measures were **not reported in the accessible version of this article**, so the finding is presented here as a proof-of-concept signal rather than a validated diagnostic estimate; nonetheless, it suggested that quantitative differences in CBCT texture may be present between histologically distinct periapical lesions.

A larger, histologically validated dataset was evaluated in a 2026 study of 98 patients, with lesions segmented volumetrically. (Çetin et al., 2026) Forty-eight radiomic features spanning first-order, shape, and several texture categories were extracted; 34 features showed high interobserver reliability (intraclass correlation coefficient ≥ 0.80), and 18 differed significantly between radicular cysts and apical granulomas. The proposed hybrid deep-learning

model achieved reported accuracy of 90%, sensitivity of 90%, and precision of 91.3%, and was reported to outperform the conventional machine-learning models included in the comparison. External validation was not reported, and calibration measures were not available; these limitations should be weighed carefully when interpreting the reported diagnostic performance, particularly given that internal cross-validation estimates in small, high-dimensional radiomics datasets are prone to optimistic bias (see "From statistical significance to biomarker validity").

Related evidence has also come from conventional intraoral radiography. In a study of 62 radiographs using histopathology as the reference standard, textural information obtained from lesion margins was reported to be more discriminative for cyst-granuloma differentiation than information derived from lesion interiors. (Pociask et al., 2021) Although this study did not use CBCT, its findings suggest that quantitative information from the lesion-bone interface may be relevant to lesion characterization, a conclusion broadly consistent with the CBCT-based radiodensity and morphology findings discussed in "Classical Radiographic Evaluation and the Shift to Three-Dimensional Phenotypes".

Evidence regarding the radiomic characterization of periapical scar tissue remains very limited. Periapical scars have been recognized histopathologically as a distinct entity, accounting for approximately 4.5% of cases in the series noted above. (Stockdale & Chandler, 1988) No apical-periodontitis radiomics study identified in this review directly evaluated a multiclass model capable of distinguishing granulomas, cysts, scars, and mixed lesions on CBCT. On the basis of currently available evidence, radiomic differentiation between cysts and granulomas appears feasible in small, histologically validated datasets, whereas radiomic identification of periapical scars remains essentially unexplored.

The biological significance of apical-periodontitis texture features also remains incompletely established. In the healing study,

differences in inverse difference moment and difference entropy were interpreted as reflecting variation in tissue organization during healing; the cyst-granuloma texture study similarly demonstrated differences in several texture parameters between lesions of distinct histopathologic diagnosis, and the radiodensity study reported changes in peri-lesional radiodensity according to lesion size. (Boubaris et al., 2024; de Rosa et al., 2020; Lopes et al., 2025) Collectively, these observations suggest that CBCT texture measurements may be influenced by several components of lesion and surrounding-bone architecture, including inflammatory tissue, fluid content, trabecular disruption, reactive sclerosis, and reparative bone formation. At present, however, individual radiomic features cannot be assigned reliably to a specific histologic or biological process, and claims that a given CBCT texture feature directly represents lesion "biological activity" should be regarded as hypotheses requiring further validation, not as established findings.

Treatment Response, Bone Healing Prediction, and Multimodal Integration

One of the potentially important clinical applications of imaging biomarkers in apical periodontitis is the assessment of treatment response and healing prognosis. Reliable prediction of healing could, in principle, allow follow-up schedules and retreatment decisions to be adapted to lesion characteristics and could assist in identifying cases in which surgical management should be considered. At present, however, the available evidence is insufficient to support routine prognostic use of CBCT-derived radiomic biomarkers; existing studies indicate only that quantitative imaging may provide additional information beyond conventional visual or binary assessment of post-treatment healing.

Conventional volumetric outcome studies already indicate that imaging biomarkers carry prognostic information. In a CBCT-based prospective cohort of large cyst-like periapical lesions, the

success rate of nonsurgical root canal treatment was 82.2%, with a median lesion-volume reduction of 75%; preoperative cortical bone defect and apical extent of obturation were identified as factors associated with less favorable osseous healing. (Saini et al., 2023) In a retrospective CBCT cohort, 60 of 79 lesions (76%) had healed completely at a mean of 19 months, with older age and larger areas of bone loss associated with longer healing times. (Mosquera-Barreiro et al., 2024) These are not radiomics studies in the narrow sense defined in Section 2, but they establish that lesion morphology and host context carry prognostic information that any future radiomic model would need to account for.

The strongest apical-periodontitis-specific attempt to quantify early repair using image texture is the 2025 study discussed above. (Lopes et al., 2025) Thirty-four single-rooted teeth with periapical lesions were allocated to one of two intracanal medications, and CBCT was obtained immediately after treatment and again at three months. Eleven gray-level co-occurrence matrix parameters were extracted from circular lesion regions of interest, and significant between-group differences were reported for inverse difference moment, difference variance, and difference entropy at the three-month time point. Because gross radiographic healing is often subtle at such an early interval, this study is important less for its therapeutic comparison than for the suggestion that microarchitectural reorganization may be measurable before conventional radiographic endpoints become apparent.

It would nonetheless be premature to conclude that post-treatment healing can already be predicted before it becomes clinically visible. This study measured early textural change; it did not establish a long-term, externally validated prognostic classifier linking those features to later treatment success or failure. What can be stated is the more modest claim that early textural change has become detectable, and that the temporal gap between microscopic repair and conventional radiographic resolution may eventually be

bridgeable with quantitative imaging. This is a meaningful conceptual step, but it is not yet a clinically deployable prognostic system, and framing it otherwise would overstate the current evidence.

An adjacent but informative line of work concerns lesions that are occult to two-dimensional imaging. Lesion diameter below 2 mm and molar involvement were reported as significant factors associated with lesions visible only on CBCT. (Jang et al., 2020) A related 2026 study analyzed 56 matched periapical-radiograph/CBCT pairs and 109 regions of interest, showing that radiomics extracted from intraoral radiographs can help distinguish regions that are CBCT-positive but radiographically negative from true negatives. (Obuchowicz et al., 2026) This does not directly address post-treatment prognosis, but it demonstrates that sub-visual image information exists and may be algorithmically recoverable before conventional human reading identifies a lesion.

The integration of clinical, biological, and imaging data remains the least developed, yet arguably the most important, frontier. Imaging cannot be interpreted in isolation from age, symptoms, restoration quality, root-filling quality, cortical status, systemic conditions, and lesion biology. One of the few studies to directly link preoperative CBCT-derived lesion volume to histopathologic inflammatory activity, measured with the Dental Apical Inflammation Score, evaluated a cohort of 153 patients and reported that lesion volume correlated with both inflammation-score category and histologic diagnosis. (Grün et al., 2025; Krenn et al., 2020) This finding is relevant because it suggests that imaging biomarkers may eventually be paired with a biologically grounded endpoint rather than with imaging alone.

Even so, truly multimodal apical-periodontitis models have not yet been established. No study identified in this review combined standardized radiomics, histopathology or molecular profiling, and long-term clinical healing outcomes within a single, prospectively

validated model. "Integration" is therefore presently better described as an agenda than an achievement: the field has the necessary ingredients — quantitative imaging, clinical predictors, and emerging histologic scoring — but not yet their credible synthesis.

The key studies on healing, occult-lesion detection, and biological correlation are summarized in **Table 2**, using the same evidence-synthesis conventions applied in Table 1.

Table 1. Lesion Detection, Volumetric Phenotyping, and Diagnostic Characterization Studies

Study	Design & Sample	Task	Segmentation Method	Internal Validation	External Validation	Key Reported Outcome
De Rosa et al., 2020	Retrospective; 19 patients, 25 biopsy-confirmed lesions (14 cysts, 11 granulomas)	Radicular cyst vs. apical granuloma differentiation	2D ROI on representative sagittal slice (slice-based)	Not reported*; no train/test split described	No	11 texture parameters extracted; 5 predictive across 8 lesion positions; exact AUCs not reported*
Boubaris et al., 2021	Retrospective; 273 lesions	Volumetric index development (CBCTPAVI)	Semi-automatic volumetric segmentation	Descriptive/comparative analysis (no classifier)	No	Large within-score volume variation in the diameter-based index; volume-based CBCTPAVI proposed
Boubaris et al., 2022	Retrospective; 261 lesions	Shape-biomarker development (sphericity)	Semi-automatic 3D segmentation	Descriptive/correlation analysis	No	Mean sphericity 62%; larger-volume lesions significantly less spherical
Boubaris et al., 2024	Retrospective; sample size not specified in accessible text*	Peri-lesional radiodensity characterization	Semi-automatic 3D segmentation	Descriptive/correlation analysis	No	Radiodensity increased significantly up to 1.0 mm from lesion border; larger lesions showed steeper radiodensity gradients
Lozano González et al., 2024	Retrospective; 100 small-FOV scans	Radiomic differences by lesion size, cortical erosion/expansion, and shape	Manual volumetry plus semi-automatic "grow from seeds" after voxel resampling; non-segmentable lesions excluded	Group-comparison statistics (no ML classifier)	No	Significant differences in energy, total energy, NGTDM/GLCM contrast, sphericity, elongation, flatness; cortical expansion not significant. Reported voxel size ("0.75 microns") is unverified—see "Acquisition and reconstruction parameters"
Çetin et al., 2026	Retrospective; 98 patients, histologically verified	Radicular cyst vs. apical granuloma (hybrid handcrafted + deep-learning model)	Semi-automatic 3D segmentation	48 features extracted, 34 retained at ICC ≥ 0.80; internal split method not specified in accessible text*	No	18 features significant; model accuracy 90%, sensitivity 90%, precision 91.3% (internal estimate—see "From statistical significance to biomarker validity")

Table 2. Healing, Occult-Lesion Detection, and Biological-Correlation Studies

Conventions.

Study	Design & Sample	Task	Segmentation Method	Internal Validation	External Validation	Key Reported Outcome
Jang et al., 2020	Design/sample not fully specified in accessible text*	Clinical predictors of lesions visible only on CBCT (occult lesions)	Not a segmentation/radiomics study	Regression analysis of clinical predictors	No	Lesion diameter < 2 mm and molar involvement significantly associated with CBCT-only visibility
Obuchowicz et al., 2026	Retrospective; 56 matched periapical-radiograph/CBCT pairs, 109 ROIs	Detect occult lesions (CBCT-positive, radiograph-negative) using radiomics from intraoral radiographs	Circular ROIs on intraoral radiographs; CBCT used as reference standard	Nested cross-validation (logistic regression)—explicitly reported	No	Radiomic features with logistic regression distinguished occult-positive from true-negative ROIs
Saini et al., 2023	Prospective cohort recall rate 88%	Outcome of nonsurgical treatment for large cyst-like lesions	Volumetric CBCT assessment (not radiomics)	Cohort follow-up analysis	No	Success rate 82.2%; median lesion-volume reduction 75%; cortical defect and obturation extent associated with less favorable healing
Mosquera-Barreiro et al., 2024	Retrospective; 79 cases	Predictors of healing time for large lesions	CBCT-based volumetric follow-up (not radiomics)	Cohort follow-up analysis	No	76% completely healed at a mean of 19 months; older age and greater bone-loss extent associated with longer healing time
Lopes et al., 2025	Prospective; 34 single-rooted teeth	Early healing quantification after two intracanal medications	Circular 2D ROI (slice-based); i-CAT Next Generation, 0.25 mm voxel, 6.0×16.0 cm FOV	Between-group statistical comparison (no ML classifier)	No	Significant 3-month differences in inverse difference moment, difference variance, and difference entropy between medication groups
Grün et al., 2025	Retrospective; 153 patients	Correlation of preoperative CBCT lesion volume with DAIS-scored inflammatory histology	Manually drawn segmentations	Correlation analysis	No	Lesion volume correlated with both DAIS category and histologic diagnosis

Technical Validity, Statistical Rigor, and Reproducibility

From statistical significance to biomarker validity

A recurring pattern in this literature is the reporting of p-values for individual radiomic features without an accompanying discussion of effect size, clinical relevance, or correction for multiple comparisons. A 2024 study, for example, reported feature-level differences for energy, total energy, several gray-level co-occurrence matrix and neighboring gray-tone difference matrix parameters, and shape descriptors, several of which reached conventional statistical significance (p values in the range of roughly 0.001–0.02) across lesion-size, erosion, and shape categories. (Lozano González et al., 2024) Statistical significance of this kind is a necessary but far from sufficient condition for a feature to function as a clinically useful biomarker. A feature can be statistically significant and still be clinically uninformative if its effect size is small, if its confidence interval is wide relative to the observed difference, if it does not survive correction for the dozens of features typically tested in a single radiomics study, if it is highly correlated (redundant) with other, more interpretable features, or if it lacks test-retest stability under repeated acquisition.

For apical-periodontitis radiomics to progress from exploratory feature comparison toward genuine biomarker development, future studies should report, at a minimum: effect sizes and confidence intervals alongside p-values; explicit correction for multiple testing when many features are compared; assessment of feature redundancy (for example, via correlation clustering) before model building; test-retest or inter-scanner stability of retained features; and, for classification tasks, discrimination (for example, area under the receiver operating characteristic curve), calibration, and a stated measure of clinical utility (for example, decision-curve analysis) rather than accuracy alone. The reported 90% accuracy,

90% sensitivity, and 91.3% precision of the hybrid cyst-granuloma model discussed in "Radiomics for Lesion Characterization and Biological Interpretation" are a case in point: (Çetin et al., 2026) these figures are internally consistent and encouraging as a proof of concept, but in the absence of external validation and calibration reporting they should be read as optimistic internal estimates, not as clinically transportable performance figures.

Acquisition and reconstruction parameters

Acquisition and reconstruction settings exert measurable effects on apical-periodontitis lesion assessment. One study reported that periapical lesion volume was significantly underestimated when CBCT slice thickness exceeded 1.00 mm, and that smaller lesions became vulnerable to false-negative diagnosis when slice thickness exceeded 0.50 mm; the authors' findings are therefore best summarized as identifying a maximum acceptable slice thickness of approximately 0.50 mm for reliable small-lesion detection, rather than a minimum threshold. (Boubaris et al., 2026) This finding is particularly relevant for longitudinal monitoring: an apparent reduction in lesion volume could, under non-standardized reconstruction, reflect technical thickening of slices rather than genuine biological healing.

One acquisition parameter reported in the primary literature warrants an explicit caveat. The 2024 radiomics study reports a CBCT resolution of "0.75 microns" for its small-field-of-view protocol. (Lozano González et al., 2024) This value, as published in the primary source, is almost certainly not the intended figure: a true voxel size of 0.75 μm would be several orders of magnitude below the physical resolution of any clinical dental CBCT unit, whereas commercially available small-field-of-view endodontic imaging modes, including the relevant manufacturer's own high-resolution protocols, typically offer voxel sizes in the range of 75–200 μm (0.075–0.20 mm), or a coarser value near 0.75 mm for standard-

resolution small-field-of-view acquisition. The figure is reproduced here exactly as reported in the source publication, with this caveat, because the correct value cannot be determined from the accessible text; readers who wish to use this parameter for methodological comparison should treat it as unverified rather than as a confirmed 0.75-micron acquisition.

Repeatability and reproducibility

Repeatability data further underscore the fragility of CBCT radiomics. In one analysis, CBCT radiomic features were found to be generally more repeatable than reproducible across reconstruction and preprocessing settings, with only a small subset of features remaining repeatable in more than 97% of tested method combinations; smoothing and noise suppression improved repeatability but reduced reproducibility. (Delgadillo et al., 2021) A separate CBCT repeatability study reported that only 25 of 107 radiomic features showed excellent repeatability (intraclass correlation coefficient greater than 0.90), with shape features generally outperforming gray-value-dependent second-order features. (Kuran et al., 2025) The practical implication for apical-periodontitis radiomics is straightforward: model development should be restricted to features with demonstrated robustness, rather than drawing on the entire available feature bank.

Segmentation variability and data leakage

Segmentation variability is not merely a nuisance but a source of systematic uncertainty. The European Society of Radiology/European Organisation for Research and Treatment of Cancer segmentation consensus recommends explicit lesion-definition policies, reproducibility assessment, and transparent handling of boundary ambiguity. (deSouza et al., 2022) This is especially important in apical periodontitis for lesions with poorly

demarcated borders, cortical perforation, fusion with adjacent marrow spaces, or close apposition to other lesions. Non-segmentable lesions with indistinct margins have been explicitly excluded in at least one apical-periodontitis radiomics study, a methodologically reasonable decision that nonetheless reveals a hidden limitation: radiomics models may be developed preferentially on "clean" lesions and then applied clinically to messier, less favorable cases. (Lozano González et al., 2024)

Automation can reduce the labor burden of segmentation, but not, by itself, the validity burden. AI-assisted and semi-automated segmentation have been directly compared for volumetric index assessment, illustrating the growing feasibility of automation in lesion-volume workflows. (Boubaris et al., 2021) A periapical-lesion detection convolutional neural network evaluated on a clinically representative CBCT dataset reported overall sensitivity of 86.7% and specificity of 84.3%, improving to 90.4% sensitivity in score-based evaluation. (Hadzic et al., 2024) A 2026 nnU-Net v2 model achieved moderate-to-good three-dimensional segmentation performance and good lesion-detection performance under routine clinical conditions, but the authors explicitly judged it more suitable as an adjunctive tool than as a stand-alone decision-maker — a conclusion this chapter endorses as appropriate for the current state of the evidence. (Öksüzoğlu et al., 2026)

The methodological problem of data leakage is especially relevant in this small-sample setting. Performing feature selection before, rather than within, cross-validation has been shown to produce optimistic bias as large as 0.15 in area under the receiver operating characteristic curve, 0.29 in F1-based area under the curve, and 0.17 in accuracy. (Demircioğlu, 2021) In radiomics, where datasets are typically high-dimensional and low-sample, this error is common and consequential; nested cross-validation is therefore not an optional refinement but a methodological necessity. One of the apical-periodontitis-specific occult-lesion studies is notable in this

regard for explicitly using nested cross-validation for its logistic-regression classification. (Jang et al., 2020) Even so, nested internal validation cannot substitute for genuine external testing.

External validation: the central deficiency

External validation remains the central deficiency of apical-periodontitis radiomics. A 2025 translational review states the point plainly: external validation on independent datasets is necessary to establish robustness, generalizability, and freedom from overfitting. (Chen et al., 2025) Across the apical-periodontitis-specific studies reviewed here, no true multicenter external validation has been identified for the cyst-granuloma texture study, the 2024 radiomics study, the healing-texture study, the occult-lesion radiomics study, or the hybrid cyst-granuloma model. (Çetin et al., 2026; de Rosa et al., 2020; Lopes et al., 2025; Lozano González et al., 2024; Obuchowicz et al., 2026) This conclusion is offered as a synthesis by the present authors rather than as a direct quotation from the original investigators, but its implication is clear: current performance metrics in this literature should be interpreted as optimistic internal estimates rather than as clinically transportable evidence. A structured breakdown of internal-validation methodology, patient-level data splitting, and external-validation status for each study is provided in Tables 1 and 2.

Clinical translation

Clinical decision support in this domain is therefore best framed, at present, as adjunctive rather than autonomous. Near-term translational opportunities are not difficult to identify: automated lesion segmentation for longitudinal monitoring; volumetric and shape-based dashboards for follow-up; probability estimates for a cyst-like phenotype in lesions selected for surgery; radiographic triage of occult lesions that warrant CBCT; and integration with

restoration- and endodontic-quality variables in outcome prediction. None of these applications require radiomics to replace the clinician. All of them require radiomics to be stable, transparent, and properly validated before they are deployed.

Conclusions

Three distinct claims can be made about CBCT-based quantitative imaging and radiomics in apical periodontitis, and it is worth stating them separately because the strength of evidence differs sharply between them.

CBCT provides higher lesion-detection sensitivity than periapical radiography under appropriate clinical indications, and three-dimensional lesion burden — volume, shape, and cortical interaction — captures information that two-dimensional indices summarize incompletely. Quantitative phenotype extraction from CBCT is technically feasible and has been demonstrated across multiple independent research groups.

Radiomic and texture-based features may contribute to lesion characterization, particularly cyst-granuloma differentiation in histologically verified, single-center datasets, and to the early, pre-visual detection of healing-related textural change after nonsurgical treatment. These findings justify further investment in better-designed studies, but they do not yet constitute validated clinical tools.

Scanner-independent quantitative biomarkers, cyst/granuloma diagnosis suitable for routine unselected clinical practice, and externally validated prediction of endodontic treatment outcome all remain unproven. No apical-periodontitis-specific radiomics study reviewed here has undergone genuine external, multicenter validation; sample sizes remain small; and at least one primary technical parameter (the voxel-size figure discussed in Section 7.2) could not be independently confirmed from the accessible literature.

The translational path forward is reasonably clear, even if it has not yet been walked. Prospective, multicenter cohorts should be assembled with standardized acquisition metadata, scanner-stratified or harmonized preprocessing, whole-volume lesion segmentation, repeatability-based feature filtering, and obligatory external validation. Histologic co-measurement should be incorporated whenever surgery provides tissue, preferably using a structured pathology score such as the Dental Apical Inflammation Score. Follow-up studies should be powered for clinically important endpoints, not only for cross-sectional lesion discrimination. Studies limited to a few dozen lesions remain useful as pilot work, but the next generation of research in this area will need to be substantially larger and more center-diverse if the field's stated goal — moving convincingly from pixels to prognosis — is to be realized rather than merely aspired to.

References

Abesi, F., & Golikani, A. (2023). Diagnostic performance of cone-beam computed tomography for apical periodontitis: a systematic review and meta-analysis. *Pol J Radiol*, 88, e597–e605. https://doi.org/10.5114/pjr.2023.134035

Boubaris, M., Chan, K. L., Zhao, W., Cameron, A., Sun, J., Love, R. M., & George, R. (2021). A novel volume-based cone-beam computed tomographic periapical index. *J Endod*, 47(7), 1129–1134. https://doi.org/10.1016/j.joen.2021.03.012

Boubaris, M., Cameron, A., Love, R., & George, R. (2022). Sphericity of periapical lesion and its relation to the novel CBCT periapical volume index. *J Endod*, 48(11), 1395–1399. https://doi.org/10.1016/j.joen.2022.08.007

Boubaris, M., Cameron, A. B., Love, R., & George, R. (2024). Influence of periapical lesion volume on the radiodensity of surrounding bone: a CBCT study. *J Conserv Dent Endod*, 27(6). https://doi.org/10.4103/jcde.jcde_178_24

Boubaris, M., Cameron, A., Manakil, J., & George, R. (2026). CBCT slice thickness impacts diagnostic accuracy of periapical lesion volume. *J Endod*.

Çetin, B., İçöz, D., Dinç, K., & Kayadibi, İ. (2026). Radiomics-based differential diagnosis of radicular cysts and apical granulomas on CBCT images using RadC-CNN architecture. *Diagnostics (Basel)*, 16(10), 1428. https://doi.org/10.3390/diagnostics16101428

Chen, M., Linton-Reid, K., Aboagye, E. O., & Copley, S. J. (2025). Translating radiomics into clinical practice: a step-by-step guide to study design and evaluation. *Clin Radiol*, 80, 107053. https://doi.org/10.1016/j.crad.2025.107053

de Paula-Silva, F. W. G., Hassan, B., Bezerra da Silva, L. A., Leonardo, M. R., & Wu, M. K. (2009). Accuracy of periapical radiography and cone-beam computed tomography scans in diagnosing apical periodontitis using histopathological findings as a gold standard. *J Endod*, 35(7), 1009–1012. https://doi.org/10.1016/j.joen.2009.04.006

de Rosa, C. S., Bergamini, M. L., Palmieri, M., Sarmento, D. J. S., de Carvalho, M. O., Ricardo, A. L. F., Hasseus, B., Jonasson, P., Braz-Silva, P. H., & Costa, A. L. F. (2020). Differentiation of periapical granuloma from radicular cyst using cone beam computed tomography image texture analysis. *Heliyon*, 6(10), e05194. https://doi.org/10.1016/j.heliyon.2020.e05194

Delgadillo, R., Bues, M., et al. (2021). Repeatability of CBCT radiomic features and their correlation to prostate CT radiomic features. *Radiother Oncol*, 154, 265–272. https://doi.org/10.1016/j.radonc.2020.11.026

Demircioğlu, A. (2021). Measuring the bias of incorrect application of feature selection when using cross-validation in radiomics. *Insights Imaging*, 12, 172. https://doi.org/10.1186/s13244-021-01115-1

deSouza, N. M., van der Lugt, A., Deroose, C. M., et al. (2022). Standardised lesion segmentation for imaging biomarker quantitation: a consensus recommendation from ESR and EORTC. *Insights Imaging*, 13, 159. https://doi.org/10.1186/s13244-022-01287-4

Eguren, M., Holguin, A. O. H., Riccer, A. O., et al. (2022). Can gray values be converted to Hounsfield units? A systematic

review. *Dentomaxillofac Radiol*, 51(1), 20210140. https://doi.org/10.1259/dmfr.20210140

Estrela, C., Bueno, M. R., Azevedo, B. C., Azevedo, J. R., & Pécora, J. D. (2008). A new periapical index based on cone beam computed tomography. *J Endod*, 34(11), 1325–1331. https://doi.org/10.1016/j.joen.2008.08.013

Grün, P., Hatamikia, S., Jadadic, R., Jansen, L., Pfaffeneder-Mantai, F., Fitzek, S., Mostegel, M., Choi, K. E. A., & Turhani, D. (2025). Volumetric measurements from manually drawn segmentations of periapical lesions in cone-beam computed tomography scans correlate with the inflammatory activity classified using the Dental Apical Inflammation Score. *Adv Oral Maxillofac Surg*, 17, 100510. https://doi.org/10.1016/j.adoms.2024.100510

Hadzic, A., Urschler, M., Press, J. N. A., et al. (2024). Evaluating a periapical lesion detection CNN on a clinically representative CBCT dataset: a validation study. *J Clin Med*, 13(1), 197. https://doi.org/10.3390/jcm13010197

Jang, Y. E., Kim, B. S., & Kim, Y. (2020). Clinical factors associated with apical periodontitis visible only in cone-beam computed tomography images. *J Endod*, 46(6), 832–838. https://doi.org/10.1016/j.joen.2020.03.010

Koçak, B., Borgheresi, A., Ponsiglione, A., et al. (2023). CheckList for EvaluAtion of Radiomics research (CLEAR): a step-by-step reporting guideline for authors and reviewers endorsed by ESR and EuSoMII. *Insights Imaging*, 14, 75. https://doi.org/10.1186/s13244-023-01415-8

Krenn, S., Gutwald, R., et al. (2020). Dental Apical Inflammation Score (DAIS): histopathological scoring for the evaluation of

apical inflammatory activity and local bone destruction. *Pathol Res Pract*, 216, 153223. https://doi.org/10.1016/j.prp.2020.153223

Kuran, A., et al. (2025). Repeatability of radiomics parameters in cone-beam computed tomography volumes. *Chin J Acad Radiol*. https://doi.org/10.1007/s42058-025-00196-x

Lopes, D. L. G., Lopes, S. L. P. d. C., Ungaro, D. M. d. T., Gomes, A. P. M., Moura, N. B. D., Gonçalves, B. C., & Costa, A. L. F. (2025). Radiomics-driven CBCT texture analysis as a novel biosensor for quantifying periapical bone healing: a comparative study of intracanal medications. *Biosensors (Basel)*, 15(2), 98. https://doi.org/10.3390/bios15020098

Lozano González, O., Salas Orozco, M. F., Mancera, J. T., Martínez Cuéllar, N. G., & Patiño Marín, N. (2024). Radiomic parameters in periapical lesions: a CBCT analysis evaluating volumetric size, cortical expansion, erosion, and shape. *Eur Endod J*, 9(4), 394–404. https://doi.org/10.14744/eej.2024.45220

Maia Filho, E. M., Calisto, A. M., de Jesus Tavarez, R. R., Segato, R. A. B., & da Silva, L. A. B. (2018). Correlation between the periapical index and lesion volume in cone-beam computed tomography images. *Iran Endod J*, 13(2), 155–158. https://doi.org/10.22037/iej.v13i2.15040

Mosquera-Barreiro, C., et al. (2024). Predictors of periapical bone healing associated with teeth having large periapical lesions following nonsurgical root canal treatment or retreatment: a cone-beam computed tomography-based retrospective study. *Int Endod J*, 57. https://doi.org/10.1111/iej.13993

Nair, P. N. R. (1998). New perspectives on radicular cysts: do they heal? *Int Endod J*, 31(3), 155–160. https://doi.org/10.1046/j.1365-2591.1998.00146.x

Obuchowicz, B., Zarzecka, J., Jakubowska, M., & Lasek, J. (2026). Radiomics as a decision support tool for detecting occult periapical lesions on intraoral radiographs. *J Clin Med*, 15(3), 971. https://doi.org/10.3390/jcm15030971

Öksüzoğlu, H., Topuz, Ö., Bilgir, E., et al. (2026). Fully automated 3D segmentation of periapical lesions on CBCT images using nnU-Net v2. *BMC Med Imaging*. https://doi.org/10.1186/s12880-026-02316-0

Patel, S., Brown, J., Semper, M., Abella, F., & Mannocci, F. (2019). European Society of Endodontology position statement: use of cone beam computed tomography in Endodontics. *Int Endod J*, 52(12), 1675–1678. https://doi.org/10.1111/iej.13187

Pociask, E., Nurzynska, K., Obuchowicz, R., Bałon, P., Uryga, D., Strzelecki, M., Izworski, A., & Piórkowski, A. (2021). Differential diagnosis of cysts and granulomas supported by texture analysis of intraoral radiographs. *Sensors (Basel)*, 21(22), 7481. https://doi.org/10.3390/s21227481

Saini, A., Nangia, R., et al. (2023). Outcome and associated predictors for nonsurgical management of large cyst-like periapical lesions: a CBCT-based prospective cohort study. *Int Endod J*, 56. https://doi.org/10.1111/iej.13860

Santinha, J., Pinto dos Santos, D., Laqua, F., et al. (2025). ESR Essentials: radiomics—practice recommendations by the European Society of Medical Imaging Informatics. *Eur*

Radiol, 35(3), 1122–1132. https://doi.org/10.1007/s00330-024-11093-9

Sousa Melo, S. L., Fayad, M. I., Gohel, A., Johnson, B. R., Kalathingal, S., Mahdian, M., Nair, M., Setzer, F. C., & Makins, S. R. (2026). AAE and AAOMR joint position statement: use of cone-beam computed tomography in endodontics, 2025 update. *Oral Surg Oral Med Oral Pathol Oral Radiol*, 141(1), 126–135. https://doi.org/10.1016/j.oooo.2025.09.013

Stockdale, C. R., & Chandler, N. P. (1988). The nature of the periapical lesion: a review of 1108 cases. *J Dent*, 16(3), 123–129. https://doi.org/10.1016/0300-5712(88)90082-4

Torabinejad, M., Rice, D. D., Maktabi, O., Oyoyo, U., & Abramovitch, K. (2018). Prevalence and size of periapical radiolucencies using cone-beam computed tomography in teeth without apparent intraoral radiographic lesions: a new periapical index with a clinical recommendation. *J Endod*, 44(3), 389–394. https://doi.org/10.1016/j.joen.2017.11.015

Wieczorek, K., et al. (2026). Methodological limitations of CBCT-derived gray values. *J Clin Med*, 15(11), 4144. https://doi.org/10.3390/jcm15114144

Zwanenburg, A., Vallières, M., Abdalah, M. A., et al. (2020). The Image Biomarker Standardization Initiative: standardized quantitative radiomics for high-throughput image-based phenotyping. *Radiology*, 295(2), 328–338. https://doi.org/10.1148/radiol.2020191145

CHAPTER 3

STANDARDIZATION, VALIDATION, ETHICS, AND DATA GOVERNANCE IN PEDIATRIC DENTAL IMAGING

Melis GÜLDALI[1]
Suay Yağmur ÜNAL[2]

Introduction

Dentistry was an early adopter of image-based artificial intelligence, and pediatric practice has followed close behind. Convolutional neural networks now detect caries on periapical and bitewing radiographs, segment developing tooth germs on panoramic images, stage third molar mineralization for age estimation, and locate cephalometric landmarks for orthodontic planning (Khanagar et al., 2021). A 2026 systematic review and meta-analysis identified a rapidly growing body of AI studies targeting caries detection, early childhood caries risk, tooth development assessment, and mesiodens identification in patients eighteen and younger (Karamüftüoğlu et al., 2026), and narrative reviews of AI in dentistry more broadly

[1] Uzm. Dt. Nişantaşı Üniversitesi Diş Hekimliği Fakültesi Ağız Diş Ve Çene Radyolojisi İstanbul/Türkiye, Orcid: 0000-0002-1165-0127
[2] Dr. Öğr. Üyesi, Nişantaşı Üniversitesi Diş Hekimliği Fakültesi Ağız Diş Ve Çene Radyolojisi İstanbul/Türkiye, Orcid: 0000-0002-8559-7461

describe pediatric applications as one of the fastest-growing subfields (Schwendicke et al., 2020). Machine learning is also expanding well beyond dentistry into pediatric medicine generally, from echocardiography to neonatal risk prediction (Hoodbhoy et al., 2021).

This growth creates a problem that is not really about the algorithms themselves. A convolutional network can be trained to find carious lesions or stage a third molar with reasonable accuracy on a held-out test set; the harder questions concern whether that performance holds up in a different clinic with a different X-ray unit and a different patient mix, whether the study that produced the model can be understood and replicated by an outside reviewer, whether the child whose radiograph trained the model was treated fairly in the process, and who remains accountable for the data once it leaves the clinic where it was acquired. These are, respectively, questions of validation, standardization, ethics, and data governance, and they are more acute in pediatric imaging than in adult imaging for reasons developed throughout this chapter: children's anatomy changes continuously with growth, children cannot give legal consent on their own behalf, radiation exposure carries a longer horizon of risk, and some pediatric dental images are put to uses, such as legal age determination, that have no equivalent in adult radiology.

This chapter focuses on radiographic and photographic imaging used in pediatric dentistry and oral and maxillofacial radiology: panoramic and periapical radiographs, bitewing radiographs, lateral and posteroanterior cephalograms, cone-beam computed tomography (CBCT), and intraoral photographic or scanner-derived images. Adult-oriented dental AI applications are not covered, nor are non-imaging applications such as chatbot-based patient triage, except where these intersect directly with the imaging discussion. Because a genuinely pediatric-specific evidence base remains narrow, this chapter also draws on the broader medical-imaging AI literature and on general dental AI studies whose populations are not restricted to minors; evidence of this second kind is used only where

pediatric dental-specific standards or studies are unavailable, and it is flagged explicitly rather than folded silently into the pediatric evidence base. Three evidentiary categories recur throughout the chapter and are worth naming once at the outset: pediatric-specific evidence, generated and validated in patients under eighteen; mixed-age evidence with a defined pediatric subgroup, in which a pediatric stratum can be isolated from a larger study population; and general dental evidence extrapolated to pediatric imaging, in which the study population is adult, mixed, or simply unreported. Much of the standardization and governance apparatus that now applies to pediatric dental AI was, in any case, built first in general radiology and adapted afterward, so some cross-reference to that literature is unavoidable.

Literature identification approach. This chapter is a narrative rather than a systematic review, and it does not follow a PRISMA-style protocol; that distinction matters for how its claims should be read. Sources were identified through targeted searches of PubMed, Scopus, and Google Scholar, combining terms for artificial intelligence, deep learning, and machine learning with terms for pediatric dentistry, dental radiography, cephalometrics, dental age estimation, and the individual imaging modalities named above, with searches concentrated on literature from 2018 onward and supplemented by citation tracking from key reviews. Pediatric dental imaging AI studies were prioritized wherever they existed; general medical-imaging AI literature was drawn on specifically to support standardization, ethics, and governance principles that have not yet been articulated in dentistry-specific form. This approach does not guarantee exhaustive coverage, and statements in this chapter about what "the literature" does or does not show should be read as a synthesis of the sources identified through this process rather than as a formal systematic estimate.

The chapter is organized around the four themes named in its title. The section on standardization reviews acquisition, annotation,

and preprocessing protocols alongside the reporting checklists, such as CLAIM and TRIPOD+AI, that increasingly govern how AI studies in imaging are designed and described. The section on validation surveys what is actually known about model performance in pediatric populations, with attention to external validation, patient-level data splitting, and task-specific performance metrics. The ethics section addresses consent, bias, radiation justification, and a detailed case study on forensic dental age estimation. The final section addresses data governance: the legal frameworks that apply to children's health data, de-identification challenges specific to craniofacial imaging, and federated learning as a partial technical solution. A closing synthesis draws the four threads together and proposes a short research agenda.

Standardization

Acquisition standardization

Before an image ever reaches an algorithm, its acquisition has to be standardized enough that the algorithm's inputs mean the same thing across sites, and this is a more unsettled problem in pediatric dentistry than it might first appear. Panoramic and cephalometric units vary in kilovoltage, exposure time, and sensor type across manufacturers and practice settings, and a model trained on images from one unit often loses accuracy when tested on images from another, a phenomenon usually described as domain shift. The same variability recurs at almost every step between the X-ray sensor and the trained model: pixel spacing and native image resolution differ across devices and are not always preserved through export; bit depth is sometimes reduced when a DICOM file is converted to an exported JPEG or PNG for research use, discarding gray-level information the algorithm might otherwise use; lossy compression, resizing, cropping, and ad hoc intensity normalization are applied inconsistently across studies and are rarely reported in enough detail for

another group to reproduce; and CBCT introduces its own layer of acquisition variability through voxel size, field of view, and reconstruction parameters, on top of motion and metal artifacts that are more frequent in pediatric patients because of positioning difficulty and mixed-dentition restorations. Preprocessing and augmentation choices made after acquisition, such as which rotations, crops, or intensity transforms are applied during training, further shape what a model actually learns and are seldom standardized across research groups. A methodological choice that cuts across all of these technical variables, and that is easy to overlook, is whether the unit of analysis in a study is the image or the patient; a single child commonly contributes several radiographs or photographs to a dataset, and treating those images as independent observations, rather than as clustered within patients, can distort both training and reported performance in ways addressed further in the validation section below.

Where intraoral photographs or scanner-derived images are used, comparable acquisition variables arise in a different form: illumination and white balance vary between clinical settings and consumer cameras, camera distance and angulation affect apparent lesion size and color, magnification is rarely calibrated against a known reference, and color rendering can differ enough between devices to affect models trained for tasks such as caries or plaque detection from photographic images.

Dentition stage deserves to be treated as a standardization variable in its own right rather than as a simple subcategory of chronological age. Primary, mixed, and permanent dentition are not smoothly interchangeable labels for the same underlying anatomy: tooth count, root development, eruption sequence, and radiographic contrast between enamel, dentin, and developing tooth germs all differ substantially across these stages, so a model trained predominantly on one dentition stage is being asked to generalize across a materially different phenotype when applied to another. Ground-truth la-

beling inherits this same variability. The tooth-numbering and staging systems used to annotate pediatric images are inconsistent across regions and traditions: the FDI two-digit notation is standard in most of the world but coexists with the Universal Numbering System in North America, and staging systems for dental development, such as Demirjian's eight-stage scheme, have several competing variants that are not directly interchangeable. When ground-truth labels for AI training are drawn from clinical records that mix these conventions, the resulting model inherits the ambiguity, and this problem compounds when annotation quality itself is not documented: the number of annotators involved, their level of clinical expertise, whether disagreements were resolved by consensus or adjudication, and formal measures of intra- and interobserver agreement are reported unevenly across the pediatric dental AI literature, so a reported accuracy figure often cannot be interpreted against a clearly defined reference standard.

Radiation protocol standardization carries the most direct clinical stakes of any acquisition variable. The European Academy of Paediatric Dentistry's policy document on prescribing radiographs sets out indication-based criteria for when a radiograph is warranted in a child and states plainly that routine, interval-based prescribing is not appropriate for young patients (Kühnisch et al., 2020). For CBCT specifically, the DIMITRA project's position statement argues that the adult-oriented ALARA principle ("as low as reasonably achievable") is not granular enough for growing patients and proposes ALADAIP, "as low as diagnostically acceptable, being indication-oriented and patient-specific," as a framework that ties dose directly to the clinical question being asked and the child's age (Oenning et al., 2018, 2021). These are not AI-specific documents, but they matter for AI standardization because any AI system trained to read pediatric CBCT or panoramic images inherits whatever protocol variability sits upstream of it, and because AI-assisted diagnosis

is sometimes proposed, without much evidence yet, as a way to justify lower-dose or reduced-field-of-view acquisitions.

Reporting guidelines for AI studies

A parallel standardization effort addresses not image acquisition but the AI studies themselves. Early AI papers in dentistry, as in medicine generally, showed wide variation in what they reported: some described dataset composition and ground-truth generation in detail, while others provided very little, making it difficult for a reader to judge whether a reported accuracy figure reflected a genuine clinical advance or an artifact of a favorable train-test split. Different study designs now have different dedicated reporting standards, and the field is best served by matching the checklist to the task rather than treating any single guideline as universal. The Checklist for Artificial Intelligence in Medical Imaging (CLAIM), first published in 2020 and updated in 2024, applies broadly to AI imaging studies and specifies what should be reported at each stage, from data provenance and label generation through model architecture, validation strategy, and failure analysis (Mongan et al., 2020; Tejani et al., 2024). TRIPOD+AI applies specifically to studies that develop, validate, or update a clinical prediction model using regression or machine-learning methods, extending the original 2015 TRIPOD statement to cover both families of method together (Collins et al., 2024), and is paired with PROBAST+AI, a companion tool for appraising risk of bias in exactly these models (Moons et al., 2025); both descend from a 2021 protocol that first proposed building AI-specific extensions to TRIPOD and its bias-assessment counterpart PROBAST (Collins et al., 2021). Diagnostic accuracy studies, the format most caries-detection and age-estimation papers fall into, are covered by the STARD-AI reporting guideline and its companion quality-assessment tool QUADAS-AI. STARD-AI began as a 2021 development protocol (Sounderajah et al., 2021a), and the guideline itself has since been finalized: the STARD-AI Steering Committee

and Consensus Group published a 40-item checklist in Nature Medicine in September 2025, developed through a multistage, multistakeholder Delphi process involving more than 240 international participants, with an author correction to the published article issued in July 2026 (Sounderajah et al., 2025, 2026). QUADAS-AI remains the companion risk-of-bias tool for the same study type (Sounderajah et al., 2021b). Clinical trials of AI interventions have their own extensions, CONSORT-AI for completed trials and SPIRIT-AI for trial protocols (Cruz Rivera et al., 2020; Liu et al., 2020), which will become more relevant to pediatric dental AI as prospective, interventional studies begin to appear alongside the retrospective diagnostic-accuracy studies that currently dominate the field.

A practical way to summarize how these instruments relate to one another is by the type of study each was built for: CLAIM for AI imaging studies broadly; TRIPOD+AI and PROBAST+AI for prediction-model development, validation, or updating studies; STARD-AI and QUADAS-AI for diagnostic-accuracy studies; and CONSORT-AI and SPIRIT-AI for AI clinical trials and their protocols. ACCEPT-AI, discussed at length in the ethics section below, functions as a pediatric-specific overlay that can be layered onto any of these rather than as a competing general-purpose checklist (Muralidharan et al., 2023). Table 1 summarizes this mapping alongside each framework's pediatric specificity.

Table 1. AI reporting and quality-assessment frameworks relevant to pediatric dental imaging AI.

Framework	Purpose	Study type covered	Pediatric-specific
CLAIM	Reporting checklist for AI imaging studies: data provenance, labeling, model architecture, validation, failure analysis	AI imaging studies, broadly	No

Framework	Purpose	Study type covered	Pediatric-specific
TRIPOD+AI	Reporting guidance for clinical prediction models using regression or machine learning	Prediction-model development, validation, or updating studies	No
PROBAST+AI	Risk-of-bias and applicability appraisal, companion to TRIPOD+AI	Prediction-model studies	No
STARD-AI	40-item reporting guideline for AI-centered diagnostic-accuracy studies (finalized 2025)	Diagnostic-accuracy studies	No
QUADAS-AI	Risk-of-bias and quality assessment, companion to STARD-AI	Diagnostic-accuracy studies	No
CONSORT-AI	Reporting guideline for completed clinical trials of AI interventions	AI clinical trials	No
SPIRIT-AI	Reporting guideline for clinical trial protocols involving AI	AI clinical trial protocols	No
FUTURE-AI	Consensus framework built around fairness, universality, traceability, usability, robustness, and explainability	Full AI life cycle, any health domain	No
ACCEPT-AI	Pediatric-specific ethical and reporting overlay: age, communication, consent/assent, equity, data protection, transparency	Any study using pediatric data for AI/ML (overlay onto the frameworks above)	Yes

These checklists sit inside a larger, more recent attempt at synthesis. FUTURE-AI, a 2025 consensus guideline built by more than one hundred experts across fifty countries, organizes trustworthy health AI around six principles, fairness, universality,

traceability, usability, robustness, and explainability, and translates each into concrete practices spanning the full life cycle of a model from design through post-deployment monitoring (Lekadir et al., 2025). None of these frameworks was written with pediatric dentistry specifically in mind, and none currently has a dentistry-specific companion checklist analogous to what radiology has built for itself. A practical implication for authors and reviewers in this field is that CLAIM and, where a prediction model is being developed or validated, TRIPOD+AI can be applied directly to a pediatric dental AI manuscript today, while the age-related considerations addressed later in this chapter, consent documentation, developmental staging, and demographic reporting, currently have to be layered on separately rather than checked against a single pediatric-dentistry-specific standard.

Valıdation

Internal and external validation in a growing population

A model that performs well on a held-out portion of its own training data has cleared only the lowest bar of validation. External validation, testing on data collected at a different site, ideally with a different scanner and a different population, tests something closer to what a clinician actually needs to know before trusting a model in a new setting. Pediatric imaging makes external validation harder to achieve than adult imaging does, for a straightforward reason: a child's dentition and skeleton change continuously, so a model validated on eight-year-olds may not generalize to twelve-year-olds even within the same clinic, let alone across sites. Age-stratified external validation is accordingly not an optional refinement for pediatric dental AI; more precisely, validation should be judged against the model's intended-use population, defined not only by chronological age but by dentition and developmental stage, since a model intended for use across the full span of childhood needs evidence

spanning that same span. This distinction is sometimes framed in the broader prediction-model literature as generalizability, whether a model performs consistently across the population it was built for, versus transportability, whether it can be moved to a different population or setting altogether; a pediatric dental AI study can, in principle, demonstrate one without the other.

Most of the published literature falls short of a fully age- and dentition-stratified standard. A 2026 systematic review and meta-analysis of AI applications across pediatric dentistry, spanning caries detection, early childhood caries risk prediction, tooth development assessment, and mesiodens identification, found that external validation was uncommon and that methodological variability across studies limited confidence in pooled accuracy estimates, even where individual models performed well (Karamüftüoğlu et al., 2026). An earlier systematic review covering a narrower thirteen-study sample of pediatric dentistry AI literature, searched across PubMed, Google Scholar, and the Cochrane Library, reached a similar conclusion: AI was judged a useful diagnostic aid across tasks including cephalometric landmark identification, early caries pattern recognition, chronological age assessment, and facial-attractiveness assessment in cleft patients, but the review's authors called for further work on clinical effectiveness rather than laboratory accuracy alone (Mahajan et al., 2023).

What the technical literature shows, by evidence type

The following synthesis is organized by task and, within each task, distinguishes pediatric-specific studies from studies whose populations are mixed-age, unreported, or adult, since the distinction bears directly on how confidently a given performance figure can be read as evidence about children specifically.

Caries detection is the most studied pediatric-relevant application, though much of the underlying evidence is not pediatric-specific in the strict sense. An early and still widely cited study trained

a GoogLeNet-based convolutional network on 3,000 periapical radiographs and reported premolar and molar diagnostic accuracies in the 82 to 89 percent range, with area-under-curve values comparable to an experienced clinician on the same task; the source population's age range is not detailed in the accessible report, so this result is best read as general dental evidence rather than pediatric-specific evidence (Lee et al., 2018). Subsequent work has diversified the imaging modality: ensemble deep-learning approaches applied to intraoral camera images have reported strong discrimination for caries presence and lesion localization, again without a clearly specified pediatric population (Kang et al., 2024), and a 2019 scoping review of convolutional networks in dental image diagnostics found consistently high performance across caries, periodontal bone loss, and periapical lesion detection tasks, while also noting that most included studies used single-center data and lacked prospective or external validation (Schwendicke et al., 2019). A related line of work applies the same architecture to periapical pathology directly, with one frequently cited study reporting that a deep network matched or approached endodontist-level accuracy in detecting apical lesions on periapical films, again in a population not restricted to children (Ekert et al., 2019). Tooth and tooth-germ segmentation and mesiodens detection, the applications named in this chapter's abstract as distinctively pediatric, remain comparatively underrepresented in the peer-reviewed literature relative to caries detection; the pediatric-focused reviews cited throughout this section identify these as active but still small application areas, and the evidence base here should be read as early-stage rather than as having reached the maturity of caries detection or cephalometric landmarking.

Cephalometric landmark detection, central to orthodontic diagnosis in growing patients, has been the subject of a formal systematic review and meta-analysis covering nineteen diagnostic-accuracy studies published between 2017 and 2020; the review does not restrict itself to pediatric populations, and cephalometric analysis is

used in growing and non-growing patients alike, so this evidence is again best treated as mixed-age rather than pediatric-specific. Pooled results showed that roughly eighty percent of landmarks were located within a two-millimeter error threshold of expert placement, a level widely regarded as clinically acceptable, but the review also found a high risk of bias across the included studies, concentrated in how reference standards were established and how test data were selected (Schwendicke et al., 2021). A separate evaluation of a customized network trained specifically for cephalometric analysis, using high-quality radiographs acquired on a single calibrated unit rather than images pooled from public repositories, reported close agreement with manual tracing and illustrated what a well-controlled single-center validation can look like even without external testing (Kunz et al., 2020).

Dental age estimation occupies a distinctive place in this literature because its outputs feed directly into legal and administrative decisions, a point developed further in the ethics section below, and because by definition its study populations are pediatric or near-pediatric. Automated staging of third molar development, the tooth most often used for age estimation once the rest of the dentition has matured, has been approached with both segmentation-based and classification-based deep-learning pipelines. One large 2024 study trained a convolutional network on more than 11,000 panoramic radiographs to classify individuals as above or below the legal age thresholds of 14, 16, and 18 years, reporting specificity between 0.80 and 0.92 across thresholds and sexes (Franco et al., 2024). The framing of that study, as a binary decision at a legal threshold rather than a continuous age estimate, reflects how this application is actually used in practice; a binary above-or-below-eighteen output carries higher stakes for an individual than a continuous estimate with an associated confidence interval, since the error that matters most is the one that falls on the wrong side of the threshold, a point returned to below.

Table 2 summarizes representative studies discussed in this section, organized by task and evidence type, to make the pediatric-specific versus extrapolated distinction concrete rather than leaving it only as a verbal qualifier attached to each citation.

Table 2. Representative pediatric dental imaging AI evidence, classified by evidence type as defined in the Introduction.

Task / study	**Evidence type**	**Sample size**	**Validation**	**Primary metric**	**Key limitation**
Caries detection, periapical radiographs (Lee et al., 2018)	General dental, extrapolated	3,000 radiographs	Internal only	82-89% accuracy; AUC near clinician level	Pediatric status of population not reported
Caries detection, intraoral camera ensemble (Kang et al., 2024)	General dental, extrapolated	Not specified	Internal	Ensemble sensitivity / specificity	Pediatric status of population not reported
CNN dental-image diagnostics (Schwendicke et al., 2019, scoping review)	General dental, extrapolated	Multiple pooled studies	Mostly internal	Varies by included study	Single-center data; little prospective or external validation
Periapical lesion detection (Ekert et al., 2019)	General dental, extrapolated	Not specified	Internal	Near endodontist-level accuracy	Population not restricted to children
Cephalometric landmark detection (Schwendicke et al., 2021, meta-analysis)	Mixed-age, 19 pooled studies	Pooled across studies	Mixed across studies	~80% of landmarks within 2 mm	High risk of bias in reference-standard and test-set selection

Task / study	Evidence type	Sample size	Validation	Primary metric	Key limitation
Cephalometric analysis, single-center CNN (Kunz et al., 2020)	Mixed-age, single-center	Single calibrated unit	Internal, well-controlled	Close agreement with manual tracing	No external validation
Pediatric dentistry AI (Karamüftüoğlu et al., 2026, meta-analysis)	Pediatric-specific	Multiple pediatric studies pooled	External validation uncommon	Pooled accuracy; high variability	Substantial study heterogeneity limits pooled estimates
Pediatric dentistry AI (Mahajan et al., 2023, 13-study review)	Pediatric-specific	13 studies, 2011-2021	Not consistently reported	Qualitative: useful diagnostic aid	Small study sample; limited clinical-effectiveness evidence
Dental age estimation, third-molar staging (Franco et al., 2024)	Pediatric-specific by definition	>11,000 panoramic radiographs	Internal	Specificity 0.80-0.92 at legal thresholds	Binary threshold framing; no external validation reported

Task-specific performance metrics deserve to be kept distinct rather than folded into a single generic notion of "accuracy." Classification and detection tasks, such as caries or lesion detection, are appropriately reported using sensitivity, specificity, precision, recall, F1, and area under the receiver-operating-characteristic curve; segmentation tasks, such as tooth or tooth-germ delineation, call for overlap measures such as the Dice coefficient or intersection-over-union, supplemented where relevant by boundary-distance metrics; landmark-localization tasks, such as cephalometric point placement, are conventionally reported using mean radial error and success detection rate at defined distance thresholds; and continuous outcome tasks, such as dental-age estimation expressed as a numeric age rather than a threshold decision, call for mean absolute error, root-

mean-square error, and an explicit assessment of systematic bias across the age range. Reducing all four of these task families to a single reported "accuracy" figure, as some of the literature synthesized above does, obscures rather than clarifies what a model can actually be trusted to do.

A further set of methodological issues cuts across all of these tasks and deserves explicit attention because it is currently underdiscussed in this literature relative to the external-validation question. Data leakage, in which images from the same patient appear in both the training and test sets, can inflate reported performance substantially if splitting is done at the image level rather than the patient level, and patient-level splitting should be treated as a baseline methodological requirement rather than a refinement. Site-level and, where feasible, temporal holdout, testing on data collected later in time or at an institution not represented in training, provide stronger evidence of robustness than a random split of a single dataset. Class imbalance, common in caries- and lesion-detection tasks where diseased regions are a minority of the image, can make raw accuracy misleading, which is part of why sensitivity, specificity, and predictive values are generally more informative than accuracy alone; reporting confidence intervals around these estimates, rather than point estimates alone, is similarly important given the small sample sizes that dominate this field. Threshold selection, calibration, and the distinction between discrimination and calibration deserve separate mention: a model can discriminate well between classes while still producing probability outputs that are poorly calibrated to true risk, and calibration is reported inconsistently, if at all, across the pediatric dental AI studies reviewed here. Finally, subgroup performance, broken down by dentition stage, age band, sex, and where relevant ethnicity, and clinically relevant error analysis, characterizing what a model's mistakes actually look like rather than reporting only an aggregate score, remain reported unevenly and would substantially strengthen the evidentiary basis of future work.

Regulatory validation

Peer-reviewed validation and regulatory validation are not the same thing, and the relationship between them in pediatric dentistry has been shifting. A 2025 cross-sectional analysis of the United States Food and Drug Administration's AI/ML-enabled device database found that the FDA does not require manufacturers to report whether clinical validation datasets included pediatric patients, or to label devices with the age range for which they were actually tested, even though the agency does require that AI/ML algorithms undergo clinical validation more generally (Brewster et al., 2025). Within dentistry specifically, a 2026 narrative review of FDA regulatory databases identified twenty-nine FDA-cleared, standalone AI products for dental imaging from thirteen companies, spanning caries detection, periodontal disease assessment, cephalometric analysis, multipathology diagnostics, automated dental charting, and three-dimensional segmentation, and found that several vendors now hold clearances for pediatric-specific modules, including dedicated pediatric caries- and periapical-lesion-detection functions (Shujaat et al., 2026). Read together, these two sources point to a more nuanced picture than a simple absence of regulatory attention: pediatric-labeled dental AI clearances now exist and are growing in number, but the regulatory framework that produced them does not itself require the kind of age- and subgroup-stratified performance reporting this chapter has argued for, so a pediatric label on a cleared device does not, by itself, indicate that pediatric-specific validation evidence of the depth described above is publicly available. The 2023 ACCEPT-AI framework, discussed in more detail below, was written partly in response to this gap: it treats "age-related algorithmic bias" as a named category of risk, arguing that combining pediatric and adult data during training, testing, or regulatory submission without clear labeling and subgroup reporting can produce systems whose real-world performance in children is effectively unknown even after formal

clearance (Muralidharan et al., 2023). Regulatory validation, in other words, should be understood as encompassing more than the clearance decision itself; intended-use specification, subgroup validation, human-factors testing of how clinicians actually interact with a device's output, post-market performance monitoring, and a defined process for evaluating model updates are all part of what a genuinely translational regulatory pathway for pediatric dental AI would need to include.

Ethics

Consent, assent, and the pediatric patient

The legal capacity of children to consent to their own care, or to the use of their data in research, varies by jurisdiction and by context, but the general pattern across most legal systems is that children require parental or guardian permission, with the child's own assent sought where the child is developmentally able to provide it, subject to jurisdiction-specific exceptions such as mature-minor doctrines or emancipation (Muralidharan et al., 2023). This two-layer structure is not a formality. A 2025 systematic review of ethical considerations in AI-driven pediatric medicine described informed consent as one of the most acute challenges in the field, in part because pediatric patients typically cannot provide it themselves and in part because retrospective datasets, the source of most training images for dental AI, were rarely collected with future AI training disclosed as a purpose at the time the original radiograph was taken (Abusamra et al., 2025). Reusing an archived panoramic radiograph to train a caries-detection model is convenient and low-cost, but it raises a real question about whether the parent who consented to the original clinical radiograph anticipated, or would have agreed to, that secondary use.

The ACCEPT-AI framework, published in 2023, was written directly to address this gap. It sets out six domains, age, communication, consent and assent, equity, data protection, and technological transparency, and translates each into concrete reporting recommendations: record who provided consent and how, document any court involvement or complex custody arrangements that bear on who can consent, record the child's age at assent separately from chronological age at enrollment, and state explicitly whether de-identified or identifiable data is being used and under which legal framework (Muralidharan et al., 2023). None of these recommendations is unique to dentistry, but dental imaging has a specific complication worth naming: unlike a chest radiograph, a dental radiograph or intraoral photograph can sometimes be re-identifying on its own, through unusual tooth morphology, orthodontic hardware, or a distinctive pattern of prior restorations, which raises the stakes of the consent conversation even for ostensibly de-identified image sets.

Bias, fairness, and developmental heterogeneity

Algorithmic bias in pediatric imaging has a dimension that adult imaging bias research, focused mostly on race, sex, and socioeconomic status, does not fully capture: bias tied to developmental stage itself. The ACCEPT-AI authors coin the term "age-related algorithmic bias" for this and give a concrete illustration: a model trained on a pooled dataset of adult and pediatric chest radiographs, without age labels, applied afterward to an adult-only population, since the training process gives no way to know whether the resulting predictions were shaped disproportionately by the pediatric subset (Muralidharan et al., 2023). The dental analogue is straightforward to construct. A caries-detection model trained predominantly on permanent dentition will encounter systematically different enamel density, restoration patterns, and interproximal spacing when applied to primary or mixed dentition, and unless the training

set explicitly stratifies by dentition stage, there is no way to know in advance whether performance will hold.

The broader medical-imaging literature offers a cautionary parallel that pediatric dental AI has not yet had to reckon with directly but has reason to anticipate. A widely discussed 2022 study found that deep-learning models could predict a patient's self-reported race from chest and other radiographs with high accuracy, using image features that human radiologists could not identify or explain, and the authors warned that this hidden capability creates a pathway for race-linked disparities to enter clinical predictions even when race is never an explicit input (Gichoya et al., 2022). No dental equivalent of this specific finding has been identified in the literature reviewed for this chapter, but the underlying mechanism, a network learning demographic signal that was never intended to be predictive and using it in ways nobody can audit, does not depend on the imaging modality, and craniofacial and dental morphology plausibly carries at least as much latent demographic signal as a chest film does. Reporting guidelines that ask authors to document the demographic composition of training data, as ACCEPT-AI and FUTURE-AI both do, are a partial answer, but they only work if the field treats demographic reporting as a genuine methodological requirement rather than an optional appendix table (Lekadir et al., 2025; Muralidharan et al., 2023).

Explainability, uncertainty, and the automation-bias risk

A substantial literature on ethical machine learning in health care treats explicability and human oversight as necessary conditions for trustworthy deployment rather than desirable extras (Chen et al., 2021). A joint statement from European and North American radiology societies applied this logic directly to imaging in 2019, arguing that the ethical use of AI requires more than accuracy, and that clinicians need enough basis for a given output to exercise independent judgment rather than defer automatically to the machine (Geis et al.,

2019). This concern, sometimes called automation bias, applies with particular force in pediatric dentistry, where the clinician reading an AI-flagged lesion or an AI-staged developmental score is often a general dentist rather than a specialist trained in the AI's underlying task. Explainability tools themselves are not a complete answer to this concern: post hoc explanation methods can highlight image regions that appear to drive a model's output without those regions being faithful to the model's actual internal reasoning, so a saliency map or feature-attribution overlay can create an impression of interpretability that outruns what it actually delivers. For that reason, human oversight, clear communication of predictive uncertainty, and clinically interpretable output, a probability accompanied by a confidence range rather than a single unqualified number, deserve at least as much emphasis as explainability tooling narrowly defined. The World Health Organization's 2021 guidance on AI ethics in health makes a related point at the policy level, framing human oversight and the ability to contest an automated output as a baseline requirement rather than an aspirational feature, a principle that applies as much to a caries-detection tool used in a pediatric dental clinic as to any other clinical AI system (World Health Organization, 2021).

A case in point: forensic dental age estimation

Few applications of dental imaging AI raise the ethical stakes of this chapter as directly as forensic age estimation. Radiographic assessment of third molar development has long been used to estimate the chronological age of individuals who lack reliable documentation, most consequentially unaccompanied minors seeking asylum, where the practical question is not a continuous age estimate but a binary one: whether a given individual is under eighteen. AI-based staging tools, including the classification model discussed earlier in this chapter (Franco et al., 2024), are now being proposed as

faster and more consistent replacements for manual staging in exactly this context.

The ethical literature on this practice, developed well before AI entered the picture and still directly applicable to its AI-assisted form, is direct in its conclusions. A 2020 analysis in the American Journal of Public Health concluded that dental radiograph-based age estimation in US asylum cases is methodologically unreliable, given the wide biological variability in third molar development across individuals and populations, and separately unethical when performed, as it often is, without informed consent from the minor or an independent advocate acting in the minor's interest (Kapadia et al., 2020). The consequences described in that literature are not abstract: an error that places a seventeen-year-old on the adult side of a threshold can mean detention in an adult facility rather than placement in the juvenile system built to protect minors.

Automating the staging step with a convolutional network changes the speed and apparent objectivity of the assessment without changing what the assessment can actually deliver. A binary classifier operating near a legal age threshold is, in practice, making a decision under a decision threshold that trades false-adult misclassification against false-minor misclassification, and reported specificity in the 0.80 to 0.92 range (Franco et al., 2024) describes performance against a particular reference sample rather than a population-independent property of the model; calibration against the population actually being assessed, and explicit uncertainty intervals around any output, matter as much as the headline specificity figure. None of this touches the underlying biological variability that the 2020 analysis identifies as the primary source of error, and a plausible risk is that a fast, computationally confident output makes it easier for a decision-maker to treat a fundamentally uncertain biological estimate as a settled fact. What AI can plausibly reduce is observer-dependent variability in the staging step itself, reading the same radi-

ograph the same way each time; what it cannot do is resolve the intrinsic biological uncertainty in the relationship between chronological age and dental development, which is a property of human biology rather than of the measurement method. Any chapter on AI ethics in pediatric imaging that omitted this application would be leaving out the case where the stakes for an individual child are most direct and severe.

Data Governance

Legal frameworks for pediatric health data

Data protection law addresses children's data with heightened protection in most jurisdictions that regulate it directly, but the specific legal mechanisms involved are easy to state imprecisely, and a chapter of this kind should be explicit about the limits of its own legal analysis: the discussion that follows describes the general structure of the GDPR as it is commonly understood, is not a substitute for jurisdiction-specific legal advice, and should be verified against national implementing legislation and reviewed by qualified counsel before being relied upon in practice. Within the GDPR, two distinct provisions are relevant and should not be collapsed into one another. Article 9 classifies health data as a special category of personal data for every data subject regardless of age, and processing it lawfully requires one of the specific legal bases set out in Article 9(2), such as explicit consent or, subject to appropriate safeguards, scientific research; this is the provision most directly relevant to pediatric dental radiographs, which are health data before they are anything else. Article 8, by contrast, addresses a narrower situation: the conditions under which a child's own consent is valid for information society services offered directly to a child, such as an online platform, and it sets a digital age-of-consent threshold, between thirteen and sixteen depending on the EU member state, below which a

holder of parental responsibility must authorize the processing. Article 8 is not the general rule governing the processing of children's health data in a clinical or research context, and describing it as such overstates its scope. The GDPR's recitals separately state that children merit specific protection because they may be less aware of the risks associated with data processing (Regulation (EU) 2016/679, 2016), a principle that informs how consent and information should be communicated to families even where Article 8 does not directly apply. In the United States, HIPAA does not distinguish adult from pediatric health information in its core de-identification standard, the Safe Harbor Rule, which instead specifies a fixed list of identifiers to be removed regardless of the patient's age (Muralidharan et al., 2023). The result, as the ACCEPT-AI authors point out, is a set of protections that differs sharply by jurisdiction: children's data receives explicit heightened treatment in some legal systems and essentially the same treatment as adult data in others, with the practical consequence that a multinational pediatric dental AI dataset can be simultaneously compliant everywhere and inconsistent in substance, meeting the letter of each local law while applying different real protections to children depending on where their data happened to be collected (Muralidharan et al., 2023).

None of these frameworks was written with imaging AI in mind, and all of them predate the current wave of large-scale, multi-institutional dataset pooling that trains most modern deep-learning systems. A 2020 ethics framework proposed for clinical imaging data more broadly argues that once an image has served its original clinical purpose, it should be treated as something closer to a public good for secondary uses such as AI development, with everyone who subsequently handles it, researcher, institution, or commercial developer, taking on a fiduciary duty to protect the patient rather than a right to exploit the data commercially (Larson et al., 2020). This framing has not been tested specifically against pediatric data, where the original clinical purpose was authorized by a parent on behalf of

a child who could not yet consent, and where the eventual secondary use may occur many years later, after the child has become an adult capable of objecting to a use nobody asked them about at the time.

De-identification and re-identification risk

Removing a name and date of birth from an image file is often assumed to be sufficient de-identification, but this assumption does not hold well for craniofacial imaging. A 2019 study demonstrated that publicly available face-recognition software could correctly match research participants' photographs to three-dimensional facial reconstructions generated from their own de-identified MRI scans in the large majority of cases tested, establishing that reconstructing a recognizable face from volumetric medical imaging data is not merely a theoretical risk (Schwarz et al., 2019). The broader medical big-data literature has flagged this problem directly, arguing that conventional de-identification techniques are increasingly inadequate against modern re-identification methods regardless of imaging modality (Price & Cohen, 2019). The same underlying concern applies to CBCT, which captures the jaw and, depending on field of view, substantial surrounding facial anatomy. A dental panoramic radiograph or set of intraoral photographs additionally carries information, such as an unusual eruption pattern, missing or supernumerary teeth, or a specific arrangement of restorations, that can function as a quasi-identifier within a small clinic population even without any conventional metadata attached. Whether primary and mixed dentition, because of the greater individual morphological variation they present relative to the more uniform adult permanent dentition, are in fact harder to de-identify robustly than adult datasets is a plausible but currently untested concern; it is raised here as a hypothesis the current legal frameworks discussed above do not address, not as an established finding.

Federated learning and privacy-preserving architectures

One technical response to this governance gap is to stop moving raw images between institutions at all. Federated learning trains a shared model across multiple sites by exchanging model updates rather than patient data, so that images never leave the institution where they were acquired (Rieke et al., 2020). A 2020 review of privacy-preserving and federated approaches to medical imaging found that federated models could achieve diagnostic performance close to centrally trained models while substantially narrowing the range of ways patient data could be exposed to attack or misuse (Kaissis et al., 2020). For pediatric dental AI specifically, where individual institutions often hold a few hundred or few thousand pediatric radiographs at most, federated learning has an additional appeal beyond privacy: it offers a path to training on the multi-site, age-stratified, demographically diverse datasets that external validation requires, discussed earlier in this chapter, without requiring any single institution to centralize a large pediatric imaging dataset and take on the governance burden of protecting it alone.

Federated learning is not a complete solution on its own. Model updates themselves can leak information under some attack scenarios, and coordinating a federated pediatric dental consortium across institutions and jurisdictions is a substantial organizational undertaking that published feasibility studies have not yet had to solve at scale. Complementary privacy-preserving techniques, including secure aggregation, which prevents any single party from inspecting another site's individual model update, and differential privacy, which adds calibrated statistical noise to limit what can be inferred about any individual patient from a shared model, address some of these residual risks and are increasingly discussed alongside federated learning rather than as substitutes for it (Kaissis et al., 2020). Taken together, this technical apparatus reframes data governance as an infrastructure problem alongside a legal one, which is a useful

reframing given how unevenly the legal protections reviewed above are applied in practice.

Toward institutional data stewardship

Taken together, the legal and technical material in this section points toward a governance role that goes beyond compliance with a single applicable law. A 2020 governance model for clinical AI, developed independently of the imaging-specific ethics framework discussed above, proposes that institutions deploying or contributing data to AI systems establish dedicated oversight, spanning data quality, algorithmic performance monitoring, and accountability for downstream harms, rather than treating governance as satisfied once a data use agreement has been signed (Reddy et al., 2020). In practical terms, such a standing governance function would need to address data minimization, defined retention periods, role-based access control, audit trails, cross-border transfer mechanisms, data-use agreements, documented data and model provenance, an incident-response process, and lifecycle governance for models after deployment, in addition to the consent and de-identification questions already discussed. Applied to pediatric dental imaging, this would mean an institution asks not only whether it had consent to collect a given image, but whether it still has a defensible basis to use that image for a given purpose five or ten years later, now that the child in it may be old enough to ask. Formal, standing review processes of this kind do not appear to be common in dental practice or academic dental programs at present, based on the literature and frameworks reviewed in this chapter, though a comprehensive census of institutional practice is beyond the scope of what this chapter can establish; the gap between the governance literature reviewed here and governance as it is actually practiced in pediatric dental AI development appears, on the available evidence, to be substantial.

Conclusion

Pediatric dental imaging AI has reached the point where proof-of-concept feasibility has been demonstrated for several high-volume tasks; caries detection, cephalometric landmarking, and age-staging models all now report accuracy figures that would have been difficult to achieve five years ago. What remains substantially unresolved is whether the infrastructure around these models, the acquisition and reporting standards, the validation evidence, the ethical safeguards, and the data governance, can keep pace with how quickly the models themselves are improving, and whether performance demonstrated in the studies reviewed here will hold up under the kind of prospective, multi-site, age-stratified scrutiny this chapter has argued is still largely absent.

This chapter has argued that these four areas are not separable concerns to be addressed one at a time but a single connected system: a model is only as trustworthy as the standardized data it was built on, only as safe as the validation evidence behind it, only as ethical as the consent and fairness practices that produced its training set, and only as sustainable as the governance structure that will still be answerable for it a decade from now, when the child in the training image has grown up. Treating these four requirements together, rather than as a checklist to satisfy sequentially, is the more accurate description of what responsible deployment in this field actually demands.

References

Abusamra, H. N. J., Ali, S. H. M., Elhussien, W. A. K., Mirghani, A. M. A., Ahmed, A. A. A., & Ibrahim, M. E. A. (2025). Ethical and practical considerations of artificial intelligence in pediatric medicine: a systematic review. *Cureus, 17*(2), e79024. https://doi.org/10.7759/cureus.79024

Brewster, R. C. L., Nagy, M., Wunnava, S., & Bourgeois, F. T. (2025). US FDA approval of pediatric artificial intelligence and machine learning-enabled medical devices. *JAMA Pediatrics, 179*(2), 212-214. https://doi.org/10.1001/jamapediatrics.2024.5437

Chen, I. Y., Pierson, E., Rose, S., Joshi, S., Ferryman, K., & Ghassemi, M. (2021). Ethical machine learning in healthcare. *Annual Review of Biomedical Data Science, 4*, 123-144.

Collins, G. S., Dhiman, P., Andaur Navarro, C. L., Ma, J., Hooft, L., Reitsma, J. B., et al. (2021). Protocol for development of a reporting guideline (TRIPOD-AI) and risk of bias tool (PROBAST-AI) for diagnostic and prognostic prediction model studies based on artificial intelligence. *BMJ Open, 11*, e048008.

Collins, G. S., Moons, K. G. M., Dhiman, P., Riley, R. D., Beam, A. L., Van Calster, B., et al. (2024). TRIPOD+AI statement: updated guidance for reporting clinical prediction models that use regression or machine learning methods. *BMJ, 385*, e078378.

Cruz Rivera, S., Liu, X., Chan, A. W., Denniston, A. K., Calvert, M. J., & SPIRIT-AI and CONSORT-AI Working Group. (2020). Guidelines for clinical trial protocols for interventions involving artificial intelligence: the SPIRIT-AI extension. *Nature Medicine, 26*, 1351-1363.

Ekert, T., Krois, J., Meinhold, L., Elhennawy, K., Emara, R., Golla, T., & Schwendicke, F. (2019). Deep learning for the radiographic detection of apical lesions. *Journal of Endodontics, 45*(7), 917-922.

Franco, A., Murray, J., Heng, D., Lygate, A., Moreira, D., Ferreira, J., Miranda e Paulo, D., Machado, C. P., Bueno, J., Mânica, S., Porto, L., Abade, A., & Paranhos, L. R. (2024). Binary decisions of artificial intelligence to classify third molar development around the legal age thresholds of 14, 16 and 18 years. *Scientific Reports, 14*(1), 4668.

Geis, J. R., Brady, A. P., Wu, C. C., et al. (2019). Ethics of artificial intelligence in radiology: summary of the joint European and North American multisociety statement. *Insights into Imaging, 10*(1), 101.

Gichoya, J. W., Banerjee, I., Bhimireddy, A. R., et al. (2022). AI recognition of patient race in medical imaging: a modelling study. *The Lancet Digital Health, 4*(6), e406-e414.

Hoodbhoy, Z., Sattar, S., Ariff, S., Iqbal, B., Chowdhury, D., & Hasan, B. (2021). Machine learning for child and adolescent health: a systematic review. *Pediatrics, 147*(3), e2020011833.

Kaissis, G. A., Makowski, M. R., Rückert, D., & Braren, R. F. (2020). Secure, privacy-preserving and federated machine learning in medical imaging. *Nature Machine Intelligence, 2*, 305-311.

Kang, S., Shon, B., Park, E. Y., Jeong, S., & Kim, E. K. (2024). Diagnostic accuracy of dental caries detection using ensemble techniques in deep learning with intraoral camera images. *PLoS ONE, 19*(9), e0310004.

Kapadia, F., Stevens, J., & Silver, D. (2020). Dental radiographs for age estimation in US asylum seekers: methodological, ethical,

and health issues. *American Journal of Public Health, 110*(12), 1786-1789.

Karamüftüoğlu, N., Yavuz Üçpunar, B., Birben, İ., Altundağ, A. E., Örnek Mullaoğlu, K., & Bal, C. (2026). Artificial intelligence in pediatric dentistry: a systematic review and meta-analysis. *Children, 13*(1), 152.

Khanagar, S. B., Al-ehaideb, A., Maganur, P. C., Vishwanathaiah, S., Patil, S., Baeshen, H. A., Sarode, S. C., & Bhandi, S. (2021). Developments, application, and performance of artificial intelligence in dentistry — a systematic review. *Journal of Dental Sciences, 16*(1), 508-522.

Kühnisch, J., Anttonen, V., Duggal, M. S., Spyridonos, M. L., Rajasekharan, S., Sobczak, M., Stratigaki, E., Van Acker, J. W. G., Aps, J. K. M., Horner, K., & Tsiklakis, K. (2020). Best clinical practice guidance for prescribing dental radiographs in children and adolescents: an EAPD policy document. *European Archives of Paediatric Dentistry, 21*, 375-386.

Kunz, F., Stellzig-Eisenhauer, A., Zeman, F., & Boldt, J. (2020). Artificial intelligence in orthodontics: evaluation of a fully automated cephalometric analysis using a customized convolutional neural network. *Journal of Orofacial Orthopedics, 81*, 52-68.

Larson, D. B., Magnus, D. C., Lungren, M. P., Shah, N. H., & Langlotz, C. P. (2020). Ethics of using and sharing clinical imaging data for artificial intelligence: a proposed framework. *Radiology, 295*(3), 675-682.

Lee, J. H., Kim, D. H., Jeong, S. N., & Choi, S. H. (2018). Detection and diagnosis of dental caries using a deep learning-based convolutional neural network algorithm. *Journal of Dentistry, 77*, 106-111.

Lekadir, K., Feragen, A., Fofanah, A. J., Frangi, A. F., Buyx, A., et al.; FUTURE-AI Consortium. (2025). FUTURE-AI: international consensus guideline for trustworthy and deployable artificial intelligence in healthcare. *BMJ, 388*, e081554.

Liu, X., Cruz Rivera, S., Moher, D., Calvert, M. J., Denniston, A. K., & SPIRIT-AI and CONSORT-AI Working Group. (2020). Reporting guidelines for clinical trial reports for interventions involving artificial intelligence: the CONSORT-AI extension. *Nature Medicine, 26*, 1364-1374.

Mahajan, K., Kunte, S. S., Patil, K. V., Shah, P. P., Shah, R. V., & Jajoo, S. S. (2023). Artificial intelligence in pediatric dentistry — a systematic review. *Journal of Dental Research and Review, 10*(1), 7-12. https://doi.org/10.4103/jdrr.jdrr_199_22

Mongan, J., Moy, L., & Kahn, C. E., Jr. (2020). Checklist for Artificial Intelligence in Medical Imaging (CLAIM): a guide for authors and reviewers. *Radiology: Artificial Intelligence, 2*(2), e200029.

Moons, K. G. M., Damen, J. A. A., Kaul, T., Hooft, L., Andaur Navarro, C., Dhiman, P., et al. (2025). PROBAST+AI: an updated quality, risk of bias, and applicability assessment tool for prediction models using regression or artificial intelligence methods. *BMJ, 388*, e082505.

Muralidharan, V., Burgart, A., Daneshjou, R., & Rose, S. (2023). Recommendations for the use of pediatric data in artificial intelligence and machine learning: ACCEPT-AI. *NPJ Digital Medicine, 6*, 166.

Oenning, A. C. C., Jacobs, R., Pauwels, R., Stratis, A., Hedesiu, M., Salmon, B., & DIMITRA Research Group. (2018). Cone-beam CT in paediatric dentistry: DIMITRA project position statement. *Pediatric Radiology, 48*(3), 308-316.

Oenning, A. C. C., Jacobs, R., & Salmon, B. (2021). ALADAIP, beyond ALARA and towards personalized optimization for paediatric cone-beam CT. *International Journal of Paediatric Dentistry, 31*(4), 676-678. https://doi.org/10.1111/ipd.12797

Price, W. N., II, & Cohen, I. G. (2019). Privacy in the age of medical big data. *Nature Medicine, 25*(1), 37-43.

Reddy, S., Allan, S., Coghlan, S., & Cooper, P. (2020). A governance model for the application of AI in health care. *Journal of the American Medical Informatics Association, 27*(3), 491-497.

Regulation (EU) 2016/679 of the European Parliament and of the Council of 27 April 2016 on the protection of natural persons with regard to the processing of personal data (General Data Protection Regulation). (2016). Official Journal of the European Union, L119, 4 May 2016 (Recital 38, Articles 8 and 9).

Rieke, N., Hancox, J., Li, W., Milletari, F., Roth, H. R., Albarqouni, S., Bakas, S., Galtier, M. N., Landman, B. A., Maier-Hein, K., Ourselin, S., Sheller, M., Summers, R. M., Trask, A., Xu, D., Baust, M., & Cardoso, M. J. (2020). The future of digital health with federated learning. *NPJ Digital Medicine, 3*, 119.

Schwarz, C. G., Kremers, W. K., Therneau, T. M., Sharp, R. R., Gunter, J. L., Vemuri, P., Arani, A., Spychalla, A. J., Kantarci, K., Knopman, D. S., Petersen, R. C., & Jack, C. R., Jr. (2019). Identification of anonymous MRI research participants with face-recognition software. *New England Journal of Medicine, 381*(17), 1684-1686.

Schwendicke, F., Golla, T., Dreher, M., & Krois, J. (2019). Convolutional neural networks for dental image diagnostics: a scoping review. *Journal of Dentistry, 91*, 103226.

Schwendicke, F., Samek, W., & Krois, J. (2020). Artificial intelligence in dentistry: chances and challenges. *Journal of Dental Research, 99*(7), 769-774.

Schwendicke, F., Chaurasia, A., Arsiwala, L., Lee, J. H., Elhennawy, K., Jost-Brinkmann, P. G., Demarco, F., & Krois, J. (2021). Deep learning for cephalometric landmark detection: systematic review and meta-analysis. *Clinical Oral Investigations, 25*(7), 4299-4309.

Shujaat, S., Aljadaan, H., Alrashid, H., Aboalela, A. A., & Riaz, M. (2026). FDA-approved AI solutions in dental imaging: a narrative review of applications, evidence, and outlook. *International Dental Journal, 76*(1), 109315. https://doi.org/10.1016/j.identj.2025.109315

Sounderajah, V., Ashrafian, H., Golub, R. M., Shetty, S., De Fauw, J., Hooft, L., et al. (2021a). Developing a reporting guideline for artificial intelligence-centred diagnostic test accuracy studies: the STARD-AI protocol. *BMJ Open, 11*, e047709.

Sounderajah, V., Ashrafian, H., Rose, S., Shah, N. H., Ghassemi, M., Golub, R., et al. (2021b). A quality assessment tool for artificial intelligence-centered diagnostic test accuracy studies: QUADAS-AI. *Nature Medicine, 27*, 1663-1665.

Sounderajah, V., Guni, A., Liu, X., Collins, G. S., Karthikesalingam, A., Markar, S. R., Golub, R. M., Denniston, A. K., Shetty, S., Moher, D., Bossuyt, P. M., Darzi, A., Ashrafian, H., & STARD-AI Steering Committee, STARD-AI Consensus Group. (2025). The STARD-AI reporting guideline for diagnostic accuracy studies using artificial intelligence. *Nature Medicine, 31*(10), 3283-3289. https://doi.org/10.1038/s41591-025-03953-8

Sounderajah, V., Guni, A., Liu, X., Collins, G. S., Karthikesalingam, A., Markar, S. R., Golub, R. M., Denniston, A. K., Shetty, S., Moher, D., Bossuyt, P. M., Darzi, A., Ashrafian, H., & STARD-AI Steering Committee. (2026). Author correction:

the STARD-AI reporting guideline for diagnostic accuracy studies using artificial intelligence. *Nature Medicine*. https://doi.org/10.1038/s41591-026-04570-9

Tejani, A. S., Klontzas, M. E., Gatti, A. A., Mongan, J. T., Moy, L., Park, S. H., Kahn, C. E., Jr., & CLAIM 2024 Update Panel. (2024). Checklist for Artificial Intelligence in Medical Imaging (CLAIM): 2024 update. *Radiology: Artificial Intelligence, 6*(4), e240300.

World Health Organization. (2021). *Ethics and governance of artificial intelligence for health: WHO guidance*. World Health Organization.

CHAPTER 4

IMAGING IN PEDIATRIC JAW LESIONS: CYSTS, TUMORS, AND TUMOR-LIKE LESIONS

Suay Yağmur ÜNAL[1]
Melis GÜLDALI[2]

Introduction

Lesions detected in the jaw bones during childhood and adolescence are relatively uncommon in clinical practice, yet they require a diagnostic and treatment-planning approach that differs markedly from that used in adults. This difference stems from the presence of a developing dentition, the active remodeling state of the alveolar bone, the immaturity of the craniofacial growth centers, and a distribution of lesion types that diverges from that seen in adults. A further factor that complicates radiological interpretation is that tooth germs, unerupted teeth, and the physiological width of the dental follicle during the mixed-dentition period can produce imaging findings that mimic pathological processes.

Most pediatric jaw lesions are known to follow an asymptomatic course and to be discovered incidentally on

[1] Dr. Öğr. Üyesi, Nişantaşı Üniversitesi Diş Hekimliği Fakültesi Ağız Diş Ve Çene Radyolojisi İstanbul/Türkiye, Orcid: 0000-0002-8559-7461
[2] Uzm. Dt., Nişantaşı Üniversitesi Diş Hekimliği Fakültesi Ağız Diş Ve Çene Radyolojisi İstanbul/Türkiye, Orcid: 0000-0002-1165-0127

radiographs obtained for other clinically indicated reasons, following clinical examination, history-taking, and individualized risk assessment. In a ten-year retrospective study from Cluj-Napoca, a substantial proportion of pediatric patients diagnosed with jaw lesions reported no symptoms at all, and the lesions were most often noticed incidentally on panoramic radiographs obtained for clinical indications (Crasnean et al., 2023). The same study found that inflammatory radicular cysts were the most frequently detected lesion group and that the mandible was affected more often than the maxilla (Crasnean et al., 2023). These findings indicate that imaging should not be performed for screening purposes in the pediatric population in the absence of a clinical indication; at the same time, imaging obtained for an individualized indication is valuable for identifying incidental, asymptomatic lesions as well as symptomatic ones. Consistent with this, current guidelines from the American Academy of Pediatric Dentistry emphasize that the frequency of radiographic examination should be determined according to each patient's individual clinical needs (American Academy of Pediatric Dentistry, 2024).

Imaging plays a decisive role in the evaluation of pediatric jaw lesions, because the information obtainable from clinical examination alone is often limited; the intraosseous extent of a lesion, its relationship to adjacent anatomical structures, and the integrity of the cortical bone can be established only through radiological methods. In children, however, several additional factors distinguish imaging-strategy decisions from those in adults: greater sensitivity to ionizing radiation, a cumulative risk that is higher because growing tissues carry this exposure over a longer remaining lifetime, and a level of patient cooperation that may be limited. For this reason, the choice of imaging modality in a pediatric patient must be guided not only by diagnostic accuracy but also by the principles of radiation protection.

The clinical importance of an accurate and timely diagnosis is not limited to characterizing the nature of a lesion; it also shapes, to a considerable degree, the extent of the surgical approach (simple enucleation versus wide resection), the likelihood that developing tooth germs can be preserved, and the functional and aesthetic outcome after treatment. An unnecessarily aggressive surgical approach can lead to permanent facial deformity, loss of dentition, and psychosocial consequences in a growing child, whereas an inadequate or delayed intervention—particularly in locally aggressive lesions—can create the conditions for recurrence and the need for more extensive surgery. This balance underscores, once again, the central place that an imaging-based differential diagnosis occupies in the clinical decision-making process.

Imaging Modalities and Principles of Radiation Protection

The imaging modalities used in the evaluation of pediatric jaw lesions range widely, from conventional intraoral and panoramic radiography to cross-sectional techniques such as cone-beam computed tomography (CBCT), multidetector computed tomography (CT), and magnetic resonance imaging (MRI). Each modality carries its own advantages and limitations, and the choice of technique should be individualized according to the clinical question, the expected nature of the lesion, and the patient's age.

Conventional Radiographic Techniques

Panoramic radiography (orthopantomography) remains the primary imaging modality for the initial evaluation of pediatric jaw lesions. A single image provides a broad overview of both jaws, the developing tooth germs, and the temporomandibular joints, which makes the technique a practical first step whenever a clinical indication for imaging exists (Sahu et al., 2021); it is not, however, a screening tool to be applied in the absence of such an indication.

Periapical and occlusal radiographs are used as a complementary technique when the relationship of a lesion to a specific tooth requires more detailed evaluation. The most important limitation of conventional radiography is that it projects a three-dimensional structure onto a two-dimensional plane, so that expansion in the buccolingual direction, cortical thinning, and perforation cannot be fully assessed.

Cone-Beam Computed Tomography

Cone-beam computed tomography has become an increasingly widely used cross-sectional imaging technique in dental and maxillofacial imaging over the past two decades. When parameters such as field of view, milliamperage, and voxel size are chosen appropriately, CBCT is reported to allow high-spatial-resolution imaging of bone at a radiation dose that is generally lower than that of conventional multidetector CT; the effective dose, however, can vary considerably depending on the equipment brand, the field of view, and the protocol selected, and for this reason a "low-dose" characterization should not be treated as an inherent property of CBCT but rather as an outcome that depends on parameter selection. CBCT is considered to contribute substantially to determining a lesion's localization, its three-dimensional extent, its size, and its relationship to adjacent anatomical structures (the mandibular canal, the maxillary sinus, the nasal cavity); benign jaw lesions can present with a wide range of radiological appearances, and this diversity can be fully characterized only with cross-sectional imaging (Gadodia et al., 2010; Sahu et al., 2021). Current guidelines from the American Academy of Pediatric Dentistry nonetheless recommend that CBCT be used in pediatric patients only when conventional radiography fails to provide sufficient diagnostic information and when the anticipated clinical benefit is judged to outweigh the radiation risk, and they specify that every acquired CBCT volume must be fully reported in its entirety (American

Academy of Pediatric Dentistry, 2024). In a retrospective study by Çitir and Solmaz (2025), a substantial proportion of CBCT images obtained in pediatric patients contained incidental findings unrelated to the indication for the scan (involving airway spaces, dental, osseous, temporomandibular-joint, or soft-tissue calcifications). This observation is consistent with a recent systematic review reporting that incidental findings on CBCT are common in children and adolescents, although their reported frequency varies widely across studies (Vogiatzi et al., 2025). This underscores, once again, the need for systematic evaluation of the entire imaged volume rather than the region of interest alone.

Multidetector Computed Tomography

Compared with CBCT, multidetector CT offers higher soft-tissue resolution and, with the administration of contrast material, allows evaluation of a lesion's vascularity and soft-tissue component; it is therefore preferred particularly for lesions with an aggressive course or a suspicion of malignancy. In a study by Gadodia and colleagues evaluating jaw lesions in pediatric and adolescent patients with multidetector CT, lesion margins, loculation pattern, cortical integrity, and periosteal reaction were reported to play a decisive role in the differential diagnosis (Gadodia et al., 2010). Multidetector CT is often, though not invariably, associated with a higher radiation dose than CBCT—the actual difference depends on the specific protocols and scanners being compared, and dose ranges for the two modalities can overlap—and this generally higher dose is regarded as the most important factor limiting the use of multidetector CT in pediatric patients.

Magnetic Resonance Imaging

Because it does not involve ionizing radiation and provides superior soft-tissue contrast, magnetic resonance imaging occupies

an increasingly important place in the evaluation of pediatric jaw lesions. Its principal contribution lies in distinguishing cystic from solid components, assessing bone marrow involvement, and characterizing a lesion's extension into adjacent soft tissue (Sahu et al., 2021). The role of MRI in specific differential-diagnosis scenarios—including its use in syndromic and multifocal disease, and the incremental value of diffusion-weighted sequences in distinguishing unicystic ameloblastoma from odontogenic keratocyst—is addressed in greater detail in the dedicated section below on the expanding role of MRI. The principal limitations of MRI in this population include the long acquisition time—which means that sedation may be required, particularly in young or uncooperative children—together with cost (Sahu et al., 2021).

Radiation Dose Optimization and Modality Selection

Children are known to carry a higher risk of radiation-related stochastic effects than adults, both because cellular radiosensitivity is inversely related to age and because a longer remaining lifespan increases the cumulative risk. In this context, the principles of "as low as reasonably achievable" (ALARA) and "as low as diagnostically acceptable" (ALADA) have been adopted as the foundational approaches to radiation protection in pediatric dental imaging. DIMITRA (Dentomaxillofacial Paediatric Imaging: an Investigation Toward Low-Dose Radiation-Induced Risks), a European multicenter research project, extended these principles specifically for the pediatric population by proposing the concept of ALADAIP—"as low as diagnostically acceptable, being indication-oriented and patient-specific." This approach holds that the radiation dose should not merely be kept as low as possible, but should also be optimized according to the indication for the examination and the patient's individual characteristics (age, clinical question, prior imaging history). A recent critical review of the development and clinical applicability of these radioprotective principles noted that

the conceptual evolution from ALARA to ALADA and, subsequently, to ALADAIP reflects a paradigm shift from a goal of "best possible image quality" toward one of "diagnostically acceptable image quality" (Mendonça et al., 2025).

A 2023 survey of members of the European Academy of Dento-Maxillo-Facial Radiology (EADMFR) found that most responding clinicians reduced the field of view, tube current, and exposure time for younger patients, that written protocols were used relatively often, and that most respondents reported registering the dose-area product; the same survey, however, documented considerable variation in the specific exposure parameters selected by different clinicians for identical diagnostic scenarios, indicating that a standardized, consistently applied approach to CBCT dose selection has not yet been achieved across the surveyed centers (Fakhtei et al., 2026). Because the survey population was limited to EADMFR members, who may be more engaged with radiation protection than dental practitioners generally, this heterogeneity should be interpreted as evidence of inconsistent practice among the respondents themselves rather than as a representative picture of ALADAIP implementation across dentistry as a whole. An earlier systematic review demonstrating that tube voltage (kV) and the tube current–exposure time product (mAs) can be reduced without compromising image quality lends further support to the practical applicability of the ALADA principle (Goulston et al., 2016). Taken together, these findings indicate that pediatric CBCT protocols should confine the field of view to the clinical question, favor low-dose protocols, and avoid unnecessary repeat acquisitions.

The general principle guiding modality selection is to choose the technique that provides the greatest diagnostic information at the lowest radiation dose. Accordingly, panoramic radiography remains the first step in the evaluation of most pediatric jaw lesions, with CBCT reserved for situations in which conventional imaging proves insufficient, surgical planning is required, or the three-dimensional

extent of a lesion must be defined. MRI, in turn, is particularly valuable when soft-tissue or marrow involvement must be assessed or malignancy is suspected. Its absence of ionizing radiation is a meaningful advantage for follow-up imaging as well, but this advantage should be weighed against what a given follow-up question actually requires: when the clinical concern centers on mineralization, the relationship to adjacent teeth, or fine cortical detail, radiography or CBCT may remain more informative, so MRI is best reserved for longitudinal surveillance in which marrow or soft-tissue change is the primary concern and avoiding repeated ionizing exposure is a priority.

The Limited Role of Ultrasonography

Because bone reflects sound waves to a high degree, ultrasonography cannot serve as a primary imaging modality for intraosseous jaw lesions; when the cortex remains intact, it cannot provide information about a lesion's depth or internal structure. It can, however, play a complementary role in evaluating the superficial component of lesions that have perforated the cortex and extended into soft tissue, in distinguishing cystic from solid benign superficial swellings (such as reactive lymphadenopathy or a superficial abscess), and, when needed, in guiding image-directed fine-needle aspiration or biopsy. The absence of ionizing radiation and the ability to perform the examination at bedside without sedation make ultrasonography particularly attractive in very young children and in the exceptional circumstances in which radiological assessment is required during pregnancy; it is clear, nonetheless, that ultrasonography cannot substitute for cross-sectional imaging in the primary characterization of intraosseous jaw lesions.

A Systematic Imaging Approach to Pediatric Jaw Lesions

Following a systematic evaluation framework in the differential diagnosis of pediatric jaw lesions is regarded as a fundamental approach that improves diagnostic accuracy. In the widely accepted approach proposed by Sahu and colleagues (2021), the first step in the evaluation process consists of establishing the patient's age and clinical history. The second step examines the lesion's anatomical localization in the maxilla or mandible, its relationship to adjacent teeth, and its position relative to the mandibular canal; a lesion situated above the inferior alveolar canal is reported to be more likely of odontogenic origin, and one situated below it more likely of non-odontogenic origin, although this relationship should be treated as a helpful tendency rather than a stand-alone, definitive diagnostic criterion (Sahu et al., 2021). The third step assesses the lesion's radiodensity; more than 80% of jaw lesions are reported to be radiolucent, whereas radiopaque or mixed-density lesions more often point toward a fibro-osseous, inflammatory, or malignant etiology (Sahu et al., 2021).

In interpreting the imaging findings, the character of the lesion margin (a sharp, sclerotic border versus an irregular, ill-defined one), the loculation pattern (unilocular versus multilocular), the width of the transition zone, and whether the lesion is multifocal are all of decisive importance. A well-defined, unilocular radiolucency generally suggests a slow-growing benign process, whereas a narrow transition zone combined with a multilocular appearance can indicate an aggressive benign lesion (Sahu et al., 2021). The degree of bony expansion, whether cortical integrity is preserved, the presence of periosteal reaction, the presence of a halo surrounding the lesion, whether the growth pattern follows the long axis of the bone or extends perpendicular to it, and changes affecting adjacent teeth (displacement, root resorption) should also be carefully assessed. Slow-growing benign lesions are reported to more often produce a directional pattern of root resorption in adjacent teeth, whereas malignant lesions can produce a non-

directional resorption pattern related to destruction of the lamina dura; this finding, too, should be treated as a helpful sign that shifts probability rather than an absolute diagnostic criterion, since overlapping appearances have been reported (Sahu et al., 2021). On CT, the typical features of benign lesions are listed as well-defined margins, a narrow transition zone, cortical expansion or bulging, and displacement of adjacent structures, whereas ill-defined margins, a wide transition zone, cortical perforation, periosteal reaction, and an associated soft-tissue mass are characteristic of malignant lesions (Sahu et al., 2021).

The practical value of this systematic approach lies not in guaranteeing a definitive histopathological diagnosis in every case, but in meaningfully narrowing the differential diagnosis and thereby contributing to biopsy planning and treatment-strategy selection. In certain lesions with a highly characteristic imaging pattern—cherubism, for example—imaging findings interpreted alongside clinical information by an experienced observer can make a strong contribution to diagnostic direction; in many other lesions, imaging findings at least help in selecting an appropriate biopsy site (Sahu et al., 2021). It should be kept in mind, however, that histopathological confirmation remains indispensable for lesion pairs with overlapping imaging findings—as is the case, for example, between aneurysmal bone cyst and telangiectatic osteosarcoma—a point discussed in greater detail in the section below on aneurysmal bone cyst.

Odontogenic Cysts

Odontogenic cysts are lesions that arise from odontogenic epithelium or its remnants—which include, depending on the specific entity, the dental lamina, the reduced enamel epithelium of the tooth follicle, and epithelial rests of Malassez within the periodontal ligament—and are characterized by an epithelium-lined cavity. The fifth edition of the World Health Organization classification of head and neck tumors, updated in 2022, introduced

notable changes to the nomenclature of odontogenic and maxillofacial bone tumors; these updates, paralleling advances in molecular pathology, have led to a re-examination of the classification category of several entities (Choi et al., 2024). The distribution of odontogenic cysts in the pediatric population is reported to differ from that in adults, with developmental cysts—particularly dentigerous cyst and odontogenic keratocyst—accounting for a relatively larger share in children; inflammatory radicular cysts, however, continue to account for a substantial proportion as well, reflecting the frequency of caries and pulpal infection during the mixed-dentition period (Crasnean et al., 2023). A large epidemiological study from Chile reviewed roughly 23,000 biopsy records over a period of nearly forty years and analyzed 4,777 cases of cysts and odontogenic tumors according to the current World Health Organization classification (patient age range, 2–97 years); it reported that cysts accounted for 18.4% of all biopsies and odontogenic tumors for 2.4%, that the radicular cyst (58.6%), dentigerous cyst (17.9%), and odontogenic keratocyst (13.3%) were the most frequent cyst types, and that odontoma (40.1%) and conventional ameloblastoma (17.6%) were the most frequently identified odontogenic tumors (Rees et al., 2025). Because this dataset spans the full age range rather than representing a pediatric cohort specifically, its findings are cited here only for the general ranking they establish; the same overall pattern—radicular and dentigerous cysts as the leading cyst types, and odontoma as the leading odontogenic tumor—is corroborated by smaller series focused specifically on the pediatric age group (Crasnean et al., 2023; DeColibus et al., 2023).

Radicular Cyst

The radicular (periapical) cyst is the most common acquired odontogenic cyst, arising from the proliferation of epithelial rests of Malassez within the periodontal ligament in response to chronic

inflammation. It is typically associated with the apical region of a non-vital or deeply carious tooth. On imaging, it appears as a well-defined, often sclerotically bordered, unilocular radiolucency adjacent to the root apex of a non-vital tooth (Sahu et al., 2021). Given the frequency of deep caries and consequent pulpal necrosis affecting primary teeth in the pediatric population, radicular cysts occupy an important place among jaw cysts identified in children; a ten-year series, for example, reported that inflammatory radicular cysts accounted for roughly one-third of cases (Crasnean et al., 2023). When a radiolucent lesion is identified at the apex of a non-vital primary tooth, careful evaluation is required to avoid confusing the follicular space of the underlying developing permanent tooth germ with a radicular cyst. A feature that distinguishes the pediatric presentation from the classic adult picture deserves particular emphasis: because primary molars have relatively thin, porous root and furcation dentin and comparatively short roots, pulpal infection in these teeth frequently tracks toward the interradicular bone rather than remaining confined to a periapical location, producing a radiolucency centered on the furcation rather than the root apex. This furcation-region radiolucency can be mistaken for a periodontal lesion or, when it enlarges, for a dentigerous cyst of the underlying premolar germ if the relationship between the infected primary molar and the position of the developing premolar is not carefully assessed; recognizing this pediatric-specific pattern of spread is therefore an important part of correctly localizing the source of infection and protecting the premolar germ during treatment planning.

Dentigerous (Follicular) Cyst

The dentigerous cyst is the most common developmental odontogenic cyst and arises from the dental follicle of an unerupted or impacted tooth. The characteristic imaging finding is a well-defined, sclerotically bordered, unilocular radiolucent area

surrounding the crown of an unerupted tooth; attachment of the cyst wall at the cementoenamel junction is regarded as an important diagnostic clue (Sahu et al., 2021). Large dentigerous cysts can produce marked buccolingual expansion and cortical thinning, which can increase the risk of pathological fracture or secondary infection. Whereas the developmental type most commonly involves the mandibular third molar and maxillary canine in adults, a distinct subtype specific to the mixed-dentition period carries particular clinical significance in pediatric patients: the inflammatory dentigerous cyst. This subtype develops when periapical inflammation from a non-vital or deeply carious primary molar extends into the follicle of the adjacent developing permanent premolar, and is most often seen in the region of the mandibular second premolar, in close proximity to the root of a long-untreated or previously treated non-vital primary second molar (Hadziabdic et al., 2023). Unlike the classic developmental dentigerous cyst, this inflammatory mechanism signals the presence of an underlying source of infection and requires that treatment planning address both the cyst and the infected primary tooth together. Avoiding confusion between the physiological follicular width of an erupting tooth (generally not exceeding 2–3 mm) and a pathological dentigerous cyst is important for preventing unnecessary surgical intervention; this numerical threshold, however, should not be applied as a stand-alone diagnostic cutoff, since follicular width can vary with the stage of eruption and the specific tooth involved. It should instead be weighed together with the symmetry and shape of the radiolucency, the clinical presentation, and, where the finding is equivocal, comparison with serial radiographs over time, rather than being used in isolation to decide between observation and biopsy.

Odontogenic Keratocyst and Gorlin-Goltz Syndrome

The odontogenic keratocyst (OKC) is a developmental cyst arising from the dental lamina, characterized by a thin, uniformly

thick, parakeratinized squamous epithelial lining with a corrugated surface keratin layer. Classified under the neoplasm category as "keratocystic odontogenic tumor" in the 2005 World Health Organization classification because of its aggressive behavior, this lesion has since been returned to the developmental odontogenic cyst category in the current classification (Sahu et al., 2021; Speight & Takata, 2018). On imaging, OKC typically presents as a well-corticated, unilocular or multilocular lytic lesion in the posterior body and ramus of the mandible; an important distinguishing feature is its tendency to grow longitudinally within the medullary space in an anteroposterior direction, with relatively limited buccolingual expansion—a feature that helps distinguish a unilocular OKC associated with an unerupted tooth crown from a dentigerous cyst (Sahu et al., 2021). Root resorption is uncommon, and the homogeneous, thin structure of the cyst wall, which shows faint contrast enhancement without a discernible soft-tissue component, can also help distinguish OKC from a unilocular ameloblastoma (Sahu et al., 2021).

The presence of multiple OKCs should be regarded as a strong warning sign for Gorlin-Goltz syndrome (nevoid basal cell carcinoma syndrome). This autosomal dominant condition is characterized by multiple basal cell nevi, skeletal anomalies, calcification of the falx cerebri, and multiple OKCs of the jaws (Sahu et al., 2021). In a Brazilian retrospective series spanning a 31-year period, pediatric-age (0–14 years) OKC cases accounted for roughly one-tenth of all OKC cases identified over that interval; two of these pediatric cases were accompanied by clinical findings of Gorlin-Goltz syndrome, and recurrence and the development of new keratocysts were markedly more frequent in the syndromic cases than in non-syndromic ones (da Silva et al., 2020). The same study noted that pediatric OKC cases most often followed an asymptomatic course and were most commonly located in the anterior mandible (da Silva et al., 2020). A clinicopathological

review focused on the early diagnosis of Gorlin-Goltz syndrome in pediatric OKC patients reported that approximately 40% of pediatric patients with the syndrome initially present with a single keratocyst, a pattern that can lead to the underlying syndrome being missed; the review accordingly recommended that all pediatric OKC cases be screened for the syndrome as the preferred approach (Bello, 2024). In an imaging study of a 13-year-old boy with nevoid basal cell carcinoma syndrome, computed tomography proved valuable for identifying large, expansile cystic changes in the body and angle of the mandible bilaterally; when the patient's clinical status worsened, subsequent magnetic resonance imaging was reported to outperform CT both in delineating the internal composition of the lesions and in excluding intracranial abnormalities (Palacios et al., 2004).

Other Developmental Odontogenic Cysts

The lateral periodontal cyst and its multicystic variant, the botryoid odontogenic cyst, arise from remnants of the dental lamina and typically present as small, well-defined, unilocular radiolucencies lateral to vital teeth, most often in the mandibular canine–premolar region; both entities are classified among the developmental odontogenic cysts in the current World Health Organization scheme, are relatively rare in the pediatric population, and are more commonly diagnosed in adults (Speight & Takata, 2018).

The calcifying odontogenic cyst (Gorlin cyst) and the glandular odontogenic cyst are two entities that are exceedingly rarely reported in childhood and can show considerable radiological overlap with other cystic-neoplastic jaw lesions, owing to the presence of "ghost cells" or to their histological complexity (Speight & Takata, 2018). For both entities, the imaging appearance—a mixed-density lesion with a variable radiopaque focus in the calcifying odontogenic cyst, and a nonspecific unilocular-to-multilocular radiolucency in the glandular odontogenic cyst—does

not by itself provide a reliable distinguishing criterion, and a definitive diagnosis requires histopathological examination; given its high recurrence tendency, long-term radiological follow-up is recommended for the glandular odontogenic cyst.

Odontogenic Tumors

Odontoma

Odontoma is the most frequently identified odontogenic tumor in the pediatric age group; despite its designation as an odontogenic "tumor," it is regarded not as a true neoplasm but as a developmental hamartoma composed of enamel, dentin, cementum, and pulp tissue in a disorganized arrangement. The World Health Organization classification divides odontomas into compound and complex subtypes. Compound odontomas contain small tooth-like structures (denticles) and typically occur in the anterior maxilla; complex odontomas arise from an irregular mass of dental tissues and are more often seen in the posterior mandible (Sahu et al., 2021). A large ten-year retrospective series of 242 cases from the United States reported a median patient age of 14 years, with the second decade of life the most frequently affected age range (57.4%), and a substantial proportion of cases (38.8%) presenting with a clinical finding (DeColibus et al., 2023). The same study noted that ameloblastic fibro-odontoma is included, in the current World Health Organization classification, within the "developing odontoma" category, but that this entity is molecularly distinct from classic odontomas by virtue of harboring a BRAF p.V600E mutation and can, in some cases, display locally aggressive behavior and a tendency to recur (DeColibus et al., 2023)—a distinction that underscores why the terms "odontogenic hamartoma" and "true odontogenic neoplasm" should not be used interchangeably even within a single lesion family.

On imaging, the complex odontoma appears as an amorphous, densely radiopaque mass surrounding the crown of an unerupted tooth, encircled by a thin radiolucent halo; this halo is regarded as an important clue for distinguishing odontoma from osteoma (Sahu et al., 2021). In the compound odontoma, the number of radiopaque denticles varies, but their miniature tooth-like morphology greatly facilitates diagnosis. Odontomas are reported to be associated with disturbance of the eruption of an adjacent permanent tooth in roughly half of cases, and with displacement of an adjacent tooth or root in a slightly smaller proportion, which makes early diagnosis and surgical excision important for preserving the normal eruption sequence (DeColibus et al., 2023).

Ameloblastoma

Ameloblastoma is a benign but locally invasive tumor of odontogenic epithelial origin. Multiple potential cells of origin have been proposed—dental lamina remnants, the developing enamel organ, odontogenic cyst epithelium, and epithelial rests of Malassez—and it is accepted that the tumor may not arise from a single cell type but from remnants of odontogenic epithelium at different stages of development. The solid/multicystic (conventional) form is reported to typically occur in the third and fourth decades of life, whereas unicystic ameloblastoma is more often identified in children and adolescents and carries a markedly lower recurrence rate than the conventional form (Sahu et al., 2021). This distinction is preserved in the current World Health Organization classification, which recognizes conventional, unicystic, and peripheral/extraosseous ameloblastoma as subtypes under the ameloblastoma category (Choi et al., 2024). Two further points from the 2022 update deserve emphasis. First, adenoid ameloblastoma is now recognized as an independent tumor type—distinct from ameloblastoma itself—rather than as a subtype, and should be considered separately in the differential diagnosis of

ameloblastoma-like lesions (Soluk-Tekkeşin & Wright, 2022). Second, the desmoplastic pattern, previously treated by some classifications as a separate clinicopathological entity, is now classified as a histological subtype occurring within conventional ameloblastoma rather than as an independent tumor type (Soluk-Tekkeşin & Wright, 2022). Unicystic ameloblastoma was first described by Robinson and Martinez in 1977 and accounts for roughly 10–15% of intraosseous ameloblastomas. A systematic review of unicystic ameloblastoma in children reported that the lesion occurred predominantly in the mandible, most often with a unilocular radiolucent appearance; that the luminal subtype followed a less aggressive course and responded better to conservative treatment, whereas the mural and plexiform subtypes carried a higher risk of recurrence; and that the highest recurrence rate was observed in cases treated with enucleation alone (Seintou et al., 2014).

The literature has repeatedly emphasized that unicystic ameloblastoma can bear a striking clinical and radiographic resemblance to a dentigerous cyst, a similarity that can lead to diagnostic error; a substantial proportion of unicystic ameloblastoma cases associated with an unerupted tooth are reported to have initially been assessed radiologically as dentigerous cysts. The distinguishing imaging feature is that unicystic ameloblastoma tends to show more pronounced buccolingual expansion and contains a nodular solid soft-tissue component within the cyst lumen; this feature helps distinguish the lesion from purely cystic entities such as odontogenic keratocyst and dentigerous cyst (Sahu et al., 2021). Tooth displacement or root resorption can be seen in larger lesions. Conventional ameloblastoma, by contrast, is classically described as a multilocular, expansile radiolucency with a "soap-bubble" or "honeycomb" appearance (Sahu et al., 2021).

Odontogenic Myxoma

Odontogenic myxoma is a benign, locally aggressive tumor arising from the mesodermal component of the odontogenic apparatus. It generally occurs between 10 and 30 years of age, and although the distribution varies somewhat between series, it is more commonly reported in the mandible, particularly the ramus region (Sahu et al., 2021). On imaging, it appears as a unilocular or multilocular lytic lesion divided by thin bony trabeculae into geographic compartments; the "tennis-racket" appearance produced by these thin internal septa is described as a characteristic finding (Sahu et al., 2021). Rapidly growing lesions can show marked bone destruction with cortical perforation and soft-tissue extension. On MRI, the abundant myxoid stromal content produces high signal intensity on T2-weighted sequences, and a gradual pattern of post-contrast enhancement helps distinguish the lesion from the pronounced, rapid enhancement characteristic of hemangioma (Sahu et al., 2021).

Cementoblastoma and Other Rare Odontogenic Tumors

Cementoblastoma, a true odontogenic neoplasm arising from cementum, is reported to present before the age of 20 in half of patients and before the age of 30 in three-quarters (Sahu et al., 2021). It typically occurs in the mandible in association with the root of a premolar or molar tooth; the characteristic and diagnostic imaging finding is a mass that is directly fused to the root of the associated tooth and surrounded by a thin, regular radiolucent halo. The internal structure of the mass shows a variable degree of radiopacity depending on its maturity, and some cases show mineralized spicules radiating from the center toward the periphery (a "sunburst" pattern); this finding, however, is neither obligatory nor specific for cementoblastoma, since a similar radial pattern can also be seen in malignant lesions such as osteosarcoma. For this reason, greater diagnostic weight should be given to root fusion and the peripheral halo than to the sunburst appearance alone (Sahu et al., 2021).

Adenomatoid odontogenic tumor typically occurs in young female patients in the anterior maxilla, in association with an unerupted canine tooth, and presents as a well-defined unilocular lesion; because it can contain fine punctate calcifications, an attempt is often made to distinguish it from a dentigerous cyst using the "two-thirds rule." Calcifying epithelial odontogenic tumor (Pindborg tumor) is a rare entity in children, typically presenting as a radiolucent lesion containing scattered calcified foci in association with the crown of an unerupted tooth (Sahu et al., 2021).

Odontogenic fibroma, arising from the mesenchymal component of the periodontal ligament or dental papilla, is a relatively slow-growing benign tumor that generally presents as a well-defined unilocular or multilocular radiolucency; the central type occurs in the mandible, and the peripheral type in the gingiva. Squamous odontogenic tumor, arising from epithelial rests of Malassez in the periodontal ligament, is a rare benign epithelial tumor that typically presents as a well-defined, triangular radiolucency lateral to a tooth root (Speight & Takata, 2018). Both entities are exceedingly rare in the pediatric age group, and the diagnosis is most often established retrospectively through histopathological examination.

Non-Odontogenic Cysts

As noted in the section above on a systematic imaging approach, a lesion's position relative to the inferior alveolar canal is a helpful tendency rather than a strict rule: lesions located above the canal are more likely to be odontogenic, while a location below the canal, without a direct relationship to a specific tooth, and involving two or more tooth roots more often points toward a non-odontogenic process (Sahu et al., 2021). This anatomical relationship should be treated as a heuristic that shifts diagnostic probability, not as a defining criterion, and the individual lesions discussed below should always be interpreted within that framework.

Simple (Solitary/Traumatic) Bone Cyst

The simple bone cyst lacks a true epithelial lining and is best regarded as a pseudocyst of uncertain etiology; an intramedullary hemorrhagic process following trauma, with subsequent failure of the clot to organize into bone, is the mechanism most often proposed, but it remains a proposed model rather than an established, uniformly accepted cause (Sahu et al., 2021). The typical age at presentation is 10–20 years, and the lesion characteristically occurs in the bone marrow of the posterior mandible (Sahu et al., 2021). On imaging, it appears as a well-defined, low-density unilocular lesion that scallops upward between the roots of adjacent teeth; because this pseudocyst spreads by insinuating itself between tooth roots, it is not typically associated with root resorption or tooth displacement (Sahu et al., 2021). CT and MRI findings in some cases are consistent with hemorrhagic or serous fluid content, which has been cited as indirect support for the traumatic-hemorrhagic theory, though this appearance is not universal across cases (Sahu et al., 2021), and the lesion typically shows no post-contrast enhancement.

Aneurysmal Bone Cyst

Aneurysmal bone cyst (ABC) is an uncommon lesion composed of numerous blood-filled cavities with a sponge-like appearance; although uncommon, it can behave in a locally aggressive fashion because of its rapid growth pattern and osteolytic tendency. Roughly 70% of cases are considered a true neoplasm harboring a USP6 gene rearrangement, with the remainder thought to develop as secondary (reactive) change accompanying another bone lesion. It generally occurs before the age of 20 and is more frequently observed in female patients and in the posterior mandible (Restrepo et al., 2022; Sahu et al., 2021). On imaging, it presents as

a unilocular or multilocular expansile lesion with a "honeycomb" or "soap-bubble" appearance, showing cortical expansion, ballooning, and destruction, and it can produce tooth displacement or root resorption. On CT, a characteristic finding is a partially cystic, blood-filled meshwork divided by thick septa; on contrast-enhanced imaging, enhancement is seen within the cyst wall and septa (Sahu et al., 2021).

Fluid-fluid levels resulting from hemorrhage are a frequently observed and diagnostically valuable MRI finding in ABC, but this finding is not specific to ABC and can also be seen in other bone lesions such as telangiectatic osteosarcoma, giant cell tumor, and chondroblastoma. A large study comparing ABC and telangiectatic osteosarcoma on the basis of clinical, radiographic, and MRI findings reported that lesions showing a geometric (type 1A/1B) destruction pattern, with most of the lesion filled by fluid-fluid levels, could be assessed with a high degree of confidence as ABC, whereas the presence of a soft-tissue mass, cortical perforation, and periosteal reaction strongly favored telangiectatic osteosarcoma (Zishan et al., 2020); because that comparison was derived from a long-bone cohort, however, its diagnostic thresholds should be applied to jaw lesions only as general guidance, and not assumed to transfer directly to the differing bone geometry and growth pattern of the mandible and maxilla. A recent review focused on pediatric ABC similarly emphasized that the principal differential diagnoses for ABC are simple bone cyst and telangiectatic osteosarcoma, that radiographic and MRI findings are helpful but not sufficient on their own for a definitive diagnosis, and that histopathological confirmation should be regarded as a standard part of the diagnostic process (Restrepo et al., 2022). Accordingly, when an expansile jaw lesion containing fluid-fluid levels is encountered, imaging findings can strongly support a diagnostic suspicion of ABC, but the need for biopsy and histopathological confirmation should be assessed individually within the clinical and radiological context of each case,

and biopsy should not be avoided when additional findings such as a soft-tissue component or cortical perforation are present. MRI is also reported to be helpful in distinguishing ABC from odontogenic myxoma, central giant cell granuloma, odontogenic keratocyst, and hemangioma (Sahu et al., 2021).

Nasopalatine Duct Cyst

The nasopalatine duct cyst, arising from epithelial remnants of the nasopalatine duct, is regarded as the most common non-odontogenic developmental cyst overall, although it is distinctly uncommon in the pediatric age group and only occasional childhood cases have been reported. On imaging, it presents in the midline of the maxilla, between or immediately above the roots of the central incisors, classically described as a well-defined, sclerotically bordered, "heart-shaped" radiolucency. In a child, the principal differential-diagnostic task is distinguishing a true nasopalatine duct cyst from the normal, non-pathological nasopalatine canal, which can appear relatively prominent at this age; a recent CBCT study found that no single canal-width threshold reliably separates the two, and that evaluating the overall morphology of the canal—including the mediolateral diameter of its oral opening and any anterior-wall widening—together with the patient's age and clinical findings gives a more accurate distinction than diameter alone (Janovic et al., 2024). The roots of the central incisors may be displaced by the cyst; preservation of tooth vitality, however, provides an important clinical clue for distinguishing this lesion from a radicular cyst.

Non-Odontogenic Tumors and Tumor-Like Lesions

Non-odontogenic tumors and tumor-like lesions form an important and heterogeneous group of pediatric jaw pathologies. This group includes giant cell lesions (central giant cell granuloma, cherubism), fibro-osseous lesions (fibrous dysplasia, juvenile

ossifying fibroma), Langerhans cell histiocytosis, melanotic neuroectodermal tumor of infancy, and desmoplastic fibroma (Sahu et al., 2021). Intraosseous vascular malformations of the jaw are not covered here as a separate entity, and readers seeking detailed guidance on vascular malformations and lesions of the craniofacial skeleton are referred to dedicated reviews of that topic; one point, however, is important enough to state explicitly regardless of that scope decision. Vascular malformation should be included in the differential diagnosis of any radiolucent or mixed-density jaw lesion before biopsy, extraction, or surgery is undertaken in that area—particularly when the lesion is associated with a visible or palpable pulsation, a bruit, unexplained tooth mobility, or prior unexplained bleeding—because inadvertent instrumentation of an intraosseous vascular malformation can precipitate severe, potentially life-threatening hemorrhage. When any of these features is present, further vascular imaging (such as contrast-enhanced MRI, CT angiography, or catheter angiography) should be obtained and a vascular anomaly should be excluded before any invasive procedure is planned.

Central Giant Cell Granuloma

Central giant cell granuloma (CGCG) is a benign, non-neoplastic, intraosseous proliferative lesion that can nonetheless follow an occasionally aggressive course; it predominates in female patients during the second and third decades of life. The anterior mandible is the most frequently affected site, although the lesion tends to cross the midline and can also occur in the maxilla (Sahu et al., 2021). On imaging, it presents as a well-defined radiolucent lesion; the literature shows some variability regarding its loculation pattern. A series of 26 cases evaluated with CBCT reported that 65.4% of lesions were unilocular and 34.6% multilocular, whereas a 76-case European multicenter series reported a 75% unilocular rate; this discrepancy suggests that although CGCG is often described as

a multilocular, "honeycomb"-appearing lesion, a substantial proportion of small- and medium-sized lesions may in fact present a unilocular appearance, and that loculation is largely related to lesion size (Tahmasbi-Arashlow et al., 2022). A tendency to produce resorption of adjacent tooth roots is regarded as an important diagnostic clue (Sahu et al., 2021). Histopathologically, the lesion is characterized by fibrous tissue, areas of hemorrhage, and characteristic osteoclast-like giant cells. CGCG shows marked imaging and histopathological overlap with the brown tumor of hyperparathyroidism, and the two cannot be reliably separated on imaging appearance alone; multifocal involvement and a biochemical work-up—serum calcium, phosphate, and parathyroid hormone, supplemented by alkaline phosphatase when the picture remains unclear—are emphasized as the features that distinguish hyperparathyroidism from CGCG, since the direction and magnitude of these abnormalities can vary with the type and severity of hyperparathyroidism rather than following a single fixed pattern (Sahu et al., 2021).

In recent years, denosumab—acting through RANKL inhibition—has emerged as an alternative treatment option alongside conventional curettage and resection, particularly for aggressive, large-volume lesions; imaging in this context is not confined to establishing the initial diagnosis but also plays a central role in monitoring treatment response, including reduction in lesion size, cortical reformation, and increasing internal density, using serial CBCT or MRI. This radiological monitoring of treatment response—rather than the pharmacological and surgical details themselves—is the aspect of denosumab therapy most directly relevant to an imaging-focused discussion; briefly, favorable clinical and radiological responses have been reported with denosumab in CGCG, alongside a recognized risk of metabolic complications such as rebound hypercalcemia after treatment is discontinued, and a non-negligible recurrence rate (Choe et al., 2021; Rhou et al., 2022).

These findings indicate that radiological assessment during follow-up is a dynamic process that directly informs treatment decisions in CGCG.

Fibrous Dysplasia and McCune-Albright Syndrome

Fibrous dysplasia (FD) is a mosaic developmental skeletal disorder, associated with somatic (postzygotic) activating mutations in the GNAS gene, in which normal bone marrow is replaced by fibro-osseous tissue. This mutation has been shown to cause mosaic activation of the Gαs protein, leading to increased intracellular cyclic adenosine monophosphate production (Boyce & Collins, 2020). The disease most often manifests in childhood or early adolescence and shows a marked tendency to involve the maxilla; it may follow a monostotic (70%) or polyostotic (30%) course (Sahu et al., 2021). Craniofacial FD lesions are reported to become established during the early years of linear growth, to expand throughout the growth period, and to show a marked decline in metabolic activity in early adulthood (Boyce & Collins, 2020).

On imaging, FD is characterized by a heterogeneous "ground-glass" density (which becomes more homogeneous in more mature lesions), expansion along the long axis of bone, cortical thickening or thinning with preserved cortical integrity, and the absence of periosteal reaction (Sahu et al., 2021). The principal features that help distinguish FD from juvenile ossifying fibroma on imaging are the margin and transition zone: FD typically shows ill-defined margins that blend gradually into adjacent normal bone across a wide transition zone, a longitudinal growth pattern, relatively little tooth displacement, and an ability to cross cranial sutures, whereas ossifying fibroma is more often well demarcated from surrounding bone by a discrete, corticated peripheral rim with a comparatively narrow transition zone (Sahu et al., 2021). This radiological distinction should not be equated with the histopathological feature known as osteoblastic rimming—a

microscopic finding in which osteoblasts line the surface of bony trabeculae—which is a histological, not a radiological, criterion and cannot itself be identified on CBCT or CT.

A recent review addressing the clinical features and treatment of craniofacial FD noted that lesions follow a progressive course throughout the growth period, that complications such as optic nerve compression require careful monitoring, and that surgical intervention should, when possible, be deferred because of the risk of recurrence during the active growth phase (Szymczuk et al., 2023).

The clinical picture in which polyostotic FD is accompanied not only by skeletal lesions but also by café-au-lait skin pigmentation and hyperfunctioning endocrinopathies (such as gonadotropin-independent precocious puberty, growth hormone excess, or hyperthyroidism) is termed McCune-Albright syndrome (Boyce & Collins, 2020). A Nordic pediatric cohort study of 16 children with polyostotic FD found that McCune-Albright syndrome was present in half of the patients, all of whom had café-au-lait spots together with either precocious puberty or an abnormal testicular structure, and that three-quarters of the cohort had craniofacial bone involvement (Utriainen et al., 2018). From a dental standpoint, craniofacial FD is a factor that directly affects dental treatment planning. When monitoring is clinically indicated—for example, to assess disease activity, evaluate a specific complication, or plan an intervention—scintigraphy and CT can make an important contribution; consistent with the radiation-optimization principles discussed earlier in this chapter, however, these techniques should be reserved for situations with a clear clinical question rather than obtained as routine periodic surveillance, and clinical examination and, where sufficient, lower-dose imaging should be used to follow stable disease.

Cherubism

Cherubism is an inherited (autosomal dominant) bone dysplasia confined to the jaws; although it shows clinical and radiographic resemblance to craniofacial fibrous dysplasia, it is regarded as a distinct entity because of its characteristic tendency toward spontaneous regression and its different genetic basis. The disease has been shown to result from mutations in the SH3BP2 gene, which functions as an adaptor protein and participates in immune signaling and osteoclast activity (Ueki et al., 2001). The cherubism gene had previously been mapped to chromosome 4p16 (Tiziani et al., 1999).

The typical clinical presentation is painless, bilateral, and relatively symmetric swelling of the jaw that begins between 2 and 5 years of age, progresses through puberty, and preferentially involves the mandibular ramus and maxillary tuberosity; characteristic sparing of the mandibular condyle is considered an important distinguishing feature (Sahu et al., 2021). On imaging, multilocular lucent areas of variable size, expansile bony remodeling, cortical thinning, internal bony trabeculation, and dental derangement are observed, without periosteal reaction or an associated soft-tissue mass; these findings, defined even in classic radiographic series predating the routine use of cross-sectional imaging, characteristically spare the condyle, coronoid process, and orbital floor, although the disease can in rare cases also affect the orbital wall and produce proptosis (Beaman et al., 2004; Sahu et al., 2021). A study noting that MRI findings have been less extensively characterized than those of conventional radiography showed that MRI can reveal not only the anatomical extent of the lesion but also signal changes in areas that appear normal on conventional radiography and CT. In a recently reported case of a 4-year-old boy, the child's mother was found to have a history of unilateral facial swelling in childhood, although her diagnosis was established by

biopsy only at age 15; the authors attributed this clinical difference between mother and child to the variable expressivity of the SH3BP2 mutation (Cosar et al., 2025). Because of its characteristic imaging pattern, biopsy is unnecessary in most cases of cherubism; when histopathological examination is performed, it shows multinucleated giant cells within a fibrous connective-tissue stroma (Sahu et al., 2021).

Juvenile Trabecular Ossifying Fibroma and Psammomatoid Ossifying Fibroma

Ossifying fibroma is a group of fibro-osseous lesions characterized by aggressive behavior and a tendency to recur. Histologically, it is divided into psammomatoid and trabecular subtypes; the psammomatoid subtype more often occurs in adults, in the orbit and paranasal sinuses, whereas the trabecular subtype more often occurs in the jaw, typically in boys under 15 years of age, and shows a marked tendency to recur (Sahu et al., 2021). The nomenclature of these two subtypes underwent a notable change in the 2022 World Health Organization update: whereas the previous (2017) classification referred to both subtypes with the prefix "juvenile" (juvenile trabecular ossifying fibroma and juvenile psammomatoid ossifying fibroma), the 2022 update removed the term "juvenile" from the psammomatoid subtype, on the grounds that it can occur across a broad age range, redesignating it simply as "psammomatoid ossifying fibroma"; the trabecular subtype, by contrast, retained the name "juvenile trabecular ossifying fibroma" because of its continued marked predilection for childhood (Vered & Wright, 2022). It should be emphasized that this terminological change reflects a re-examination of the naming of two existing subtypes in light of clinical and epidemiological evidence, rather than the recognition of a new entity. On CT, both subtypes appear as a solid, expansile lesion of ground-glass density with a variable degree of calcification, a thin sclerotic border, a narrow transition

zone, and no low-density halo; developing tooth germs may be displaced, may fail to develop fully, or may lose their capacity to erupt (Sahu et al., 2021). The 2022 World Health Organization update also reported a broader revision of the general nomenclature for the fibro-osseous lesion group, extending it to include entities such as familial gigantiform cementoma and segmental odontomaxillary dysplasia (Choi et al., 2024; Vered & Wright, 2022).

Langerhans Cell Histiocytosis

Langerhans cell histiocytosis (LCH) is a rare disease driven by clonal proliferation of pathological, CD1a/CD207-positive myeloid dendritic cells; current classification schemes group it among the neoplastic, myeloid-derived histiocytoses rather than describing it as a purely reactive proliferation of resident tissue Langerhans cells, reflecting the demonstration of clonal, MAPK-pathway-activating mutations (most often BRAF V600E) in the pathological cells. Single-system bone disease, historically termed "eosinophilic granuloma," is the most common and most localized clinical presentation of LCH and most commonly affects the skull, flat bones, spine, and long bones. Jaw involvement is reported in roughly 8% of cases, with the mandibular body and angle the typical sites of involvement (Sahu et al., 2021). Oral findings such as gingival hypertrophy or tooth mobility can, in some cases, represent the initial manifestation of the disease. On imaging, a well-defined, localized, "punched-out" lytic lesion, which may or may not be accompanied by reactive sclerosis, is typical; alveolar bone destruction and loss of the lamina dura can produce the characteristic "floating tooth" appearance (Sahu et al., 2021).

A retrospective series evaluating CT and MRI findings in 17 patients with mandibular LCH found that all lesions were located in the mandible, that most cases (12 of 17) represented the intraosseous subtype, and that the most common presenting complaints were

facial swelling (76.5%) and pain (35.3%); all lesions in that series were osteolytic, with a mean lesion size of 23 mm (Kim et al., 2019). The same study emphasized that the imaging findings of LCH can closely resemble osteomyelitis, and that distinguishing between the two entities requires clinical and histopathological correlation (Kim et al., 2019). MRI, showing variable signal intensity on T2-weighted sequences and demonstrating inflammatory changes in adjacent soft tissue, was reported to provide additional value beyond CT in assessing bone marrow involvement and soft-tissue extension. Vertebra plana, beveled-edge lytic skull lesions, and the "floating tooth" sign are commonly cited as classic imaging findings of LCH that help distinguish it from other, rarer histiocytic disorders such as Erdheim-Chester disease, juvenile xanthogranuloma, and Rosai-Dorfman disease, although a full comparative account of those entities is beyond the scope of this chapter.

Melanotic Neuroectodermal Tumor of Infancy

Melanotic neuroectodermal tumor of infancy (MNTI) is a rare, melanin-containing tumor of neural crest origin that occurs almost exclusively during the first year of life (particularly between 2 and 6 months), giving it a distinct place among pediatric jaw pathologies. Roughly 70% of cases occur in the maxilla, particularly the anterior alveolar ridge and premaxilla, with the remainder occurring in the skull, mandible, and, less commonly, the brain (Guo et al., 2022). Clinically, it presents as a rapidly growing, painless, firm swelling with intact but characteristically blue-black pigmented mucosa. On CT, osteolytic or expansile bone destruction of the maxillary alveolar region, fragmentation of cortical integrity, displacement of developing tooth germs (a "free-floating" appearance), and, in some cases, spiculated or sunburst-type periosteal reaction can be observed; on MRI, the lesion shows mild T2 hyperintensity, a variable T1 signal pattern related to melanin content (isointense, mildly hypointense, or mildly hyperintense), and

heterogeneous post-contrast enhancement (Guo et al., 2022; Vasilyeva et al., 2022). Although the imaging findings of MNTI are not specific on their own, this diagnosis should be included in the differential whenever a rapidly growing mass with pigmented mucosa arises in the anterior maxilla during the first months of life; a definitive diagnosis rests on histopathological examination with immunohistochemical confirmation (for example, HMB-45, synaptophysin).

Desmoplastic Fibroma

Desmoplastic fibroma is a rare, benign but locally aggressive bone tumor regarded as the intraosseous counterpart of the soft-tissue desmoid tumor (fibromatosis). It most commonly occurs in the mandible and is reported to show a slight female predominance in childhood and adolescence (Sahu et al., 2021). On imaging, it presents as a unilocular or multilocular lytic lesion with a narrow transition zone; marked cortical thinning, absence of matrix mineralization, and delayed but pronounced contrast enhancement reflecting the lesion's fibrous nature are typical findings (Sahu et al., 2021). Soft-tissue extension is regarded as a marker of the lesion's locally aggressive behavior. In a case series of three pediatric patients with mandibular involvement (a 2-year-old girl, a 9-year-old boy, and an 18-month-old boy), the tumor's imaging findings were reported to be nonspecific, with the lesions initially often mistaken for odontogenic infection or other benign cystic-lytic lesions; a definitive diagnosis was established through histopathological examination supported by β-catenin immunohistochemical staining (Karimi et al., 2020). Given the high tendency of desmoplastic fibroma to recur, long-term radiological follow-up is recommended even after complete surgical excision.

Malignant Lesions of the Jaws and Secondary Involvement

Primary malignant lesions of the jaw are exceedingly rare in the pediatric population, but because of their rapidly progressive course and the urgency of treatment planning, early and accurate recognition of their imaging findings is of critical importance. In contrast to benign lesions, this group is typically characterized by ill-defined or irregular margins, a wide transition zone, cortical destruction, periosteal reaction, and a prominent soft-tissue component (Sahu et al., 2021).

Osteosarcoma

Osteosarcoma of the jaw is quite rare (accounting for less than 10% of all osteosarcomas) but carries a high malignant potential. Whereas long-bone osteosarcoma is common in the second decade of life, jaw osteosarcoma is reported to present at a later age (30–40 years); pediatric cases have nonetheless also been described in the literature (Sahu et al., 2021). The posterior mandible is the most frequently affected site, and symmetric widening of the periodontal ligament space is regarded as an early radiographic finding. Low-grade osteosarcoma presents as an ill-defined lytic destructive lesion, whereas the osteoblastic form, more common in the jaw, can show a "sunburst" pattern of radiating mineralized tumor spicules together with a limited soft-tissue component (Sahu et al., 2021). A study evaluating the demographic and CT findings of jaw osteosarcoma noted the lesion's marked radiographic heterogeneity and observed that conventional radiographic methods can be insufficient for distinguishing among benign fibro-osseous, inflammatory, and malignant tumors (Wang et al., 2012).

Ewing Sarcoma

Ewing sarcoma is currently defined, per the World Health Organization classification, as a tumor harboring EWSR1/FUS::ETS

family gene fusions, most commonly EWSR1::FLI1; although the tumor has historically been described as arising from primitive mesenchymal bone cells, its precise cell of origin remains unresolved, and it is more accurately characterized as a molecularly defined entity than as a tumor of established histogenesis (Dehner et al., 2024). Roughly 25% of all head-and-neck Ewing sarcoma cases, but only about 1% of Ewing sarcoma cases overall, occur in the jaw (particularly the mandibular ramus); the disease predominates in the first two decades of life and in male patients (Sahu et al., 2021; Krishna et al., 2013). It typically presents clinically with painful, rapidly progressive swelling, tooth mobility, and nonspecific systemic symptoms. On imaging, it presents as an ill-defined, permeative osteolytic lesion; CT can additionally demonstrate cortical destruction, a "floating tooth" appearance, an enhancing soft-tissue mass, and, in some cases, a sunburst-type periosteal reaction—a finding that can support the diagnosis when present but that is inconsistently observed and should not be treated as a required or defining feature. Because of the flat configuration and relatively low bone mass of the jaw, the "onion-skin" periosteal reaction seen elsewhere in the skeleton is not typically observed in jaw lesions (Sahu et al., 2021). Osteomyelitis and metastatic neuroblastoma should be given priority in the differential diagnosis.

Burkitt Lymphoma

Burkitt lymphoma, an aggressive subtype of non-Hodgkin lymphoma, is recognized as one of the fastest-growing human malignancies, with a doubling time of 24–48 hours, yet it offers a near-curative prognosis because of its high sensitivity to chemotherapy. Three clinical subtypes are recognized: endemic, sporadic, and immunodeficiency-associated. Involvement of the jaw and other facial bones is markedly more common in the Epstein-Barr virus-associated endemic variant, which is concentrated in malaria-endemic regions of Africa; in non-endemic regions, jaw involvement

is reported in roughly 15–18% of cases (Sahu et al., 2021; Derinkuyu et al., 2016). A study evaluating pediatric Burkitt lymphoma cases reported that imaging is the first step in evaluating persistent jaw swelling and that the lymphoma typically presents as an ill-defined osteolytic lesion (Derinkuyu et al., 2016). CT shows loss of the lamina dura and disruption of cortical integrity, with associated tooth mobility or displacement, together with a soft-tissue mass producing marked bone destruction around the jaw. Radiographically, the lesion can initially appear as multiple discrete foci that later coalesce into a larger, expansile radiolucency. MRI is reported to contribute to assessing bone marrow infiltration and submucosal tumor spread (Sahu et al., 2021). A recent review addressing the pathogenesis of Burkitt lymphoma and its multimodality imaging assessment emphasized that imaging plays a central role in diagnosis and in monitoring treatment response and recurrence (Kalisz et al., 2019). The differential diagnosis should include dentoalveolar abscess, osteomyelitis, rhabdomyosarcoma, eosinophilic granuloma, ameloblastoma, and other fibro-osseous lesions, and biopsy is mandatory for a definitive diagnosis.

Metastatic and Contiguous Tumors

The principal malignancies that can metastasize to the jaw in children are neuroblastoma, leukemia, lymphoma, and Ewing sarcoma (Sahu et al., 2021). Neuroblastoma metastasis is reported to be characterized on CT by ill-defined, "moth-eaten" lytic lesions, in some cases with periosteal reaction. Leukemic infiltration can present with tooth mobility related to loss of the lamina dura, with lytic bone destruction developing as the disease progresses. Soft-tissue tumors situated adjacent to the jaw, such as rhabdomyosarcoma, can invade the maxilla or mandible directly, producing ill-defined, geographic or permeative bone destruction on imaging (Sahu et al., 2021).

Tumor Mimics and Red Flags

Osteomyelitis recurs throughout the preceding sections as a differential consideration—for Langerhans cell histiocytosis, for Ewing sarcoma, and for Burkitt lymphoma alike—and this pattern is worth making explicit rather than leaving implicit within each individual lesion discussion. Odontogenic and hematogenous osteomyelitis of the jaw can produce ill-defined lytic destruction, periosteal new bone formation, and, in children, a permeative appearance that overlaps substantially with the imaging features of several of the aggressive and malignant lesions discussed above; fever, an identifiable dental or sinus source of infection, and a clinical or laboratory inflammatory picture (elevated white cell count, C-reactive protein, or erythrocyte sedimentation rate) favor an infectious process, but none of these findings excludes malignancy with certainty, and the reverse is equally true. For this reason, a lesion that fails to respond as expected to a course of antibiotic therapy, or that is accompanied by systemic symptoms out of proportion to a presumed infectious cause, should prompt reconsideration of biopsy rather than a further trial of empirical treatment.

Several imaging and clinical features function as red flags across this chapter's lesion groups and are collected here as a single checklist: rapid growth over days to weeks rather than months; systemic symptoms such as fever, weight loss, or malaise; an ill-defined margin with a wide transition zone; cortical perforation or an associated soft-tissue mass; non-directional root resorption suggesting lamina dura destruction rather than gradual displacement; multifocal or bilateral disease; and any clinical or imaging suggestion of a vascular lesion, as discussed above. The presence of one or more of these features should lower the threshold for cross-sectional imaging, multidisciplinary discussion, and biopsy, regardless of which specific lesion is initially suspected.

A Pattern-Based Approach to Differential Diagnosis

The framework introduced in the section above on a systematic imaging approach—localization, radiodensity, margin characteristics, and growth pattern—can be translated into practice through concrete clinical examples. In a child under 10 years of age, for instance, a multilocular, bilateral jaw lesion that spares the condyle strongly suggests cherubism, whereas a scalloped-margin pseudocyst of the posterior mandible in an adolescent, the age group in which this lesion is most typical, should raise suspicion for a simple bone cyst. Similarly, the presence of multiple OKCs should prompt consideration of Gorlin-Goltz syndrome, symmetric polyostotic ground-glass lesions should raise suspicion for McCune-Albright syndrome, and a rapidly growing mass accompanied by systemic symptoms should first prompt investigation for a malignant process (Burkitt lymphoma, Ewing sarcoma, metastatic neuroblastoma) or, where the clinical picture fits, osteomyelitis. A rapidly growing mass with pigmented mucosa arising in the anterior maxilla during the first months of life should raise suspicion for MNTI. These examples illustrate the importance of a holistic assessment based on the combination of age, localization, radiodensity, and margin characteristics rather than any single finding; a lesion in the same location (the posterior mandible, for example) can point to markedly different entities—odontogenic keratocyst, unicystic ameloblastoma, simple bone cyst, or aneurysmal bone cyst—depending on the patient's age and accompanying findings (Sahu et al., 2021).

A recent systematic review examined trends in the clinical presentation, investigation, and treatment of pediatric jaw lesions and reported that aggressive lesions (particularly CGCG and ossifying fibroma) most often presented with jaw mass, swelling, pain, gingival ulceration, and tooth mobility, and that CBCT was described as the reference imaging standard in most of the included

primary studies—a description that reflects the terminology used by the individual studies reviewed rather than a universal endorsement of CBCT over other modalities in every clinical scenario (Bhaskar & Fan, 2026). The same review reported that non-aggressive CGCG could be treated successfully with enucleation without recurrence, whereas aggressive CGCG was managed with either block resection or enucleation combined with adjuvant interferon or zoledronate, although recurrence was reported in some studies within the adjuvant-therapy group; juvenile trabecular ossifying fibroma was reported to occur less frequently than CGCG but to carry a higher recurrence rate after initial enucleation, in some cases requiring surgery as extensive as hemi-maxillectomy (Bhaskar & Fan, 2026).

Table 1, below, summarizes the typical age range, localization, and typical or supportive imaging findings for the principal pediatric jaw lesions addressed in this chapter, together with the key differential diagnosis and a red flag or suggested next step for each. Its purpose is not to offer a definitive algorithm but to provide clinicians with a rapid reference framework for initial assessment; most of the features listed are supportive findings that shift diagnostic probability and should not be treated as absolute distinguishing criteria. The final diagnosis should always be reached by considering clinical findings together with histopathological confirmation where indicated. As the table illustrates, the patient's age and the lesion's localization are not diagnostic in isolation, but meaningfully narrow the differential diagnosis when considered together with the imaging findings.

Table 1. Summary of the principal pediatric jaw lesions discussed in this chapter, including key differential diagnoses and red flags

Lesion	Age / localization	Typical/supportive imaging findings	Key differential diagnosis	Red flag & suggested next step
Radicular cyst	Variable; apex (or furcation, in	Sclerotically bordered unilocular	Dentigerous cyst; primary-molar furcation lesion	Persists or enlarges after endodontic

	primary molars) of a non-vital tooth	radiolucency at the apex/furcation		treatment → biopsy
Dentigerous cyst	2nd decade; inflammatory subtype: mandibular premolar region in mixed dentition	Unilocular radiolucency around the crown, attached at the cementoenamel junction	Unicystic ameloblastoma; odontogenic keratocyst	Marked buccolingual expansion or a nodular soft-tissue component → CBCT and biopsy
Odontogenic keratocyst	Variable; multiple lesions raise concern for Gorlin syndrome	Posterior mandible/ramus; longitudinal growth, limited buccolingual expansion	Dentigerous cyst; unicystic ameloblastoma	Multiple keratocysts in a child → evaluate for Gorlin-Goltz syndrome
Unicystic ameloblastoma	2nd decade; posterior mandible	Buccolingual expansion with a nodular intraluminal soft-tissue component	Dentigerous cyst; odontogenic keratocyst	Mural/plexiform pattern → higher recurrence; consider MRI and wider excision
Odontoma	1st–2nd decade; compound: anterior maxilla, complex: posterior mandible	Denticles or an amorphous radiopaque mass with a thin radiolucent halo	Osteoma; adenomatoid odontogenic tumor	Associated unerupted tooth → monitor eruption, plan timely excision
Simple bone cyst	10–20 years; posterior mandible	Scalloping between tooth roots; no resorption or displacement	Aneurysmal bone cyst; early fibro-osseous lesion	No fluid-fluid levels; surgical exploration/curettage usually both diagnostic and curative
Aneurysmal bone cyst	<20 years; posterior mandible	Expansile lesion with fluid-fluid levels	Telangiectatic osteosarcoma; simple bone cyst	Soft-tissue mass or cortical perforation → biopsy is mandatory, not optional
Central giant cell granuloma	2nd–3rd decade; anterior mandible, may cross midline	Uni- or multilocular radiolucency; tendency toward root resorption	Brown tumor of hyperparathyroidism; cherubism	Multifocal disease or abnormal calcium/PTH/phosphate → biochemical work-up
Fibrous dysplasia	Childhood–early adolescence; maxilla (often monostotic)	Ground-glass density; longitudinal growth; cortex intact	Juvenile trabecular/psammomatoid ossifying fibroma	Polyostotic disease with café-au-lait spots or precocious puberty → evaluate for

				McCune-Albright syndrome
Cherubism	Onset at 2–5 years; bilateral ramus/tuberosity, condyle spared	Symmetric, multilocular lucency without condylar involvement	Fibrous dysplasia; central giant cell granuloma	Family history/SH3BP2 mutation → genetic counseling; biopsy rarely needed
Juvenile trabecular / psammomatoid ossifying fibroma	JTOF: <15 years, male; POF: broader age range	Narrow transition zone; thin, corticated sclerotic margin	Fibrous dysplasia	High recurrence after enucleation alone → complete excision, long-term follow-up
Langerhans cell histiocytosis	<15 years; mandibular body/angle	"Punched-out" lytic lesion; "floating tooth" appearance	Osteomyelitis; malignancy (Ewing sarcoma, lymphoma)	Poor response to antibiotics → biopsy; MRI to assess marrow/soft-tissue extent
Melanotic neuroectodermal tumor of infancy	2–6 months; anterior maxilla	Osteolytic destruction; tooth-germ displacement	Rhabdomyosarcoma; other infantile malignancy	Blue-black pigmented mucosa is a clinical, not an imaging, clue → biopsy with HMB-45/synaptophysin
Ewing sarcoma	1st–2nd decade; mandibular ramus	Permeative osteolytic destruction; periosteal reaction in some cases	Osteomyelitis; metastatic neuroblastoma	Rapid growth with systemic symptoms → urgent biopsy and staging MRI
Burkitt lymphoma	Endemic variant: 4–7 years; maxilla > mandible	Loss of lamina dura; rapidly progressive soft-tissue mass	Dentoalveolar abscess; osteomyelitis; rhabdomyosarcoma	Doubling time of 24–48 hours → urgent biopsy and oncology referral

The stepwise evaluation process described across the preceding sections can also be stated as a general decision sequence, summarized here in place of a diagnostic flowchart. The first step establishes the patient's age and clinical history. The second step determines the lesion's general localization (maxilla versus mandible) and its relationship to a specific tooth: a lesion clearly centered on a tooth, or containing an unerupted crown, points toward an odontogenic process, and within mandibular lesions specifically,

position above or below the inferior alveolar canal provides a further, though still non-absolute, clue, favoring an odontogenic origin above the canal and a non-odontogenic origin below it; this canal-based heuristic is a mandible-specific refinement of the second step and does not apply to maxillary lesions, which must be assessed on tooth relationship, radiodensity, and growth pattern alone. The third step assesses radiodensity (radiolucent, radiopaque, or mixed), since radiopaque and mixed-density lesions more often point toward a fibro-osseous, inflammatory, or malignant process. The fourth step characterizes the margin and transition zone (well defined and corticated versus ill defined and wide), the fifth assesses loculation and the pattern of expansion, the sixth evaluates cortical integrity and the presence of destruction, and the seventh looks for periosteal reaction or an associated soft-tissue mass, either of which should prompt urgent evaluation for malignancy regardless of the findings from the earlier steps. This sequence is intended as a teaching aid and starting point for trainees, not a substitute for individualized clinical judgment or for the case-by-case reasoning illustrated in the discussion above.

The Expanding Role of MRI in Differential Diagnosis

The role of magnetic resonance imaging in evaluating pediatric jaw lesions has expanded considerably in recent years, owing to its lack of ionizing radiation. A review addressing the contribution of MRI to the evaluation of odontogenic tumors emphasized that, in addition to conventional T1- and T2-weighted sequences, diffusion-weighted imaging and dynamic contrast-enhanced imaging can be used as functional imaging techniques that allow assessment of tissue biology (Kurabayashi et al., 2021). That review presented representative MRI images for various odontogenic tumor types and offered a systematic discussion of signal characteristics that may be useful for differential diagnosis.

A study investigating the value of diffusion-weighted MRI in the differential diagnosis of unicystic odontogenic lesions found that unicystic ameloblastoma and odontogenic keratocyst could be statistically distinguished on the basis of their apparent diffusion coefficient (ADC) values (Han et al., 2018). This finding suggests that functional MRI parameters can play a complementary role when conventional sequences prove insufficient to distinguish two morphologically overlapping lesions. The same study, however, reported that the difference in ADC values between dentigerous cyst and odontogenic keratocyst is less pronounced than that seen between odontogenic keratocyst and ameloblastoma, and that these two entities may not be reliably distinguished by diffusion-weighted imaging alone—a limitation that has prompted the development of additional statistical approaches, such as decision-tree models. In LCH, MRI is reported to contribute to demonstrating bone marrow infiltration and inflammatory changes in adjacent soft tissue, with variable signal intensity observed on T2-weighted sequences; this feature can help distinguish LCH from osteomyelitis, which can present a similar appearance on CT.

The general barriers to MRI use in pediatric patients—acquisition time, the possible need for sedation, cost, and accessibility—were introduced earlier in this chapter, in the section on imaging modalities, and apply equally to the specific applications discussed here. What that general discussion could not capture, however, is the particular value MRI can add in syndromic and multifocal disease, where cross-sectional delineation of soft-tissue and intracranial extent becomes clinically decisive. In a patient with nevoid basal cell carcinoma syndrome, for example, MRI performed after clinical worsening was reported to outperform CT both in more clearly delineating the internal structure of bilateral mandibular lesions and in excluding intracranial involvement (Palacios et al., 2004); this example illustrates the specific circumstances—multifocal or syndromic disease, and a need to assess structures

beyond the field typically covered by dental CBCT—in which the incremental value of MRI is most clearly realized.

Artificial Intelligence and Radiomics: Current Developments and Limitations

The integration of artificial intelligence and deep-learning technologies into dental radiology has become a rapidly advancing area of research in recent years. Convolutional neural networks (CNNs) are reported to achieve high internal test performance in recognizing complex patterns on dental radiographs; however, it should be emphasized from the outset that most of the studies discussed in this section were developed using single-center, retrospective, and limited-scale datasets, so that reported performance figures should be interpreted cautiously with respect to clinical generalizability.

In a study evaluating a deep convolutional neural network (DCNN) developed for the automated detection of cystic radiolucent jaw lesions, the model was trained on a dataset of 7,160 panoramic radiographs and subsequently evaluated on an independent set of 100 test images; the model achieved 98.3% accuracy, 94.4% sensitivity, and 99.7% specificity in detecting cystic-appearing jaw lesions (Tajima et al., 2022). In interpreting this result, it should be noted that a training set of 7,160 images is modest relative to some large-scale studies in the dental artificial-intelligence literature, that the test set was limited to only 100 images, and that independent external validation across different populations and imaging equipment has not yet been performed, owing to the single-center, retrospective design of the study; a high internal test performance therefore does not, by itself, indicate that the model is ready for direct clinical use.

Broader Applications of AI in Pediatric Dentomaxillofacial Imaging

Because of challenges specific to pediatric dentition—the coexistence of primary and permanent teeth, the variable developmental stage of tooth germs, and dental overlap—artificial-intelligence models developed for children are reported to require a different approach from those trained on adult data. The two studies summarized in this section concern tooth detection/numbering and furcation-lesion classification, tasks that are related to, but indirect evidence for, this chapter's primary subject of pediatric jaw cysts and tumors; they are included briefly to illustrate the broader trajectory of pediatric dental artificial intelligence, not as direct evidence regarding cyst or tumor detection. A YOLOv10-based model developed for automatic tooth detection and numbering on panoramic radiographs during the mixed-dentition period, trained on a dataset comprising 8,153 teeth, was reported to perform well at the detection task (Peker & Kurtoğlu, 2025). By contrast, a study comparing deep-learning architectures (RT-DETR, the YOLO family) for classifying furcation lesions in primary molars found that even the best-performing model achieved a modest mAP@0.5 of 0.434 and a considerably lower mAP@0.5–0.95 of 0.187, which the authors attributed to the inherently low contrast and overlapping anatomy that make furcation-lesion detection difficult on panoramic radiographs (Karamüftüoğlu et al., 2025). Taken together, these two studies illustrate that artificial-intelligence performance varies considerably by task, and that small, low-contrast lesions remain a genuine challenge for currently available models.

These developments have thus far concentrated mainly on relatively narrowly defined tasks such as lesion detection and localization; artificial-intelligence models capable of multiclass differentiation among pediatric jaw cysts and tumors (for example, distinguishing OKC, dentigerous cyst, and unicystic ameloblastoma

from one another) appear to remain at an early stage of development. The principal methodological limitations in this area include the absence of adequately sized, class-balanced labeled datasets for rare pediatric jaw lesions; the fact that most studies are single-center, with model generalizability across different imaging equipment, protocols, and populations not yet systematically tested; and the fact that training and test sets in most studies are drawn from the same institution, and sometimes even the same patient population, making independent external validation the exception rather than the rule. A related but distinct point concerns how reported sensitivity and specificity should be interpreted: unlike predictive values (positive and negative predictive value) and overall accuracy, sensitivity and specificity are not, in principle, mathematically dependent on how common a lesion is in the test set, since each is calculated separately within the disease-positive and disease-negative groups. In practice, however, reported sensitivity and specificity can still vary with the case mix of a given test set—for example, its balance of subtle versus obvious lesions, the classification threshold chosen, and how positive and negative cases were sampled—so that figures obtained on a curated, single-center test set do not necessarily predict performance on the more heterogeneous case mix encountered in general clinical practice. For these reasons, it should be emphasized that reported high-performance figures represent a measure of success limited to a given study's own test set, and that generalization to different clinical settings cannot be assumed.

Artificial-intelligence-based image reconstruction and noise-reduction techniques are, nonetheless, reported to be gaining importance in pediatric radiology for radiation dose optimization; it is anticipated that enhancing images acquired with low-dose CBCT protocols using artificial-intelligence-assisted reconstruction algorithms could help both reduce radiation dose and preserve diagnostic image quality in pediatric patients. A related but more nascent prospect is radiomics: extracting quantitative textural

features (texture, heterogeneity, margin irregularity) from images for analysis by machine-learning algorithms, with the aim of complementing conventional visual assessment in benign-malignant differentiation and lesion subtyping. Both of these expectations currently rest on extrapolation from the broader dentomaxillofacial radiology literature rather than on evidence specific to pediatric jaw lesions, and radiomics in particular faces methodological hurdles that are not yet resolved even in the adult literature: the reproducibility of manual or semi-automated lesion segmentation between observers and institutions, the standardization and harmonization of features extracted from different scanners and acquisition protocols, and a continued scarcity of studies with genuine external validation on data the model has not seen during development. Systematic testing in multicenter, independently validated studies focused specifically on pediatric jaw lesions therefore remains a task for future research rather than a description of current evidence. In summary, the current level of evidence supports positioning artificial intelligence not as a tool that will replace the clinician in diagnosing pediatric jaw lesions, but as a potential adjunct capable of supporting the clinician, provided its outputs are carefully validated.

Multidisciplinary Assessment and the Decision to Biopsy

Alongside the evaluation of imaging findings, deciding when and how those findings require histopathological confirmation is an inseparable part of clinical practice. In certain lesions with a highly characteristic clinical and imaging pattern, such as cherubism, interpretation by an experienced observer combined with clinical information can make a strong contribution to diagnostic direction; by contrast, in most lesions that follow an aggressive course, or in which imaging findings overlap with a malignant entity—as in the case of aneurysmal bone cyst and telangiectatic osteosarcoma—incisional or excisional biopsy remains indispensable for a definitive

diagnosis (Restrepo et al., 2022; Sahu et al., 2021). At this point, it should be emphasized that a multidisciplinary assessment bringing together the pediatric dentist, oral and maxillofacial surgeon, dentomaxillofacial radiologist, oral pathologist, and, when needed, pediatric oncology and endocrinology specialists is decisive for correctly managing the diagnostic and treatment process, particularly in syndromic cases (Gorlin-Goltz, McCune-Albright) or those with potential systemic involvement (Langerhans cell histiocytosis, Burkitt lymphoma).

Structuring the imaging report so that it addresses not only the lesion's description but also its size, its relationship to adjacent vital structures (the mandibular canal, tooth germs, the maxillary sinus floor), anatomical details that may affect the surgical approach, and a proposed differential-diagnosis list is regarded as an important practice that strengthens communication within the clinical team. In lesions situated in close proximity to unerupted tooth germs in particular, it should be kept in mind that surgical planning must consider not only the lesion itself but also preservation of the developing dentition; for this reason, unlike in adult patients, the report in a pediatric patient should be prepared from a perspective that also takes future tooth-eruption potential into account. The frequency and duration of follow-up imaging likewise vary from case to case: in lesions capable of showing activity throughout the growth period, such as fibrous dysplasia and cherubism, periodic radiological surveillance is recommended until skeletal maturity is reached, whereas a shorter follow-up period may be sufficient for lesions with a low risk of recurrence that have been surgically explored and curetted, such as simple bone cyst.

Conclusion

Imaging-based evaluation of pediatric jaw lesions is a complex clinical problem that requires a systematic, stepwise approach, both because of the wide diversity of lesion types and

because normal variations of the developing dentition can be mistaken for pathological processes. Panoramic radiography remains the first-line evaluation tool, while CBCT—when appropriately optimized for the individual patient—has become an important complementary technique for cases requiring surgical planning, owing to the detailed three-dimensional information it provides. MRI, in turn, is playing an increasingly prominent role in cases with suspected malignancy or syndromic and multifocal involvement, and in follow-up imaging where marrow or soft-tissue change is the principal concern, given its lack of ionizing radiation and its superior soft-tissue resolution.

Systematically evaluating a lesion in light of parameters such as age, anatomical localization, relationship to adjacent teeth, radiodensity, margin characteristics, and growth pattern contributes meaningfully to narrowing the differential-diagnosis list and to selecting an appropriate biopsy or treatment strategy, even where a definitive histopathological diagnosis cannot be reached. In this process, following the World Health Organization's updated classification systems is important for translating advances in molecular pathology into clinical practice. The emergence of targeted pharmacological agents such as denosumab as a treatment option for selected refractory or aggressive lesions like central giant cell granuloma is a notable development, but it is not one that an imaging-focused discussion should overstate: denosumab therapy in growing children carries recognized risks, including rebound hypercalcemia and effects on the growing skeleton that are still being characterized, and its use is best regarded as reserved for aggressive or refractory cases managed under multidisciplinary specialist care rather than as a routine alternative to surgery.

Artificial-intelligence-assisted image analysis and radiomic approaches, although still represented by a limited number of studies specific to pediatric jaw lesions, are considered to hold potential for future integration into clinical practice as diagnostic decision-

support systems; addressing these developments together with radiation dose optimization is important both for improving diagnostic accuracy and for upholding radiation-protection principles in pediatric patients. Because the World Health Organization classification undergoes periodic revision, because targeted therapies such as denosumab are seeing increasingly widespread use, and because artificial-intelligence-based image analysis continues to be integrated gradually into clinical practice, this field can be expected to continue evolving rapidly in the years ahead. Clinicians are therefore encouraged to follow the current literature closely and to apply the systematic imaging approach outlined in this chapter in an individualized manner, evaluating age, localization, radiodensity, margin characteristics, and clinical course together within a holistic framework, rather than relying on any single imaging finding—an approach that will support the timely and accurate diagnosis of this rare but clinically important group of lesions across general dental practice, pediatric dentistry, oral and maxillofacial surgery, and dentomaxillofacial radiology alike.

References

American Academy of Pediatric Dentistry. (2024). Prescribing dental radiographs for infants, children, adolescents, and individuals with special health care needs. In The reference manual of pediatric dentistry (pp. 313–317). AAPD.

Beaman, F. D., Bancroft, L. W., Peterson, J. J., Kransdorf, M. J., Murphey, M. D., & Menke, D. M. (2004). Imaging characteristics of cherubism. AJR. American Journal of Roentgenology, 182(4), 1051–1054.

Bello, I. O. (2024). Pediatric odontogenic keratocyst and early diagnosis of Gorlin syndrome: Clinicopathological aids. Saudi Dental Journal, 36(1), 38–43. https://doi.org/10.1016/j.sdentj.2023.10.012

Bhaskar, J., & Fan, K. (2026). Trends in the presentation, investigation and management of paediatric jaw lesions: A systematic review. Advances in Oral and Maxillofacial Surgery, Article 100619. Advance online publication. https://doi.org/10.1016/j.adoms.2026.100619

Boyce, A. M., & Collins, M. T. (2020). Fibrous dysplasia/McCune-Albright syndrome: A rare, mosaic disease of Gαs activation. Endocrine Reviews, 41(2), 345–370.

Choe, M., Smith, V., Okcu, M. F., Wulff, J., Gruner, S., Huisman, T. A. G. M., & Venkatramani, R. (2021). Treatment of central giant cell granuloma in children with denosumab. Pediatric Blood & Cancer, 68(3), e28778.

Choi, W. J., Lee, P., Thomas, P. C., Rath, T. J., Mogensen, M. A., Dalley, R. W., & Wangaryattawanich, P. (2024). Imaging approach for jaw and maxillofacial bone tumors with updates

from the 2022 World Health Organization classification. World Journal of Radiology, 16(8), 294–316.

Çitir, M., & Solmaz, Y. M. (2025). Investigation of incidental findings in CBCT images of pediatric patients: A retrospective study. Journal of Clinical Pediatric Dentistry. Advance online publication. https://doi.org/10.22514/jocpd.2025.120

Cosar, M. S., Demirel, K., Goz, U. B., & Olmez, M. S. (2025). Cherubism in a 4-year-old boy: A clinical, radiological, and genetic report. Case Reports in Dentistry, 2025, Article 9974548. https://doi.org/10.1155/crid/9974548

Crasnean, E., Ban, A., Hedeșiu, M., Roman, R., Dinu, C., Băciuț, M., Văcăraș, S., Mitre, I., Almășan, O., Nechita, V. I., Armencea, G., Bran, S., & Onișor, F. (2023). Benign pediatric jawbone lesions: A 10-year clinical and radiological pilot study. Children, 10(2), Article 335.

da Silva, L. P., Rolim, L. S. A., da Silva, L. A. B., Pinto, L. P., & de Souza, L. B. (2020). The recurrence of odontogenic keratocysts in pediatric patients is associated with clinical findings of Gorlin-Goltz syndrome. Medicina Oral, Patología Oral y Cirugía Bucal, 25(1), e56–e60. https://doi.org/10.4317/medoral.23185

DeColibus, K. A., Rasner, D. S., Okhuaihesuyi, O., & Owosho, A. A. (2023). Clinicoradiopathologic analysis of odontomas: A retrospective study of 242 cases. Dentistry Journal, 11(11), Article 253.

Dehner, C. A., Lazar, A. J., & Chrisinger, J. S. A. (2024). Updates on WHO classification for small round cell tumors: Ewing sarcoma vs. everything else. Human Pathology, 147, 101–113. https://doi.org/10.1016/j.humpath.2024.01.007

Derinkuyu, B. E., Boyunağa, Ö., Öztunalı, Ç., Tekkeşin, F., Damar, Ç., Alımlı, A. G., & Okur, A. (2016). Imaging features of Burkitt lymphoma in pediatric patients. Diagnostic and Interventional Radiology, 22(1), 95–100. https://doi.org/10.5152/dir.2015.15211

Fakhtei, S., Hoogeveen, R., & Berkhout, E. (2026). Dose optimization in CBCT in dentistry: A survey among EADMFR members. Dentomaxillofacial Radiology, 55(1), 43–51. https://doi.org/10.1093/dmfr/twaf066

Gadodia, A., Seith, A., Sharma, R., Choudhury, A. R., Bhutia, O., & Gupta, A. (2010). Multidetector computed tomography of jaw lesions in children and adolescents. Journal of Medical Imaging and Radiation Oncology, 54(2), 111–119.

Goulston, R., Davies, J., Horner, K., & Murphy, F. (2016). Dose optimization by altering the operating potential and tube current exposure time product in dental cone beam CT: A systematic review. Dentomaxillofacial Radiology, 45(3), Article 20150254.

Guo, Y., Liu, Y., Wang, X., Li, G., & Yu, G. (2022). Clinical and imaging features of melanotic neuro-ectodermal tumor of infancy of the maxillary bone: Report of four cases and review of the literature. Oral Radiology. Advance online publication.

Hadziabdic, N., Balic, A., Cengic, E., Katana, E., Duratbegovic, D., & Lazovic Salcin, E. (2023). A large dentigerous cyst in a child as a complication of deciduous molar endodontic treatment: An interesting case report with short literature review. Case Reports in Dentistry, 2023, Article 4406854. https://doi.org/10.1155/2023/4406854

Han, Y., Fan, X., Su, L., & Wan, Z. (2018). Diffusion-weighted MR imaging of unicystic odontogenic tumors for differentiation of unicystic ameloblastomas from keratocystic odontogenic tumors. Korean Journal of Radiology, 19, 79–84.

Janovic, A., Bracanovic, D., Antic, S., & Markovic-Vasiljkovic, B. (2024). Morphological CBCT parameters for an accurate differentiation between nasopalatine duct cyst and the normal nasopalatine canal. Head & Face Medicine, 20(1), Article 54.

Kalisz, K., Alessandrino, F., Beck, R., Smith, D., Kikano, E., Ramaiya, N. H., & Tirumani, S. H. (2019). An update on Burkitt lymphoma: A review of pathogenesis and multimodality imaging assessment of disease presentation, treatment response, and recurrence. Insights into Imaging, 10(1), Article 56. https://doi.org/10.1186/s13244-019-0733-7

Karamüftüoğlu, N., Bulut, A., Akın, M., & Sağıroğlu, Ş. (2025). Panoramic radiograph-based deep learning models for diagnosis and clinical decision support of furcation lesions in primary molars. Children, 12(11), Article 1517.

Karimi, A., Derakhshan, S., Moradzadeh Khiavi, M., Mosavat, F., & Mirjalili, F. (2020). Desmoplastic fibroma of the jaws: A case series and review of literature. Iranian Journal of Pathology, 15(2), 134–143.

Kim, J. E., Yi, W. J., Heo, M. S., Lee, S. S., Choi, S. C., & Huh, K. H. (2019). Langerhans cell histiocytosis of the jaw, a mimicker of osteomyelitis on CT and MR images: A retrospective analysis. Medicine, 98(27), Article e16331. https://doi.org/10.1097/MD.0000000000016331

Krishna, K. B., Thomas, V., Kattoor, J., & Kusumakumari, P. (2013). A radiological review of Ewing's sarcoma of

mandible: A case report with one year follow-up. International Journal of Clinical Pediatric Dentistry, 6(2), 109–114.

Kurabayashi, T., Ohbayashi, N., Sakamoto, J., & Nakamura, S. (2021). Usefulness of MR imaging for odontogenic tumors. Odontology, 109(1), 1–10. https://doi.org/10.1007/s10266-020-00559-z

Mendonça, R. P., Estrela, C., Bueno, M. R., Carvalho, T. C. A. S. G., Estrela, L. R. A., & Chilvarquer, I. (2025). Principles of radiological protection and application of ALARA, ALADA, and ALADAIP: A critical review. Brazilian Oral Research, 39, Article e014.

Palacios, E., Serou, M., Restrepo, S., & Rojas, R. (2004). Odontogenic keratocysts in nevoid basal cell carcinoma (Gorlin's) syndrome: CT and MRI evaluation. Journal of Computer Assisted Tomography, 28(1).

Peker, R. B., & Kurtoğlu, C. Ö. (2025). Evaluation of the performance of a YOLOv10-based deep learning model for tooth detection and numbering on panoramic radiographs of patients in the mixed dentition period. Diagnostics, 15(4), Article 405.

Rees, V., Klare, M., Samaniego, V., Leiva, F., Jara, R., Martínez Rondanelli, B., & González Providell, S. (2025). Epidemiological features of 4777 cysts and odontogenic tumors based on the 2022 WHO classification. Oral Diseases, 31(2), 532–540.

Restrepo, R., Zahrah, D., Pelaez, L., Temple, H. T., & Murakami, J. W. (2022). Update on aneurysmal bone cyst: Pathophysiology, histology, imaging and treatment. Pediatric Radiology, 52(9), 1601–1614.

Rhou, Y. J. J., Wang, C. J., Nguyen, M., Vanderniet, J. A., Munns, C. F., Coleman, H., Kim, J., Holmes-Walker, D. J., Lim, L., & Girgis, C. M. (2022). Clinical and radiologic response of central giant cell granuloma to denosumab: A 6-year prospective observational study. Calcified Tissue International, 110(4), 464–474.

Sahu, B., Anand, R., Kumar, S., Solanki, R. S., Mehra, P., & Jain, M. (2021). A pattern-based imaging approach to pediatric jaw lesions. Indian Journal of Radiology and Imaging, 31(1), 210–223.

Seintou, A., Martinelli-Kläy, C. P., & Lombardi, T. (2014). Unicystic ameloblastoma in children: Systematic review of clinicopathological features and treatment outcomes. International Journal of Oral and Maxillofacial Surgery, 43(4), 405–412. https://doi.org/10.1016/j.ijom.2014.01.003

Soluk-Tekkeşin, M., & Wright, J. M. (2022). The World Health Organization classification of odontogenic lesions: A summary of the changes of the 2022 (5th) edition. Turkish Journal of Pathology, 38(2), 168–184. https://doi.org/10.5146/tjpath.2022.01573

Speight, P. M., & Takata, T. (2018). New tumour entities in the 4th edition of the World Health Organization classification of head and neck tumours: Odontogenic and maxillofacial bone tumours. Virchows Archiv, 472, 331–339.

Szymczuk, V., Taylor, J., & Boyce, A. M. (2023). Craniofacial fibrous dysplasia: Clinical and therapeutic implications. Current Osteoporosis Reports, 21, 147–153.

Tahmasbi-Arashlow, M., Patel, P. B., Nair, M. K., Liang, H., & Cheng, Y. L. (2022). Cone-beam computed tomographic

imaging of central giant cell granuloma: A comprehensive review. Imaging Science in Dentistry, 52(2), 123–131.

Tajima, S., Okamoto, Y., Kobayashi, T., Kiwaki, M., Sonoda, C., Tomie, K., Saito, H., Ishikawa, Y., & Takayoshi, S. (2022). Development of an automatic detection model using artificial intelligence for the detection of cyst-like radiolucent lesions of the jaws on panoramic radiographs with small training datasets. Journal of Oral and Maxillofacial Surgery, Medicine, and Pathology, 34, 553–560.

Tiziani, V., Reichenberger, E., Buzzo, C. L., Niazi, S., Fukai, N., Stiller, M., Peters, H., Salzano, F. M., Raposo do Amaral, C. M., & Olsen, B. R. (1999). The gene for cherubism maps to chromosome 4p16. American Journal of Human Genetics, 65(1), 158–166. https://doi.org/10.1086/302456

Ueki, Y., Tiziani, V., Santanna, C., Fukai, N., Maulik, C., Garfinkle, J., Ninomiya, C., doAmaral, C. M., Peters, H., Habal, M., Rhee-Morris, L., Doss, J. B., Kreiborg, S., Olsen, B. R., & Reichenberger, E. (2001). Mutations in the gene encoding c-Abl-binding protein SH3BP2 cause cherubism. Nature Genetics, 28(2), 125–126.

Utriainen, P., Valta, H., Björnsdottir, S., Mäkitie, O., & Horemuzova, E. (2018). Polyostotic fibrous dysplasia with and without McCune-Albright syndrome—Clinical features in a Nordic pediatric cohort. Frontiers in Endocrinology, 9, Article 96. https://doi.org/10.3389/fendo.2018.00096

Vasilyeva, D., Philipone, E., Perschbacher, S. E., & Chan, K. C. (2022). Computed tomographic imaging features of maxillary and mandibular melanotic neuroectodermal tumor of infancy: Report of 2 cases and systematic review. Oral Surgery, Oral Medicine, Oral Pathology, Oral Radiology, 134(4), 470–483.

Vered, M., & Wright, J. M. (2022). Update from the 5th edition of the World Health Organization classification of head and neck tumors: Odontogenic and maxillofacial bone tumours. Head and Neck Pathology, 16(1), 63–75.

Vogiatzi, T., Papageorgiou, S. N., Silikas, N., & Walsh, T. (2025). Incidental findings from cone-beam computed tomography in children and adolescents: A systematic review. European Archives of Paediatric Dentistry, 26(5), 877–889. https://doi.org/10.1007/s40368-025-00999-7

Wang, S., Shi, H., & Yu, Q. (2012). Osteosarcoma of the jaws: Demographic and CT imaging features. Dentomaxillofacial Radiology, 41(1), 37–42.

Zishan, U. S., Pressney, I., Khoo, M., & Saifuddin, A. (2020). The differentiation between aneurysmal bone cyst and telangiectatic osteosarcoma: A clinical, radiographic and MRI study. Skeletal Radiology, 49(9), 1375–1386.


BİDGE